Studies on the novel selective β-O-4 cleavage method of lignins by E1cB type elimination reaction assisted by the sulfone group -γ-TTSA method-

2014

Daisuke Ando

Contents

List of Figures

List of schemes

List of Tables

Introduction

Petroleum-based chemical products are indispensable for the chemical industry today. However, the fossil refinery processes give rise to some environmental problems, such as degradability and toxicity. In addition, the price of petroleum has risen steadily for several years. Thus, our society is facing the shift from a fossil-fuel-based society to a new sustainable society that is based on renewable resources, such as biomass. Especially, wood biomass, representing about 146 billion tons a year, is drawing attention. The sustainable use of bio-based resources suggests integrated manufacturing in biorefineries. Wood biomass is a polymer complex consisting of biomaclomolecles, such as cellulose, lignin and hemicellulose. Thus, the utilization of each component according to its feature is needed. The biorefinery concept embraces a wide range of technologies able to separate biomass into the building blocks, which can be converted to value-added products, chemicals, and biofuels (Cherubini and Stromman 2011). However, the development and application of lignocellulosic biomass fractionation technologies that are technically and economically feasible is still in its infancy. That is, the biorefinery of wood biomass should be ideally initiated with the highly selective separation of their components, i.e., cellulose, hemicellulose and lignins, without large chemical modifications which have been carried out by the conventional chemical modification of wood, such as wood-pulping and saccharification.

Of these components in wood biomass, lignin is the key component for biorefinery because lignin is connected between microfibrils in a plant cell wall. Lignin is, after cellulose, the second abundant biomacromolecule as natural organic materials and comprised about 20-30% of woods and 15-20% of grasses. Its structure is built of phenylpropanoid units, linked with various types of ether and carbon-carbon bonds and gives stiffness, strength, waterproof and rotproof of the cell wall (Boerjan et al. 2003). However, the lignin's chemical structure has not yet been completely elucidated because some different kinds of bonds are formed by random-coupling of some radicals derived from monolignols. That is, lignin's chemical structure and features are quite different from polysaccharides.

Thus, it is considered that a separation of biomass to lignin and polysaccharide is the first step for biorefinery. Therefore, the knowledge of structures between components is needed in these days. Indeed, there are the interactions between the components, such as entangling and chemical bonding. Especially, the chemical bondings between lignin and polysaccharide, called Lignin-Carbohydrate-Complex (LCC), have been studied for many years in lignin chemistry. Several chemical bonds have been proposed to be prevalent between lignin and polysaccharides such as phenyl glycoside, benzyl ester and benzyl ether linkages (Watanabe 1995; Koshijima and Watanabe 2003; Lawoko et al. 2005; Balakshin et al. 2007, 2011). Many investigations have been conducted to isolate and elucidate the LCC's chemical structure. Besides the above industrial interest, studies on the chemical structure of LCC in wood are of significance for the elucidation of the LCC biosynthesis in cell-wall construction. Much knowledge is obtained by degradation techniques such as alkaline hydrolysis, acid hydrolysis and Smith degradation. In these approaches, wood samples are degraded to afford the resulting products, followed by identification of the products. The useful information could be got in spite of indirect evidence. Moreover, valuable information of LCC's type and quantity in biomass has been obtained without any modification by using 2D-NMR analysis recently. However LCC's structures are still unknown despite many researches. In past methods, information was lost by cleavage of LCC linkages in degradation approaches and knowledge about low-content LCC linkages is undetectable in 2D-NMR analysis. Therefore, the isolation and chemical structural determination of LCC bonding sites is an important approach for new knowledge. Indeed, direct proofs such as the isolation of LCC bonding site is not yet reported.

The selective degradation of each component is needed for LCC isolation. So, there are two approaches. One is an approach to degrade in order of polysaccharide, lignin. The other is an approach to decompose in order of lignin, polysaccharide. It is considered that the latter is useful for this purpose. This is because the obtained degradation products of the latter have easier structure than that of the

former. The key point is to degrade lignin, that has the complicated structure, in the first step. Thereby, the polysaccharide-rich degradation products can be obtained in high molecular weight moiety. In subsequent step, the degradation products, such as LCC bonding sites and oligosaccharide, can be separated easily. However, there are no lignin degradation methods, in coarse of which LCC linkages are intact without damaging. A novel selective degradation method for LCC analysis is needed.

In order to clarify the exact chemical structure of lignin on the basis of intact degradation products of it and to obtain the LCC molecules, such as that linked with benzyl ether, the author has developed the novel selective degradation method for β-O-4 substructures in lignin, named as γ-TTSA method which consists of four steps; selective tosylation (T) of a primary hydroxyl group at γ-position, subsequent thioetherification (T), sulfonylation (S) and mild alkali treatment (A).

Thus, in this study, two lignin degradation methods (α-TSA method and γ-TTSA method) were established in model experiment. In α-TSA methods, it was clear that β-elimination reaction of sulfone compound is appropriate for the β-O-4 cleavage. Then, the utilities and detail reaction mechanism of the γ-TTSA method for LCC chemical structure analysis were investigated with using lignin model compounds; dimeric β-O-4 lignin model compounds, artificial lignin (dehydrogenative polymer: DHP). And then, purified milled wood lignin (pMWL) as native lignin was also analyzed by γ-TTSA method. Finally, LCC in crude MWL (cMWL) was analyzed by γ-TTSA method. These results were summarized in five chapters.

In Chapter 1, the author describes the novel lignin degradation method, named as α-TSA method. The cleavage of the β-O-4 linkage by the effect of a sulfone group that was a neighboring carbon of β-O-4 linkage is discussed in dimer model experiment.

In Chapter 2, the author describes development of novel lignin degradation method, named as γ-TTSA method. An introduction of the sulfone group to a carbon at γ-position is discussed for the retention of LCC bonding sites. The availability of the method for LCC analysis was discussed.

In Chapter 3, the degradation behavior of a lignin polymer model, a so-called dehydrogenation polymer (DHP, prepared from coniferyl alcohol), by the γ-TTSA method is described. Each reaction step of the method was followed by Fourier transform infrared (FT-IR) spectrometry and heteronuclear single quantum coherence nuclear magnetic resonance (HSQC-NMR) analysis. The obtained degradation product was analysed by some spectroscopy methods. The applicability of γ-TTSA method to lignin polymer is discussed in this chapter.

In Chapter 4, the γ-TTSA degradation of purified milled wood lignin (pMWL) from *E. globulus* is described. The MWL is a β-O-4 unit rich native lignin. Depolymerization by the cleavage of β-O-4 linkages in native lignin was comfirmed by using HSQC-NMR and GPC analyses. On the other hand, the β-β linkage was investigated after the reaction, too. The effect of γ-TTSA method on the molecular distribution of lignin is discussed.

In Chapter 5, selective degradation of lignin in crude MWL (cMWL) from *E. globulus* by the γ-TTSA method is described. The cMWL is a LCC fractiom consisting of lignin and xylan. The β-O-4 linkages were cleaved selectively without transforming of the other structures to degrade the only lignin moiety of cMWL. The obtained degradation products were fractionated with some different solvents to get new LCC fractions. The chemical structures of the fractions are discussed.

The detailed experimental methods and data of compounds are summarized in Experimental Section.

Development of γ-TTSA method

Chapter 1. Cleavage of the β-O-4 linkage by the effect of sulfone group

The cleavage of β-O-4 linkage proceeded without side reactions by β-elimination of α-sulfone derivative. It found that the cleavage of β-O-4 linkage associated by sulfone group at neighboring carbon of the linkage.

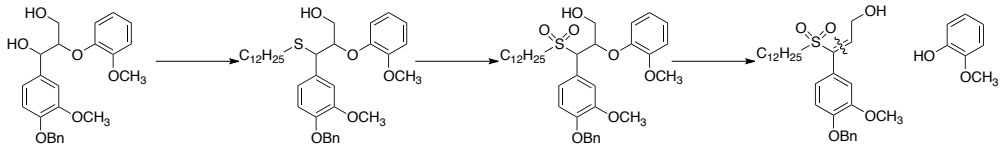

Chapter 2. Novel lignin degradation method for LCC analysis -dimer model-

γ-TTSA method were established. The introduction of sulfone group to γ-position and sequent cleavage of β-O-4 linkage were succeeded in lignin model dimer. The method was useful for LCC analysis because side reactions at α-position were not proceeded.

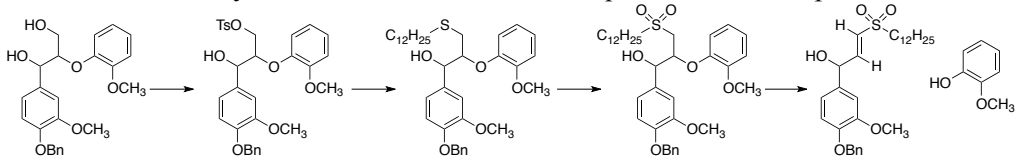

Chapter 3. Novel lignin degradation method for LCC analysis -polymer model-

In polymer model experiment with artificial lignin (DHP), β-O-4 linkage was cleaved selectively and other linkages were intact under γ-TTSA reaction sequence. As a result, molecular weight of DHP was decreased. Accordingly, it found that γ-TTSA method was useful for lignin polymer.

Application of γ-TTSA method

Chapter 4. Degradation of Native lignin

The purified MWL (pMWL) from *Eucalyptus globulus* was degraded by γ-TTSA method. β-O-4 linkages in pMWL were cleaved selectively and molecular weight of pMWL was decreased. As expected, lignin was degraded by the cleavage of β-O-4 linkages.

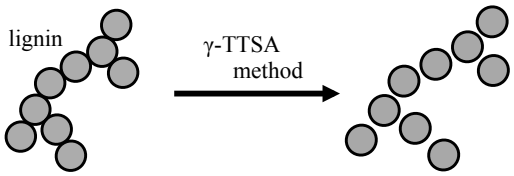

Chapter 5. Degradation of LCC

LCC (crude MWL) from *Eucalyptus globulus* was degraded by γ-TTSA method to obtain new LCC fractions. It was suggested by the structure analysis of these fraction that syringaresinol-type β-β substructure played an important role for linking between lignin and xylan.

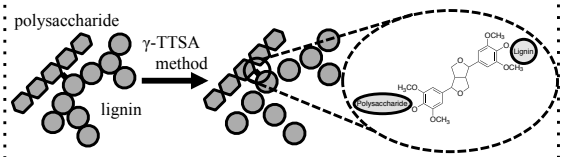

Development and application of new degradation method, named as γ-TTSA method, for LCC analysis were described in this study. The fact that this method is useful for LCC analysis was established. This method will open a new possibility for studies on LCC.

Figure 0 Schematic representation of the outline of this thesis

Chapter 1

Cleavage of the β-O-4 linkage by the electron-withdrawing effect of the sulfone group that exist in a neighboring carbon of the β-O-4 linkage: the development of the novel lignin degradation method named α-TSA method

1.1 Introduction

Lignin is the most abundant aromatic natural macromolecules existing in the plant cell walls. Some degradation methods of lignin have been reported for the elucidation of lignin chemical structure. Specifically, the degradation methods such as acidolysis (Lundquist 1992), thioacidolysis (Lapierre et al. 1986; Roland et al. 1992) and DFRC (Lu and Ralph 1997 a,b), by which β-O-4 linkages were cleaved selectively to give monomers, oligomers and low-molecular weight products, have been used well to gain the various knowledge about the lignin structure. (e.g. the quantity of β-O-4 linkage, S/G ratio, condensed linkages such as 5-5, β-β and β-1 substructures, the functional group information at γ-position). On the other hand, the unexpected secondary condensation reactions at benzylic positions are presumed to occur because all these methods carried out under acidic reaction conditions to form benzylic cations, which easily react with neighboring electron-rich aromatic rings having methoxy and alkoxy groups to cause condensation reactions, just like those of the Klason lignin formation. Thus, the degradation method under the milder condition is required for getting the more detailed knowledge.

It was reported in some studies (Forzelius et al. 1963, Jerkeman and Lindberg 1964, Ljunggren et al. 1983) that a sulfonyl group at the α-position of lignin facilitated the cleavage of β-O-4 linkages under an alkali condition. Indeed, in normal β-O-4 linkages, a temperature of 170 ^{o}C is required for the cleavage to occur at a reasonable rate. On the other hand, the corresponding temperature is less than 0 ^{o}C in β-O-4 linkages with the sulfone at α-position (Ljunggren et al. 1983). This reaction mechanism is that the sulfonyl group activated the β-elimination (E1cB type reaction) from the

α-position. However, it was difficult to introduce the sulfone group quantitatively at the α-position of the β-O-4 substructure model: the yield was 51% even in the case of lignin model compound without γ-hydroxy methyl group, 1-(3,4-dimethoxyphenyl)-2-(2-methoxyphenoxy)-ethanol (Jerkeman and Lindberg 1964). Therefore, we focused on the nucleophilicity of thiol at the α-position, as revealed at the initial stage of the thioacidolysis strategy (Roland et al. 1992), and tried to introduce the sulfone structure to the α-position of the β-O-4 substructure by 2-step reactions (the nucleophilic reaction of thiol and the oxidation of sulfur atom).

In this chapter, an selective β-O-4 linkage degradation method, named as α-TSA method, is proposed via a α-sulfone intermediate, which consists of three reactions: (1) α-thioetherification (T), (2) sulfonylation (oxidation) (S), and (3) mild alkali treatment (A), i.e., the α-TSA reaction. It is demonstrated that the β-O-4 linkage is cleaved under the mild condition by the effect of a sulfone group that was a neighboring carbon of β-O-4 linkage.

1.2 Results and discussion

1.2.1 Strategy

There are two-type synthesis methods of a sulfone structure in organic chemistry (Scheme 1). One is the addition of sodium sulfinates. Sulfinate anions normally react with electrophiles at sulfur to give sulfones. (Durst, T. 1979). The other is the oxidation of sulfides. The sulfur is oxidized after the C-S bond formation to transform the sulfone structure. The nucleophlic addition of the sulfone anion by the former method proceeded only in a low yield and the strong acid condition was needed. Then, a series of the TSA reaction, thioetherification, sulfonylation with oxidation and cleavage of β-O-4 linkage under alkali treatment, was attempted.

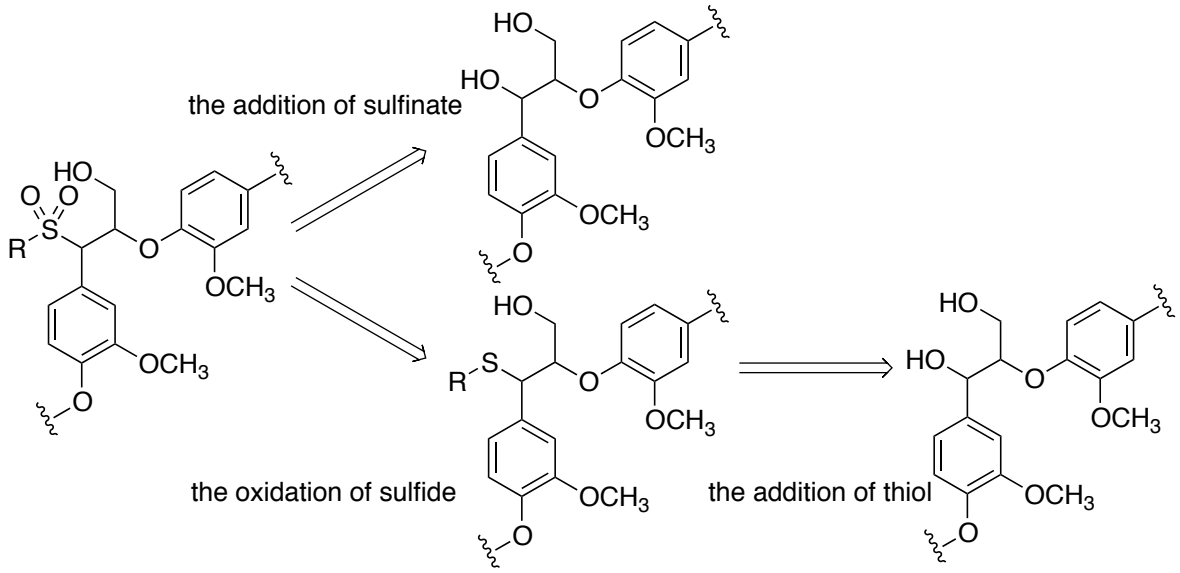

Scheme 1 Retro-synthesis of a sulfone structure at α-position of β-O-4 substructure

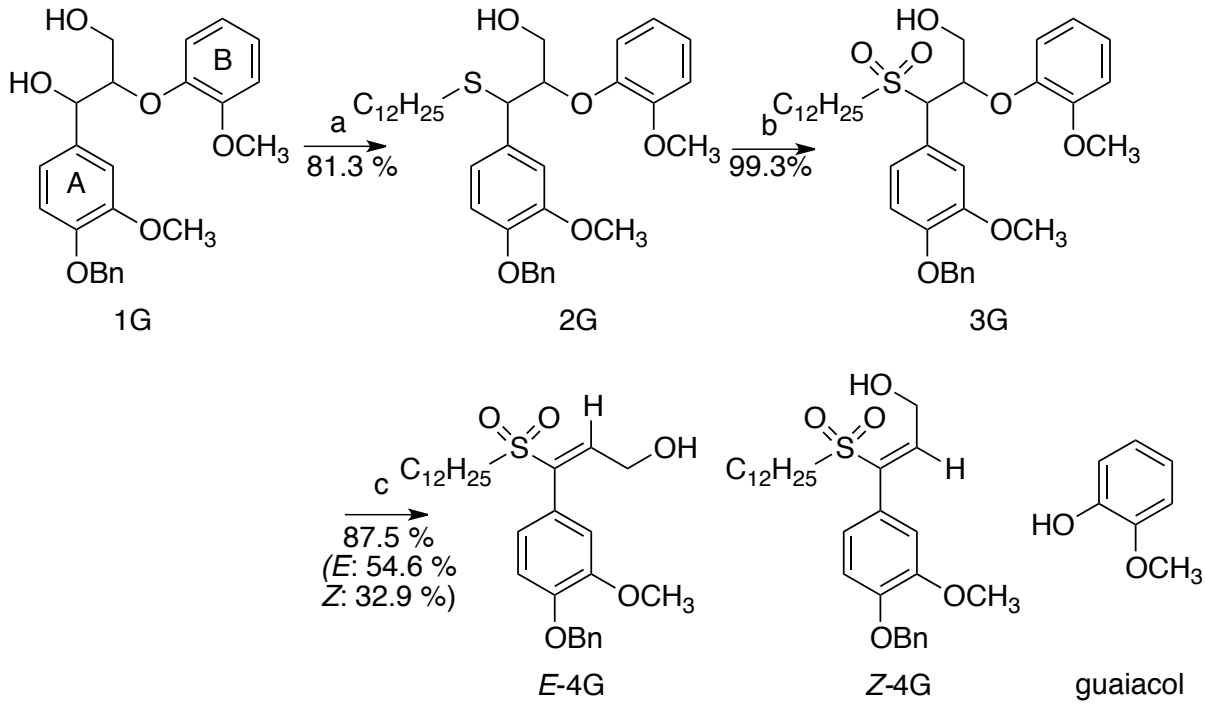

[a] $C_{12}H_{25}SH/BF_3$-Et_2O/CH_2Cl_2/r.t./1h [b] oxone/dioxane:H_2O=9:1/r.t./2h

[c] 0.1M NaOH(dioxane:H_2O=9:1)/r.t./12h

Figure 1-1 α-TSA method

1.2.2 α-TSA method

Figure 1-1 outlines the essential steps of the α-TSA method based on the non-phenolic β-O-4 dimeric model compounds (**1G**). Each reaction product was determined by spectroscopy analyses i.e., IR(Figure 1-2), ^{1}H-NMR(Figure 1-3) and 2D-NOESY-NMR (Figure 1-4).

1.2.2.1 α-Thioetherification

The carbocation formation from *erythro*-**1G** with BF_3-Et_2O in CH_2Cl_2 and the subsequent nucleophilic addition of Dod-SH to the carbocation were proceeded to afford the product **2G** in 81.3 % yield consisting of *erythro* and *threo* isomers. In ^{1}H-NMR spectrum of **2G**, two α-proton peaks attributed to the isomers with 3 to 2 peak area were observed at δ 4.18 and 4.35 ppm, respectively, as shown in Figure 1-3b. The relative configuration of **2G** could not be determined from these ^{1}H-NMR data, but we assumed temporarily at this stage that the former peak at 4.18 ppm with the higher product yield corresponds to *erythro* isomer and the latter peak at 4.35 ppm with lower yield to *threo* one, because an *erythro* isomer is reported to be produced in higher yield than that of *threo* one in the case of nucleophilic addition to the α-position of quinonemethide intermediate having the same sp^2 hybride orbital as the carbocation (Nakatsubo et al. 1976).

After thioetherification, the IR spectrum of **2G** reveals new absorption bands of the alkyl group in the dodecylthioether moiety at 2919 (ν CH) and 2852 (ν CH) cm^{-1} (Figure 1-2b). ^{1}H-NMR spectrum of **2G** is presented in Figure 1-3b. The α-methine proton signal is shifted to upfield (from δ 4.97 ppm to δ 4.18 (*erythro*) and 4.35 (*threo*) ppm) by the electron-donating effect of the thioether. Proton signals of the alkyl group (at δ 0.88, 1.25, 1.50 and 2.37 ppm) from Dod-SH are also visible. The MALDI-TOF MS spectrum of **2G** shows an Na-adduct ion with *m*/*z* $[M+Na]^+$=617.43. These data confirm that the product is the desired α-thioether **2G**; in other words, that a sulfur-carbon (S-C) linkage had definitely formed. In preliminary experiments, this reaction also proceeded with thiols such as

ethanethiol, used in thioacidolysis, and thiophenol as a nucleophile in place of Dod-SH. However, we selected Dod-SH because the experimental work can be carried out without disagreeable odor.

1.2.2.2 Sulfonylation (oxidation)

Oxidation of **2G** consisting of *erythro* and *threo* isomers with 3 to 2 ratio was carried out with oxone in dioxane/ H_2O (9/1) solution and the product **3G**, consisting of two isomers, was obtained in 99.3% yield. The *erythro* and *threo* ratio of the isomers was founded to be 3 to 2 by ^{1}H-NMR spectroscopy, which is the same value as that of **2G**. Naturally, the oxidation on the sulfur atom in **2G** does not alter the relative configuration of **3G**. The isomers of **3G** were easily separated by P-TLC.

The IR spectrum of **3G** reveals one sharp absorption band at 1113 cm^{-1} and another broad band as a shoulder in the range of 1329-1281 cm^{-1} (Figure 1-2c), which correspond to 1160-1120 cm^{-1} (ν_s SO_2) and 1350-1300 cm^{-1} (ν_{as} SO_2) (Silverstein 1967). ^{1}H-NMR spectra of **3G** are presented in Figures 1-3c (*erythro*-**3G**) and 1-3d (*threo*-**3G**). The α-methine proton signal is shifted downfield (from δ 4.18 (*erythro*) to 4.53 (*erythro*) ppm and from δ 4.35 (*threo*) to 4.70 (*threo*) ppm, respectively) by the formation of an electron-withdrawing sulfonyl group at the α-position. The methylene proton in dodecyl group at the α-position of the sulfone structure is also shifted (from δ 2.37 ppm to 2.77 (*erythro*) and 3.27 (*threo*) ppm, respectively). The MALDI-TOF MS spectrum of **3G** shows an Na-adduct ion, with *m*/*z* $[M+Na]^+$=649.05, which corresponds to the calculated values of an Na-adducted **3G** ion. These data support the expectation that the product is exactly converted to the sulfone **3G**.

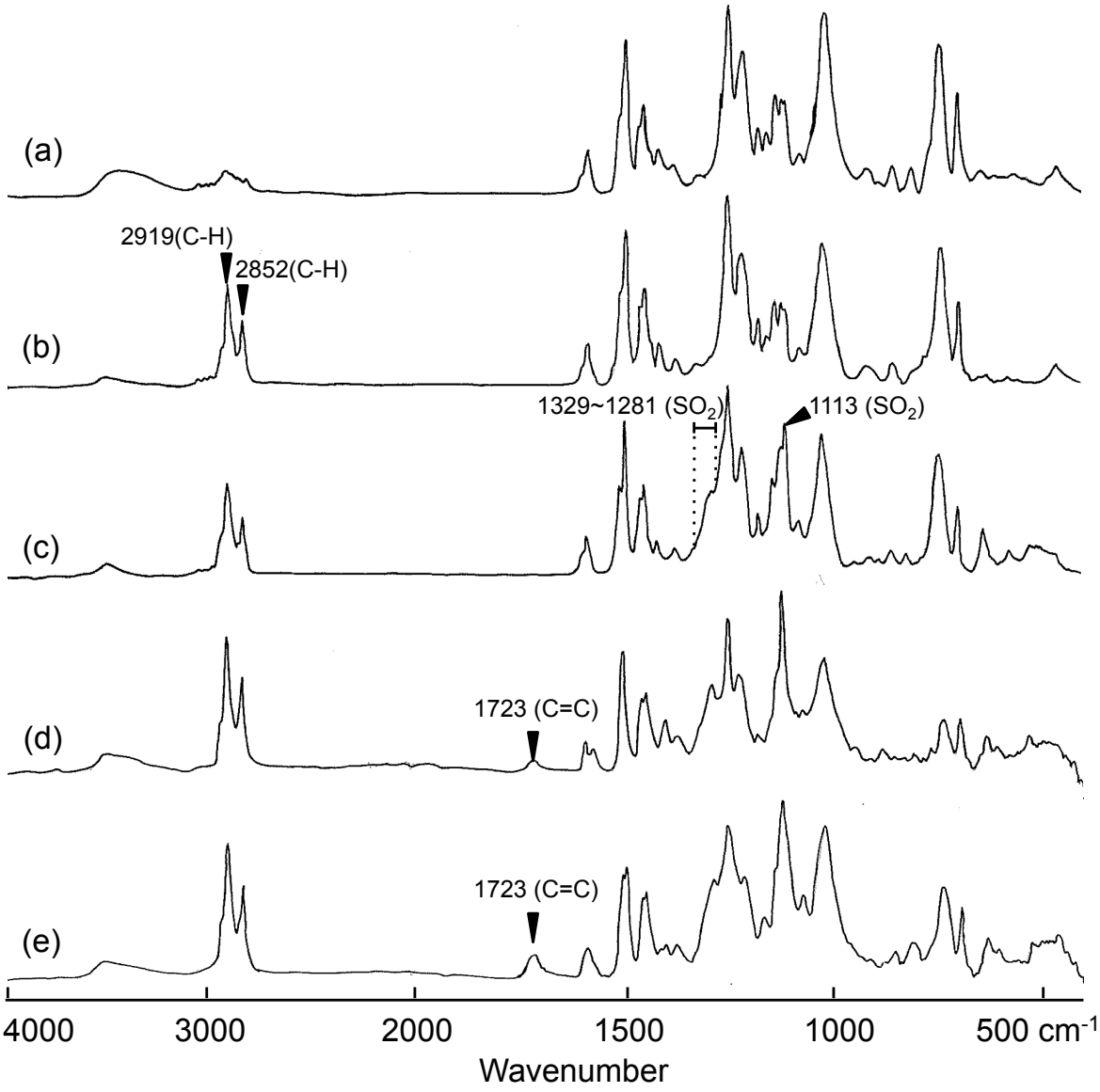

Figure 1-2 FT-IR spectra of compounds (a) **1G**, (b) **2G**, (c) **3G**, (d) *E*-**4G**, and (e) *Z*-**4G**

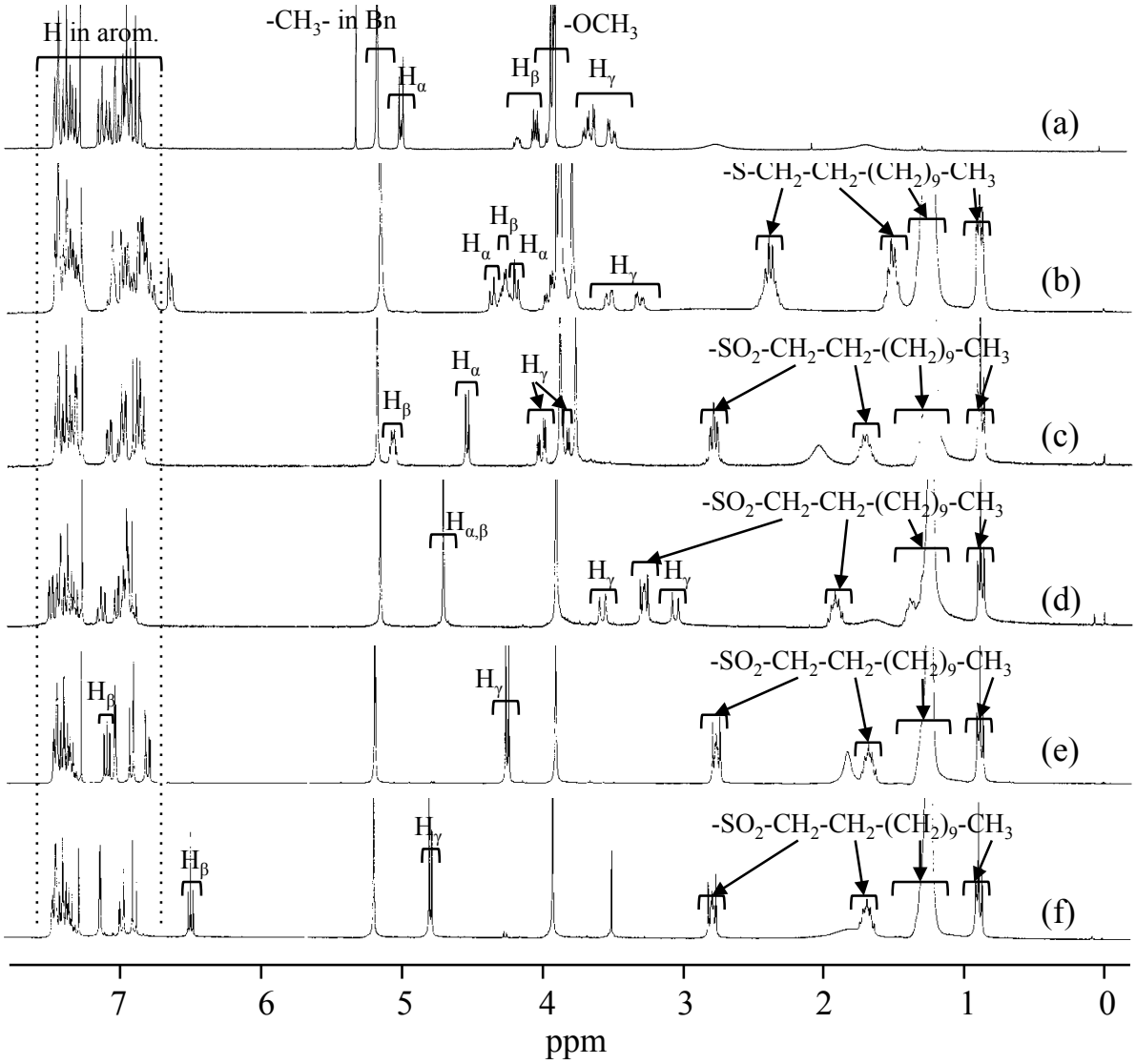

Figure 1-3 ^{1}H-NMR spectra of compounds (a) **1G**, (b) **2G**, (c) *erythro*-**3G**, (d) *threo*-**3G**, (e) *E*-**4G** and (f) *Z*-**4G**

1.2.2.3 Alkali treatment

The α-sulfone **3G** consisting of a mixture of *erythro*- and *threo*- isomers (3/2) was treated with 0.1 M NaOH solution (dioxane/H_2O=9/1) to afford cleanly three products: *E*-**4G**, *Z*-**4G** and guaiacol as expected. On the other hand, the isolated pure *erythro*-**3G** gave only *E*-**4G** and *threo*-**3G** gave only *Z*-**4G**. That is to say, the present elimination reaction was found to proceed completely stereoselectively.

The structure of *E*-**4G** and *Z*-**4G** were determined by the following spectroscopic data. The IR spectra of both *E*-**4G** and *Z*-**4G** revealed a new sharp absorption band of the olefin in the vinyl sulfone structure at 1723 (ν C=C) cm^{-1} (Figure 1-2d and 1-2e). In ^{1}H-NMR spectra shown in Figure 1-3e and 1-3f, signals of the B-ring, which formed guaiacol, and the α-proton signals completely disappeared after the cleavage of β-O-4 linkage. The β-proton (7.08 ppm) of *E*-**4G** appeared at lower magnetic field as compared to that (6.47 ppm) of *Z*-**4G**. On the other hand, the γ-proton (4.24 ppm) of *E*-**4G** is appeared at higher magnetic field as compared to the γ-proton (4.77 ppm) of *Z*-**4G**. Fantoni and Maroñón (1996) reported that the predominant conformation of methyl vinyl sulfone has the C=C bond eclipsed with one of the S=O bonds. Therefore, it is considered that the oxygen of sulfone forms intramolecularily-stabillized hydrogen bond to the β-proton in *E*-**4G** or the γ-proton in *Z*-**4G**, respectively, with this stable eclipsed conformation, resulting in the down-magnetic field shift of these protons. Moreover, in the NOESY-NMR spectrum of *E*-**4G**, the correlation signals of H_γ and H_2, H_6 were observed at 4.24/7.02 and 4.24/6.79 ppm, respectively (Figure 1-4a). By contrast the signals in the NOESY-NMR spectrum of *Z*-**4G** were appeared between H_β and H_5, H_6 at 6.47/6.87 and 6.47/6.96 ppm, respectively (Figure 1-4b). Consequently, these data clearly indicate that *E*- and *Z*-**4G**s exactly have *Entgegen* and *Zusammen* configuration, respectively. Thus, the configuration of **4G**s was determined.

We found that the present elimination reaction proceeds with high stereo-selectivity, that is,

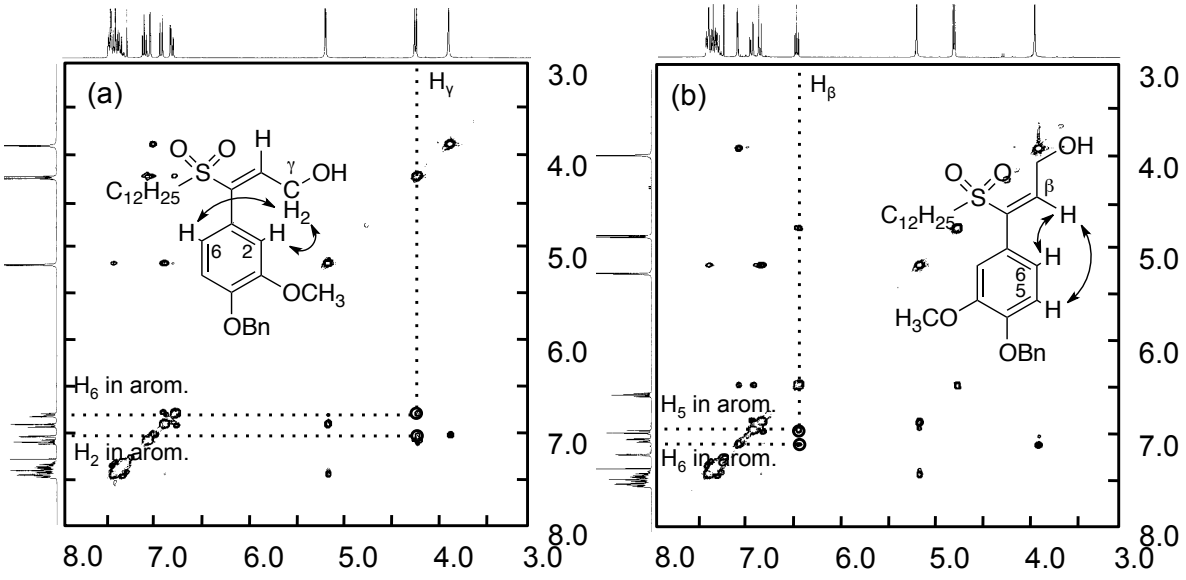

Figure 1-4 NOESY-NMR spectra of (a) *E*-**4G** and (b) *Z*-**4G**

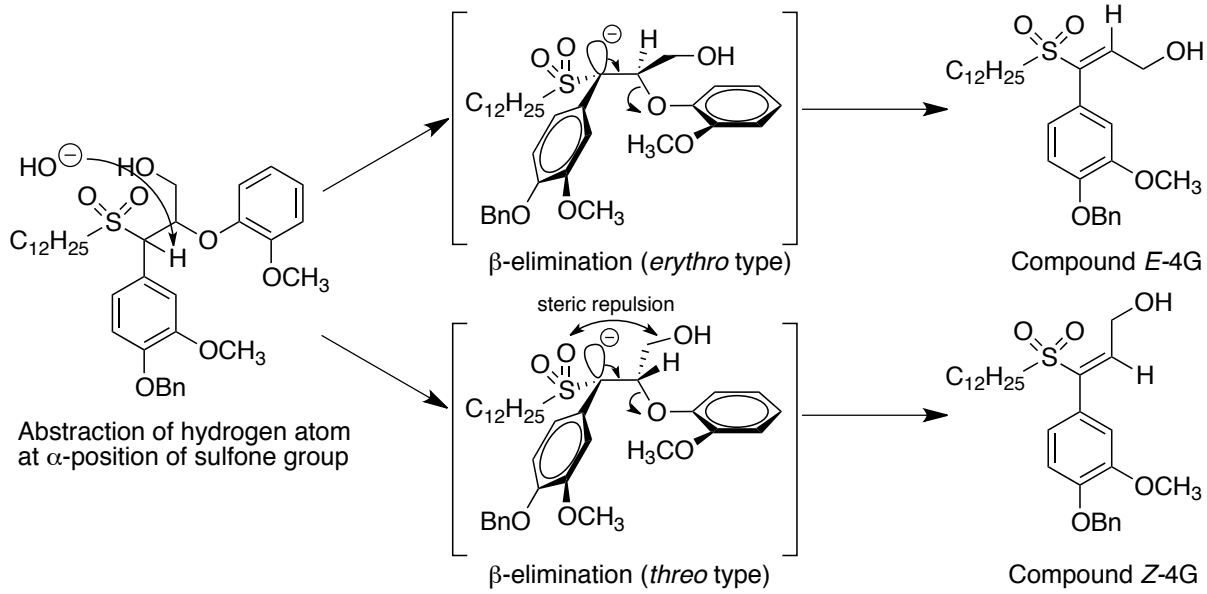

Figure 1-5 Reaction mechanism of β-elimination

one isomer **3G** gives conclusively one isomer of **4G**. Consequently, the *E*-**4G** was obtained only from *erythro*-**3G** and *Z*-**4G** only from *threo*-**3G** via transition state shown in Figure 1-5. The present elimination reaction was thought to proceed by E1cB mechanism via preferred anti-periplanar conformation, i.e., it is reasonable to explain that the reaction takes place with anti-periplanar arrangement that α-hydrogen atom and β-phenoxy group depart from opposite sides of the molecule in the same plan as shown in Figure 1-5.

Thus, it was confirmed that our assumption that *erythro*/*threo* configuration of **2G** and **3G** described in the previous section "α-thioetherification" in this report was exactly right as expected.

1.2.2.4 Monitoring of the β-elimination reaction

The monitoring experiments with **3G** by HPLC were carried out under the mild alkaline condition to understand the reaction process in more detail. It was found that this reaction is a clear reaction, i.e., any byproducts were never seen in the HPLC chromatograms (Figure 1-6). Figure 1-7 illustrates the yields of **3G**, *E*-**4G**, *Z*-**4G**, and guaiacol as a function of the degradation time. Starting material **3G** gradually decreased and completely disappeared after 6 h, whereas the yield of guaiacol increased and became constant after 6 h. Moreover, the yield of *E*-**4G** increased rapidly and the yield of *Z*-**4G** increased gradually, then, both yields became constant after 6 h.

The difference of the reaction rate between *erythro*- and *threo*-**3G**s can be explained from the β-elimination reaction mechanism. The elimination proceeds via *anti*-periplanar of E1cB elimination as described above. In the case of *threo*-**3G**, a steric repulsion between the sulfone group and the hydroxymethyl group interrupt a desirable *anti*-periplanar conformation (Figure 1-5), but no such steric repulsion in the case of *erythro*-**3G**, resulting in the slower reaction rate of the *threo* isomer than that of *erythro* one.

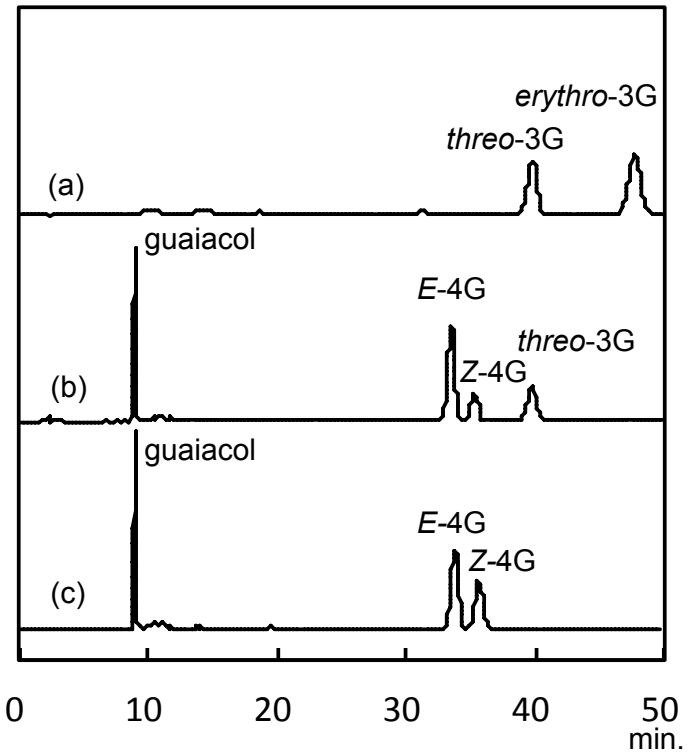

Figure 1-6 HPLC chromatograms with (a) **3G**s, (b) the reaction mixture after 1h, and (c) the reaction mixture after 12h

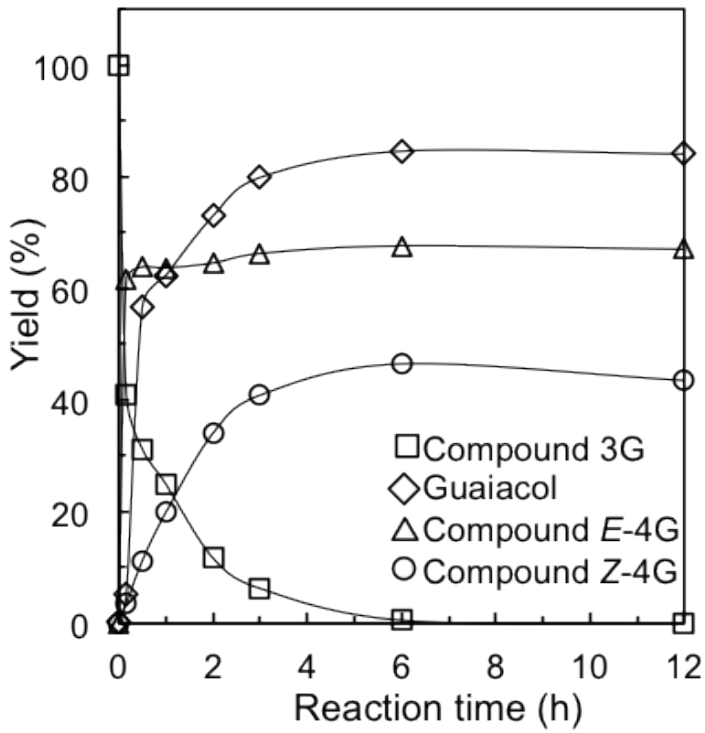

Figure 1-7 Mild alkali treatment of **3G** in 0.1 M NaOH solution (dioxane/H_2O=9/1)

1.3 Summary

The three-step α-TSA method, consisting of α-thioetherification, sulfonylation, and mild alkali treatment, afforded the expected products in high yields. The α-sulfone derivative promoted the mild alkali degradation efficiently. Accordingly, the cleavage reaction is initiated from the α-position and the reaction proceeds with only a weak alkali solution and not an acid catalyst as is the case in former methods (acidolysis, thioacidolysis, and DFRC etc.). The advantage of the method is that side reactions don't proceed in the mild alkali treatment. The α-TSA method may be useful for the chemical structural analysis of lignin. The results suggested that the sulfone group at neighboring carbon of β-O-4 linkage promoted the cleavage of β-O-4 linkage under the mild alkali condition.

Chapter 2

Development of selective lignin degradation method, named γ-TTSA method, for Lignin-Carbohydrate-Complex (LCC) bonding site isolation -dimer model experiment-

2.1 Introduction

The elucidation of structures in lignin-carbohydrate complexes (LCCs) is a challenge in lignin chemistry. Several chemical bonds have been proposed to be prevalent between lignin and polysaccharides, such as phenyl glycoside, benzyl ester, and benzyl ether linkages (Watanabe 1995; Koshijima and Watanabe 2003; Lawoko et al. 2005; Balakshin et al. 2007, 2011). However, to the authors' knowledge, direct isolation of the binding sites in LCCs has not yet been reported. Degradation methods are also sought that lead to the retention of the bonds in the α-position, to obtain direct proof for the chemical structure of LCCs.

It is well-known that β-O-4 linkage is the most abundant linkage in lignin (Higuchi 2006). Therefore, a new degradation method must focus on the cleavage of this linkage. The known methods in this regard are acidolysis (Lundquist 1992), thioacidolysis (Lapierre et al. 1986; Roland et al. 1992), and the DFRC method (Lu and Ralph 1997a,b). These afford information about the number of β-O-4 linkages and substituents at the γ-position (Ralph and Lu 1998; Holtman et al. 2003). However, information about α-linkages of the C6-C3 basic units, postulated to be abundant in LCCs (Enoki et al. 1983), is lost in the course of the chemical reactions.

In chapter 1, the novel lignin degradation method, called α-TSA method, was reported. In the method, the final cleavage reaction under the mild condition proceeds without side reactions, unlike the conventional methods. The key of this reaction is that the ether-cleavage is assisted by the neighboring sulfonyl group at α-position of ether linkage. However, in the first step, the information of α-functional groups in lignin is disappeared for a nucleophilic substitution of thiol to carbocation at α-position as is

the case with the conventional methods. Accordingly, a selective degradation for β-O-4 linkages with the retention of α-linkages would be sought for LCC research.

The methods, in which α-linkages are intact, were reported. These methods are Katahira's TIZ method and Matsumoto's lignin degradation method. In these methods, the cleavage of β-O-4 linkage is assisted by functional groups, introduced to γ-position of β-O-4 substructure in the derivatization.

Katahira et al. (2003) proposed the so-called TIZ method for the cleavage of β-O-4 linkages, consisting of the reaction steps: (1) γ-tosylation, (2) substitution reaction with iodine, and (3) reduction cleavage by zinc powder. The reactions are carried out under almost neutral conditions and the β-O-4 cleavage initiated from the γ-position retains some information about the α-linkage (Katahira et al. 2006). However, a disadvantage in this reaction chain is the solid state of the zinc powder as the catalyst. This circumstance is problematic if the splitting is applied to native lignin or wood, because the heterogeneous catalysis may reduce the reactivity significantly. A soluble catalyst working under mild conditions is sought.

Matsumoto et al. (1980, 1982) developed four-step β-O-4 linkage degradation: (1) γ-tosylation, (2) substitution reaction with iodine, (3) substitution reaction with sulfinate (sulfinylation), and (4) mild alkali degradation. Here, the key reaction (cleavage of β-O-4 linkage) was effected by mild alkali (NaOH) splitting the ether bond in the presence of an electron-withdrawing sulfinyl group at the γ-position. The key reaction proceeded easily and afforded the cleaved product in high yield. However, an unexpected sulfinyl derivative was found, which was characterized by infrared (IR) analysis. In this case, sulfinyl compound was obtained by the substitution of γ-iodine model compound in the presence of sodium *p*-toluenesulfinate, although another paper showed that sulfone compound is obtained in high yield with substitution of a bromo compound with the reagent (sodium *p*-toluenesulfinate) (Lenihan and Shechter 1998). It is unknown whether the degradation of ether bond was assisted by a sulfinyl or

sulfonyl group at the γ-position of lignin, as it was not possible to distinguish between sulfinyl and sulfonyl groups using the IR data.

Therefore, the introduction of a sulfonyl group to the γ-position seemed to be attractive for a new degradation method for the isolation of the binding sites of LCC. Lindberg and Lundström (1966) found that the ether bond (C1-O-C5) in methyl 6-deoxy-6-*p*-tolylsulfonyl-β-D-glucopyranoside is cleaved under weakly alkaline conditions. The substructure of the glucopyranoside is similar to that of β-O-4/γ-sulfone lignin, because a sulfonyl group is introduced in the neighboring primary carbon of the ether bond. This report suggests that β-elimination is also assisted by a sulfonyl group in the γ-position. Moreover, based on the result of chapter 1, the β-O-4 linkage is also expected to be cleaved by the neighboring sulfonyl group at the γ-position of β-O-4 substructure.

In this chapter, an alternative β-O-4 linkage degradation method, named as γ-TTSA method, is proposed via a γ-sulfone intermediate, which consist of four reactions: (1) γ-tosylation (T), (2) thioetherification (substitution reaction with thiol) (T), (3) sulfonylation (oxidation) (S), and (4) mild alkali degradation (A) (Figure 1), i.e., the γ-TTSA reaction chain. The reactions (the substitution reaction and oxidation) are selected to synthesize a γ-sulfone derivative with a defined structure. It is demonstrated that γ-TTSA method can degrade β-O-4 linkage without reactivity loss in representative lignin model compounds, quantitatively.

2.2. Results and discussion

2.2.1 Strategy

In Chapter 1, it was described that the β-O-4 linkage with the sulfone at α-position was easily cleaved under the mild alkali condition and β-elimination reaction of sulfone compound was effective in degrading lignin. In this chapter, the introduction of sulfone group to the γ-position of β-O-4 substructure was tried.

Tosyl group is well used as a leaving group and has the reaction selectivity for its bulkiness in its introduction. The only primary hydroxyl groups at γ-position were converted to tosyl group in tosylation of lignin, such as previous reports (Freudenberg1949, Matsumoto et al. 1980, Katahira et al. 2006). Then, it is expected that the subsequent substitution of thiol and oxidation of sulfur atom cause to introduce a sulfone group selevitvely to the γ-position.(Scheme 2)

Therefore, a series of the TTSA reaction, tosylaiton, thioetherification, sulfonylation with oxidation and cleavage of β-O-4 linkage under alkali treatment was attempted (Figure 2-1).

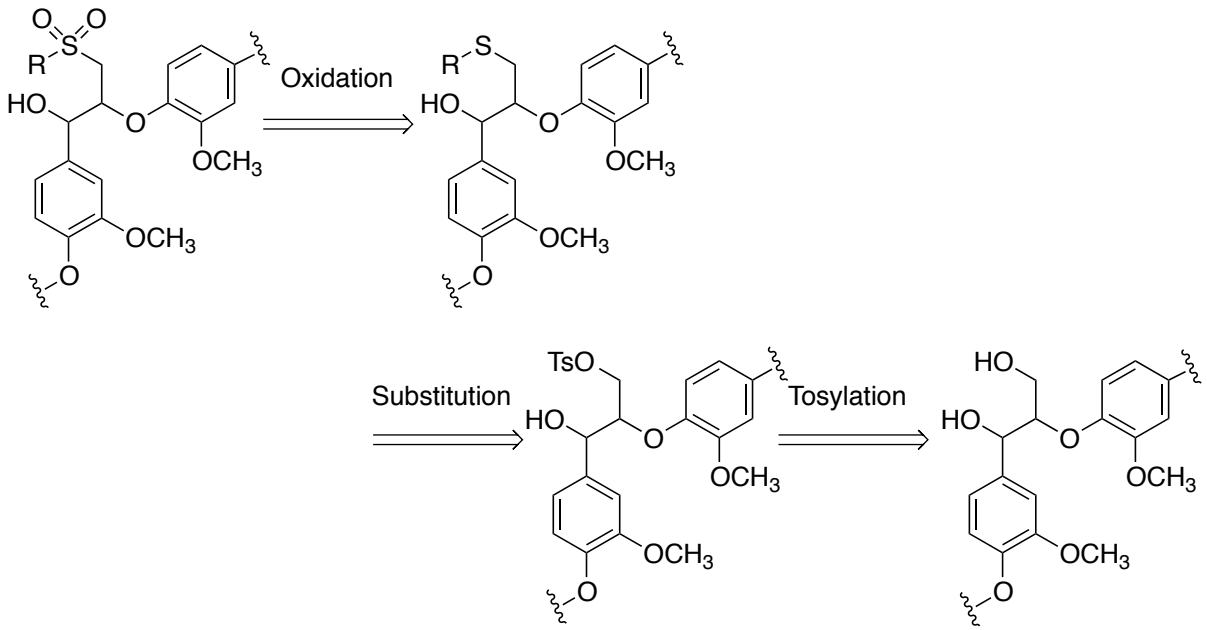

Scheme 2 Retro-synthesis of a sulfone structure at γ-position of β-O-4 substructure

2.2.2 γ-TTSA method

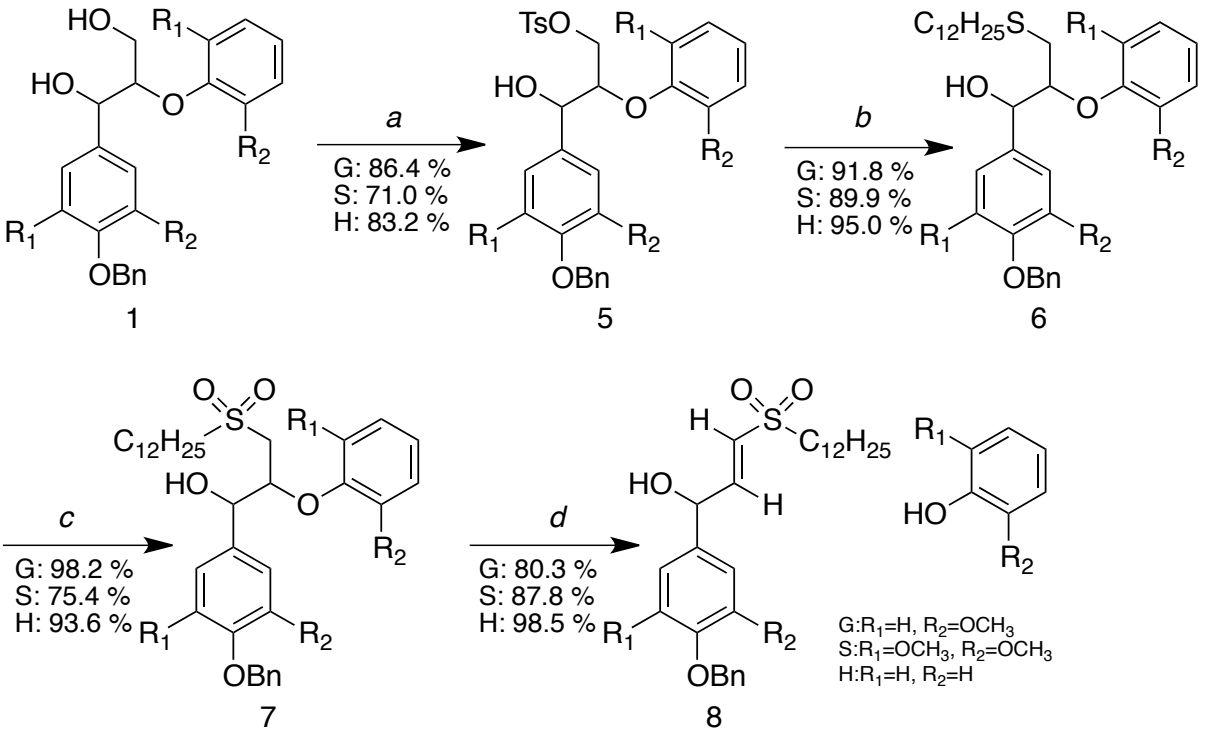

[a]Ts-Cl/pyridine/r.t./over night, [b]Dod-SH/K_2CO_3/KI/acetone/reflux/over night,

[c]MCPBA/dioxane:H_2O=9:1/r.t./2h, [d]0.03 M NaOH (dioxane:H2O=9:1)/r.t./2h

Figure 2-1 γ-TTSA method

2.2.2.1 γ-Tosylation

The tosylation of **1G**, **1S**, and **1H** with tosyl chloride and pyridine was conducted according to Katahira et al. (2003), for 5 h, and the substances **5G**, **5S**, and **5H** were obtained in 86.4%, 71.0%, and 83.2% yields, respectively.

2.2.2.2 Thioetherification

Thiols are effective nucleophiles for the substitution at saturated carbon atoms, but the experimental work is aggravated by their very disagreeable odor, like ethanethiol for thioacidolysis for lignin degradation. Node et al. (2001) reported that the foul smell of thiols toward the human olfactory cell is

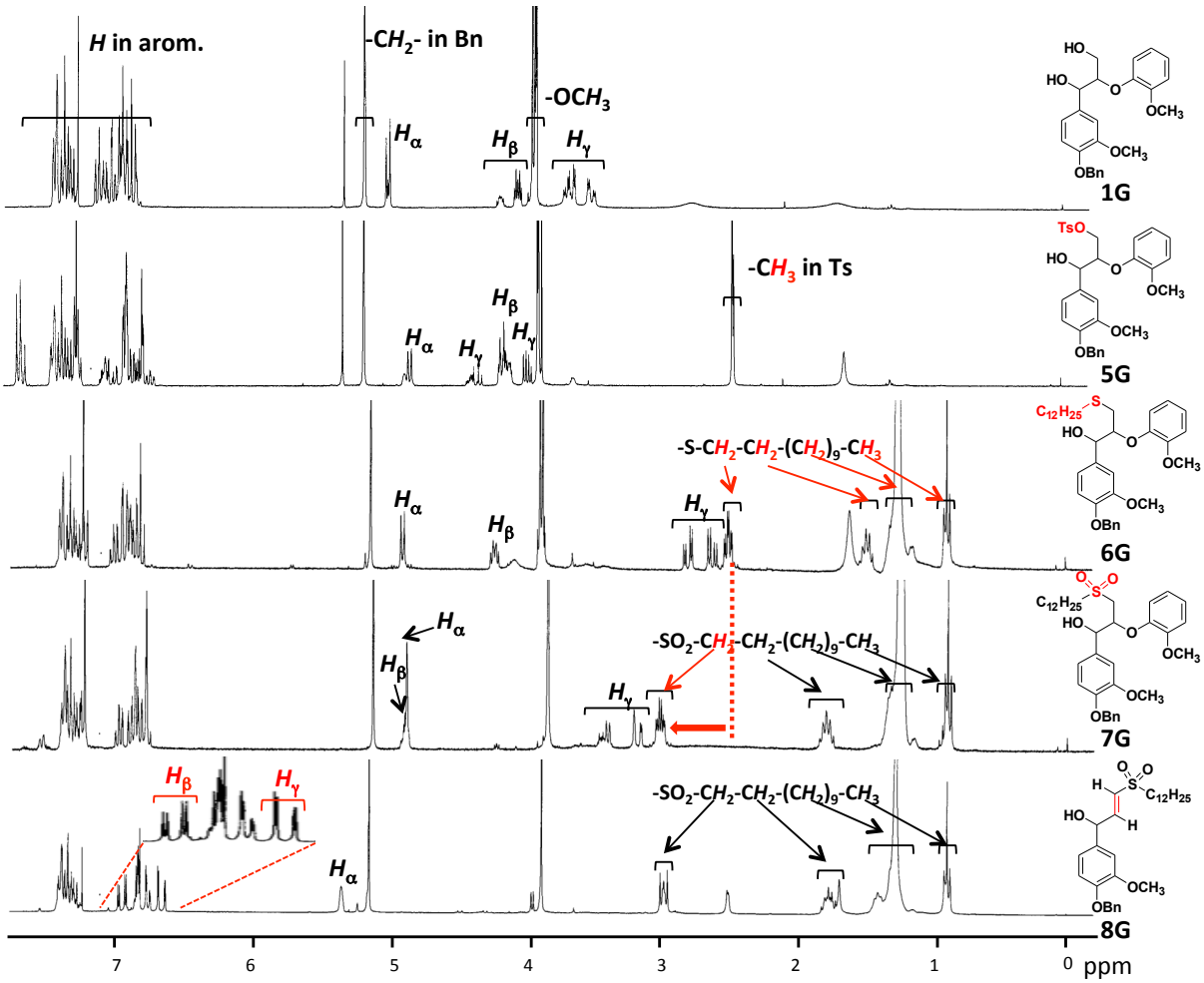

Figure 2-2 ^{1}H-NMR spectra of compounds **1G**, **5G-8G**.

related to the length of its carbonchain; and Dod-SH, with 12 tandem-linked carbons, was found to be odorless compared to the commonly used malodorous thiols. The introduction of a long alkyl group may improve the solubility of the intermediates. This is the reason why Dod-SH was selected as a nucleophile.

The nucleophilic substitution of **5G** with Dod-SH was conducted in the presence of K_2CO_3 in acetone under reflux overnight without a bad odor to afford the product **6G** in 91.8% yield. Product **6G** was identified by several spectroscopic analyses. ^{1}H-NMR spectra of **5G** and **6G** are shown in Figure 2-2. After the substitution reaction with Dod-SH, the methyl signals (at δ 2.40 ppm) and aromatic signals (at δ 7.21–7.28, δ 7.63–7.70 ppm) derived from the tosyl group have disappeared. The γ-methylene proton

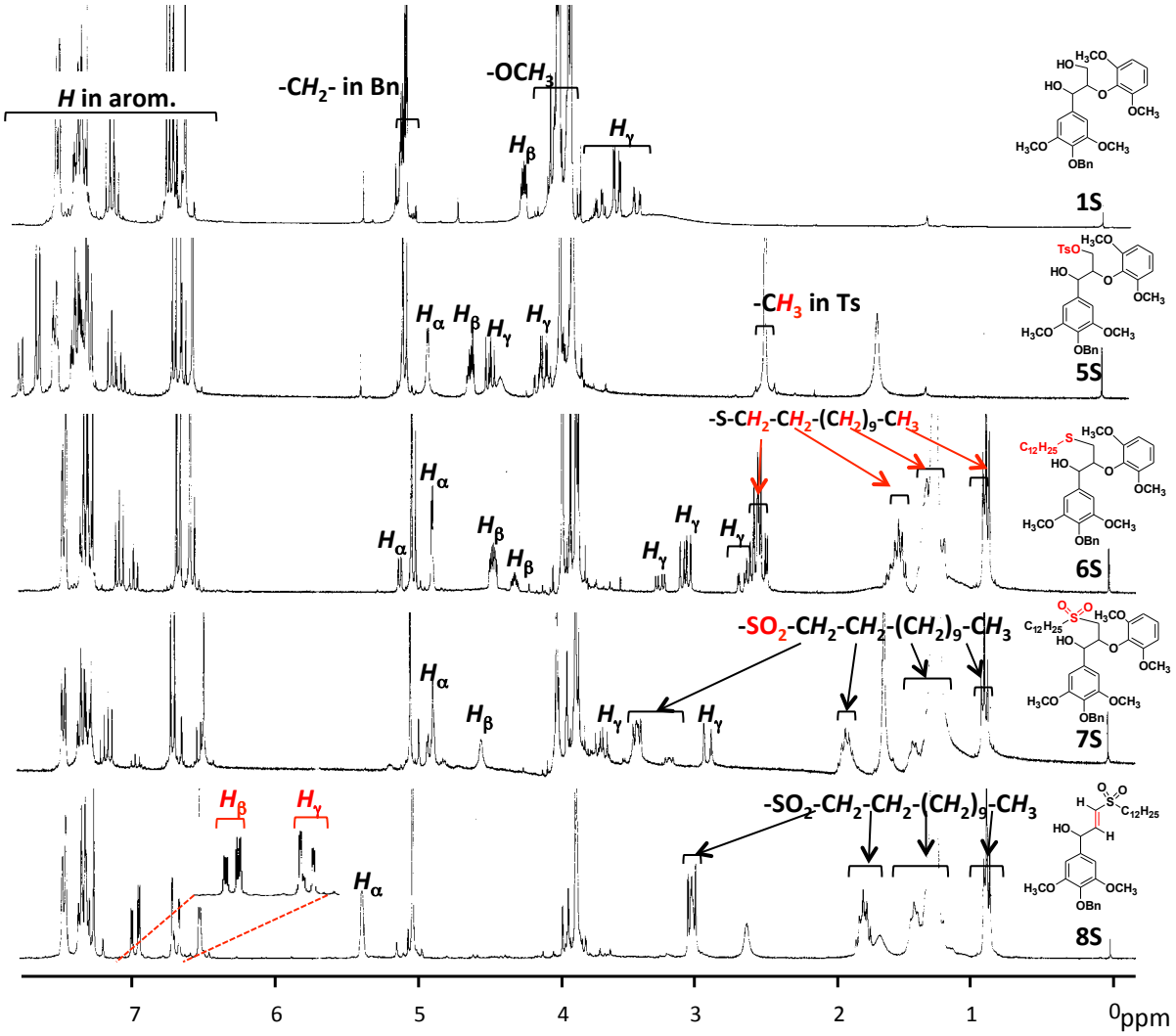

Figure 2-3 ^{1}H-NMR spectra of compounds **1S**, **5S-8S**.

signals are shifted to the upfield (from δ 4.07 and 4.31 ppm to δ2.61 and 2.79 ppm) by the electron-donating effect of the thioether. Proton signals of the alkyl group (at δ 0.89, 1.25, 1.47, and 2.49 ppm) from Dod-SH are visible. The MALDI-TOF MS spectrum of **6G** shows an Na-adduct ion with *m/z* $[M+Na]^{+}$=617.62. These data confirm that the product is the desired thioether **6G**; in other words, that a sulfur-carbon (S-C) linkage had definitely formed. The nucleophilic substitution of **5S** and **5H** with Dod-SH also proceeded to give the corresponding thioethers in high yields, namely **6S** and **6H**, which were identified by ^{1}H-NMR spectra [Figure 2-3 (6S) and Figure 2-4 (6H)] and MALDI-TOF MS (experimental section).

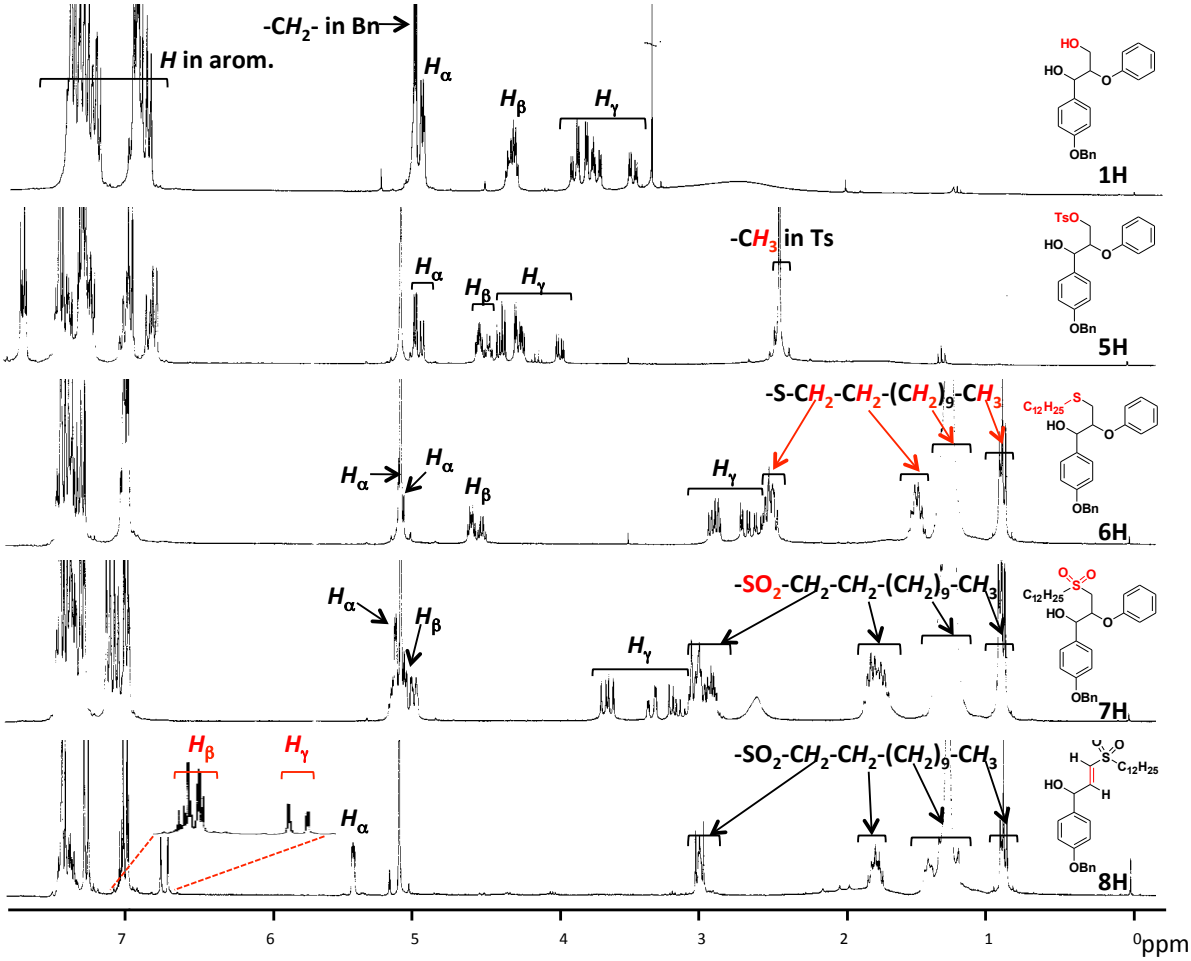

Figure 2-4 ^{1}H-NMR spectra of compounds **1H**, **5H-8H**.

2.2.2.3 Sulfonylation (oxidation)

Oxidation of **6G** was carried out with *m*-chloroperbenzoic acid (MCPBA) in dioxane/ H_2O (9/1) solution for 3 h and the product **7G** was obtained in 98.2% yield. The oxidation was found to proceed step by step, i.e., first the oxidation of thioether to sulfoxide occurred and subsequently the sulfoxide converted to sulfone. TLC analysis was helpful with this regard, e.g., **6G** (Rf-value: 0.5) was quantitatively converted to sulfoxide (Rf-value: 0.1) with one equivalent of MCPBA and then **7G** (Rf-value: 0.3) with another equivalent of the reagent. Similar results have been reported for the oxidation of dehydroepiandrosterone (William and Boehm 1995). Product **7G** was identified by

spectroscopic analyses. ^{1}H-NMR spectra of **6G** and **7G** are presented in Figure 2-2. The signals from the methylene protons at the γ-position of the product are shifted downfield (from δ 2.61 and 2.79 ppm to δ 2.76 and 3.65 ppm) by the formation of an electron-withdrawing sulfone group at the γ-position. The MALDI-TOF MS spectrum of **7G** shows an Na-adduct ion, with m/z $[M+Na]^{+}$=649.52, which corresponds to the calculated values of an Na-adducted **7G** ion. The IR spectrum of **7G** reveals one sharp absorption band at 1122 cm^{-1} and another broad band as a shoulder in the range of 1320–1290 cm^{-1}, which correspond to 1160–1120 cm^{-1} (ν_s SO_2) and 1350–1300 (ν_{as} SO_2) (Silverstein 1967). These data support the expectation that the product is converted to the sulfone **7G**. Oxidation of **6S** and **6H** was also performed in the same manner as **6G** to give **7S** and **7H**, the structures of which were confirmed by ^{1}H-NMR [Figure 2-3 (**7S**) and Figure 2-4 (**7H**)], MALDI-TOF MS, and FT-IR data (experimental section).

2.2.2.4 Alkali treatment

γ-Sulfone **7G** was treated with 0.03 M NaOH solution (dioxane/H_2O=9/1) to afford two main products: **8G** and guaiacol. Product **8G** was spectroscopically identified. ^{1}H-NMR spectra of **7G** and **8G** are presented in Figure 2-2. The signals of the B-ring, which formed guaiacol, have disappeared. The γ- and β-olefinic proton signals of **8G** appear at δ 6.69 (dd, J=15.2 and 1.8) and δ 6.98 ppm (dd, J=15.2, 3.3), indicating *entgegen* (*E*)-configuration of the double bond. The MALDI-TOF MS spectrum of **8G** indicates a Na-adduct ion with m/z $[M+Na]^{+}$=525.26, which is the molecular weight of the desired compound **8G**. The formation of **8G** and guaiacol proves that the desired alkali degradation took place, i.e., the electron-withdrawing sulfonyl group induced β-elimination from both the γ-position and the α-position.

The monitoring experiments with **7G** were carried out under mild alkaline conditions to understand the reaction in detail. HPLC was more helpful than TLC as a separation method, because

the Rf-values of the starting material **7G** and product **8G** were almost the same in TLC analysis. Figure 2-5a illustrates the changing yield of **7G**, **8G**, and guaiacol as a function of the degradation time. Starting material **7G** rapidly decreased and was completely consumed after 2 h, whereas the yields of product **8G** and guaiacol were increased and maintained after 2 h, at 70% and 80%, respectively. At reaction times longer than 2 h, the yield of **8G** gradually decreased, but the yield of guaiacol increased slightly. This is a hint that **8G** is not stable under the alkaline conditions, and that long reaction times are not favorable in this step.

Mild alkaline degradations of **7S** and **7H** with 0.03 M NaOH solution (dioxane/H_2O=9/1) were found to give the two main products, **8S** and 2,6-dimethoxyphenol, **8H** and phenol as well as **7G** **8S** and **8H** were found only as *E*-isomers by ^{1}H-NMR analysis [Figure 2-3 (**8S**), Figure 2-4 (**8H**)], which was also the case for **8G**, indicating that both *erythro* and *threo* isomers gave only unsaturated sulfone with an *E*-configuration by the reaction. Figure 2-5 (b,c) shows the time-course changing of the yields of starting materials and products of the degradation reaction of **7S** and **7H**, respectively. The behavior of **7S** and **7H** was the same as that of **7G**, that is, the starting materials were almost consumed after 2 h. After more than 2 h, the yield of **8S** was decreased to some extent, whereas that of **8H** was nearly stable. Clearly, **8S** and **8H** are not as stable as **8G** under the conditions tested, and **8S** is the most unstable among them. The degradation of **7S** and **7H** with 0.03 M NaOH solution (dioxane/H_2O=9/1) for 2 h gave **8S** and **8H** in 63.4% and 82.5% yields, respectively. Thus, β-O-4 linkages in **7G**, **7S**, and **7H** were found to be easily cleaved under mild alkaline conditions to give *E*-unsaturated sulfones 8G, **8S**, and **8H**, respectively, in high yields. The side reactions of **8G**, **8S**, and **8H** after more than 2 h reaction time remain to be investigated. It is confirmed that β-elimination beginning from the γ-position proceeded efficiently under the weakly alkaline conditions in the three types of lignin model compounds.

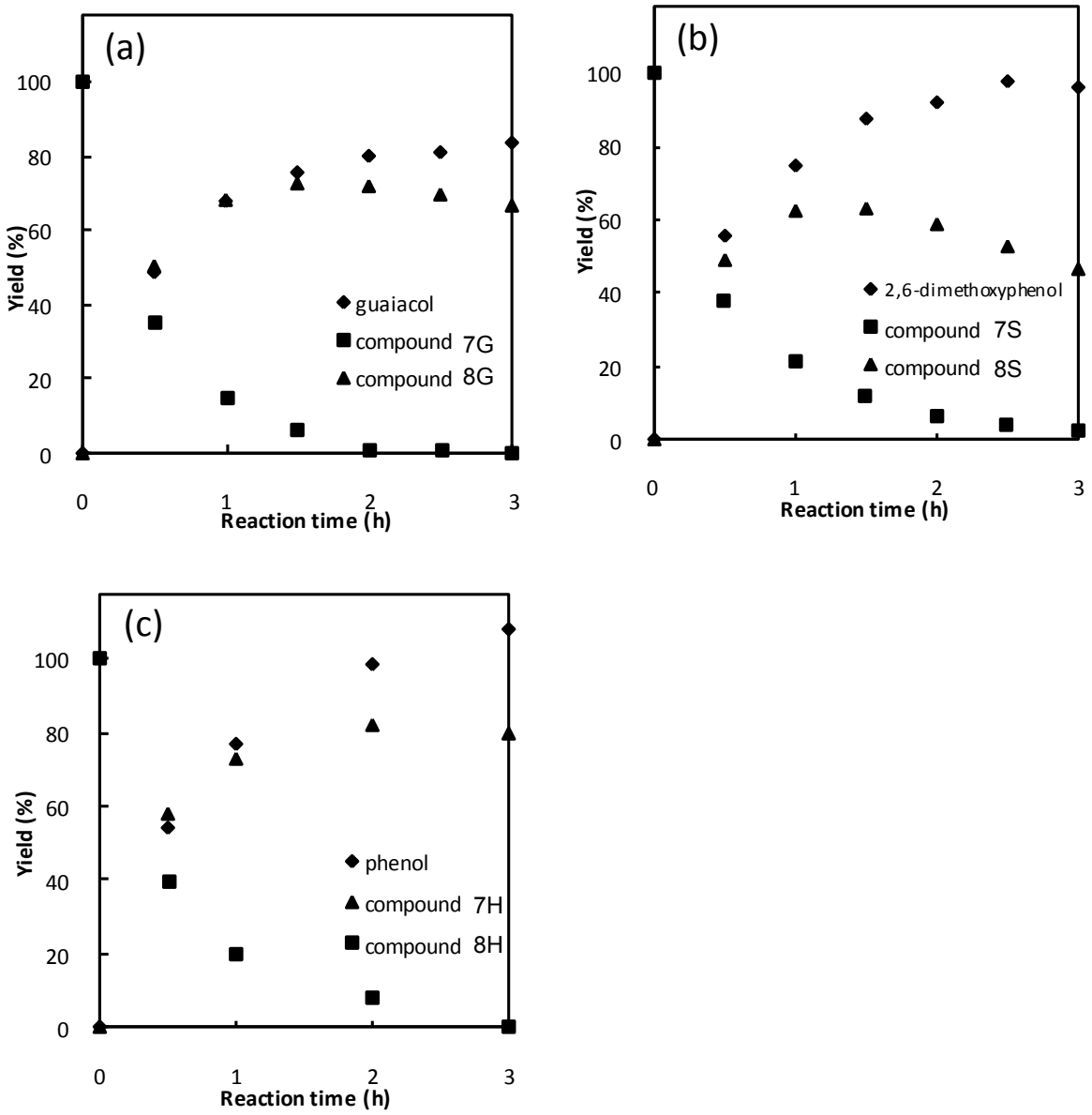

Figure 2-5 Alkali treatment of (a) **7G**, (b) **7S**, and (c) **7H** in 0.03 M NaOH solution (dioxane/H_2O=9/1).

2.3 Summary

The four-step γ-TTSA method, consisting of γ-tosylation, thioetherification, sulfonylation, and mild alkali degradation, afforded the expected products in high yields. The γ-sulfone derivatives promoted the mild alkali degradation efficiently, which can be explained by the electron-withdrawing effect of the sulfone group that assists the cleavage of ethers in both the γ- and α-positions of lignin model compounds. Accordingly, the cleavage reaction is initiated from the γ-position and the reaction needs only a weak alkali solution and not a solid catalyst as was the case in former experiments. The advantage of the method is that the structures at the α-position are kept. The γ-TTSA method may be useful for the analysis of LCCs, where the α-position of lignin is involved in linkages to polysaccharides.

Chapter 3

Development of selective lignin degradation method, named γ-TTSA method, for Lignin-Carbohydrate-Complex (LCC) bonding site isolation -polymer model experiment-

3.1 Introduction

Lignin is the second biomacromolecule as natural organic materials. Its structure is built of phenylpropanoid units, linked with various types of ether and carbon-carbon bonds. Of these, β-O-4 linkage is the most abundant linkage in lignin (Higuchi 2006). However, the other linkages, such as β-5 and β-β linkages, account for about 50%. Therefore, the lignin's chemical structure has not yet been completely elucidated. Moreover, it is difficult to evaluate its reactivity.

A so called dehydrogenation polymers (DHPs) are widely used as model lignin polymers for investigating the structure, reactivity and properties of native lignins, although structural differences between DHPs and native lignins such as milled wood lignin (MWL) have pointed out. It is reported that DHPs contain β-O-4, β-5, β-β substructures, olephinic end sturucture and α-O-4 linkages (Terashima et al. 1995, 1996). Moreover, DHPs are prepared easily by the hydrogenation of monolignols such as coniferyl alcohol and various structural DHPs can be obtained by changing the circumstance of polymerization.

In Chapter 2, γ-TTSA method for LCC analysis, that was able to cleave β-O-4 linkages selectively, was developed. The method consists of four reaction steps, namely, tosylation (T), thioetherification (T), sulfonylation (S) and mild alkali treatment (A). The β-O-4 linkage was cleaved without the reaction involving the carbocation at α-position in the method and LCC bonding sites such as benzyl ether linkage might be intact after the TTSA treatment. But the applicability of the method to the more complex lignin macromolecule was not yet tested. Therefore, the influence of other linkages and the reactivity of polymer under the application of γ-TTSA method are needed to investigate.

More precisely, the degradation behavior of a lignin polymer model, a so-called dehydrogenation polymer (DHP, prepared from coniferyl alcohol), by the γ-TTSA method (Figure 3-1) is described in this chapter.

3.2 Results and discussion

In chapter 1 and 2, it was possible to follow easily each reaction with ^{1}H-NMR spectroscopy because the side-chain signals of the models were well separated. In case of a polymer model (DHP), however, the side-chain signals are broad and overlapping, both in the ^{1}H-NMR and in the ^{13}C-NMR spectra. The 2D-NMR method, in which the correlation between ^{1}H and ^{13}C atoms directly bonded to each other is visible, is helpful in this regard (Ralph et al. 1999, 2004; Capanema et al. 2001, 2004, 2005; Balakshin et al. 2003; Ibarra et al. 2007). The quantitative distribution of the main substructures in

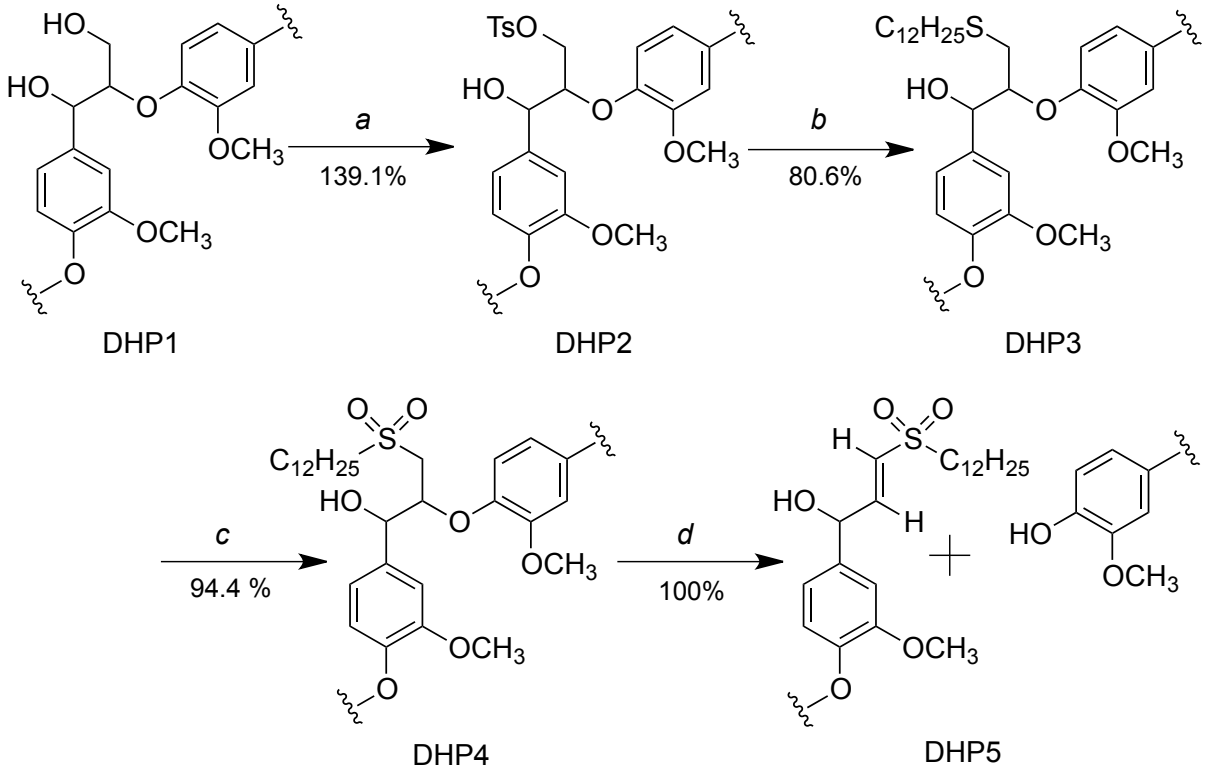

[a] Ts-Cl/dry pyridine/r.t./5h, [b] Dod-SH/K_2CO_3/DMF/70°C, [c] oxone/dioxane:H2O=9:1/r.t./3h, [d] 0.03M NaOH (dioxane:H_2O=9:1)/25°C/2h

Figure 3-1 Application of γ-TTSA method to dehydrogenation polymer (**DHP1**)

lignins have been evaluated by HSQC-NMR, which is one of the 2D-NMR techniques (Heikkinen et al. 2003; Ralph et al. 2006; Ibarra et al. 2007; Zhang and Gellerstedt 2007). Therefore, each reaction step of the method will be followed by Fourier transform infrared (FT-IR) spectrometry and heteronuclear single quantum coherence nuclear magnetic resonance (HSQC-NMR) analysis.

3.2.1 Preparation of Dehydrogenation Polymer (DHP)

The double bond moieties (in *E* configuration) of the terminal cinnamyl alcohol groups of the DHP were hydrogenated to give hydrogenated DHP (**DHP1**) to avoid overlapping of the Hγ/Cγ correlation signals of cinnamyl alcohol with those of the β-O-4 and β-5 substructures appearing at 3.4–4.1/60–62 ppm. The number average molecular weight (*Mn*=2900) and the dispersion (*Mw*/*Mn*=1.71, where *Mw* is the weight-average molecular weight) of the acetylated **DHP1** were determined by GPC.

The FT-IR spectrum of **DHP1** is shown in Figure 3-2b. Both the stretching vibration band at 1656 cm^{-1} (ν C=C) and the bending band at 965 cm^{-1} (δ C=C) of the DHP almost disappeared after the hydrogenation (Figure 3-2 a and b). The HSQC-NMR spectrum of **DHP1** is presented in Figure 3-3a. Cross-signals were assigned on the basis of published data (Ralph et al. 2004, Rencoret et al. 2008). The main side-chain assignments are listed in Table 3-1. The Hα/Cα, Hβ/Cβ, and Hγ/Cγ signals of the β-O-4 substructure are at 4.75/71.2, 4.26/84.2, and 3.41, 3.63/59.9 ppm, respectively. The Hα/Cα, Hβ/Cβ, and Hγ/Cγ signals of the β-5 substructure are visible at 5.45/86.6, 3.45/53.2, and 3.68/62.8 ppm, respectively, whereas the Hα/Cα, Hβ/Cβ, and Hγ/Cγ signals of the β-β substructure are observable at 4.51/82.9, 3.04/53.4 and 3.75, 4.15/70.8 ppm, respectively. The Hα/Cα signals of the α-O-4 substructure are at 5.41/79.1 ppm. The relative percentages of the main linkages (β-O-4, β-5, and β-β) in **DHP1** were calculated from the Hα/Cα correlation peak area by the method described by Rencoret et al. (2008) to be 28%, 50%, and 22%, respectively. The Hγ/Cγ signal of the cinnamyl alcohol moiety still appears at 4.10/61.4 ppm because of the incomplete hydrogenation, but the signal was well separated.

3.2.2 Application of γ-TTSA method to DHP1

The γ-TTSA method consisting of the four reaction steps was applied to **DHP1** (Figure 3-1). In the first step, **DHP1** was reacted with TsCl in pyridine at r.t. for 5 h and yielded 139.1% **DHP2** as gravimetrically determined. In the second reaction, the thioetherification of **DHP2** with Dod-SH was conducted in the presence of K_2CO_3 in DMF at 70°C for 20 h, resulting in an 80.6% yield of **DHP3**. In the third reaction, oxidation of **DHP3** was carried out with an oxone in dioxane/H_2O (9:1) solution at r.t. for 3 h to obtain a 94.4% yield of **DHP4**. Oxone was used as an oxidation reagent in place of MCPBA because the excess of water-soluble oxone is easy to remove. In the final reaction, **DHP4** was treated with a 0.03 M NaOH solution (dioxane/H_2O, 9:1) at 25°C for 2 h to afford a 100% yield of **DHP5**. **DHP2** to **DHP5** were characterized by FT-IR (Figure 3-2) and HSQC-NMR (Figure 3-3). The cross-signals were assigned by comparing with data of model compounds in Chapter 2 (Experimental section).

The red and blue arrows in Figure 3-3 show the dynamic shifting of the Hγ/Cγ signals of β-O-4 and β-5 by each reaction step. The assignments of the main side-chain signals are listed in Table 3-1. The numbers in parentheses in Table 3-1 are for the difference in the chemical shifts before and after each reaction: the bold and bold italic numbers indicate the higher and lower magnetic field shifts, respectively.

3.2.2.1 γ-Tosylation

In the FT-IR spectrum of **DHP2** (Figure 3-2c), the absorption bands at 1386 (ν_{as} SO_2), 1172 (ν_s SO_2), 811(ν SO), 660(ν SO), and 551(ν SO) cm^{-1}, attributable to the tosyl (Ts) groups, are prominent. In the ^{1}H-NMR spectrum of **DHP2**, both typical signals at 2.35 ppm (methyl in Ts) and 6.6–7.6 ppm (aromatic ring in Ts) are visible. In the HSQC-NMR spectrum of **DHP2** (Figure 3-3b), the H/C correlation signals of the methyl group and the aromatic ring in the Ts group are observed at 2.35/20.2

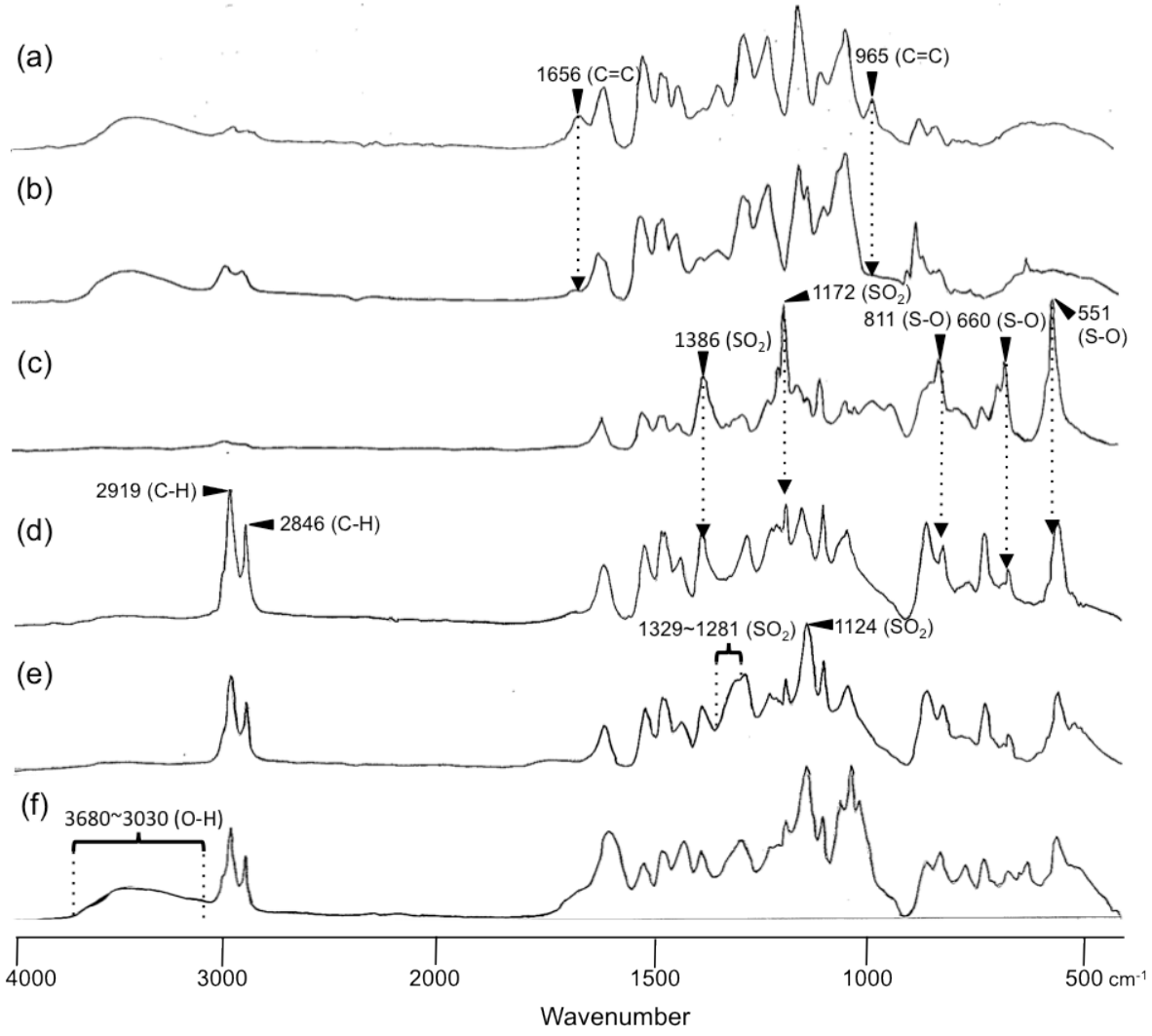

Figure 3-2 FT-IR spectra of (a) **DHP**, (b) **DHP1**, (c) **DHP2**, (d) **DHP3**, (e) **DHP4** and (f) **DHP5**

and 7.38/129.5, 7.69/127.0 ppm. The Hγ/Cγ signals in the β-O-4 and β-5 substructures of **DHP1**, which appeared at 3.41, 3.63/59.9, and 3.68/62.8 ppm, respectively, disappeared completely after tosylation, and those signals were newly observed in **DHP2** at lower magnetic fields, i.e., at 4.07, 4.33/68.8, and 4.38/70.3 ppm, respectively, as shown by the red and blue arrows in Figure 3-3b. The chemical shifts of the Hα/Cα signal of the β-O-4 substructure did not change after tosylation. Thus, concerning the hydroxyl groups in the aliphatic region, the tosylation was found to proceed selectively at the primary hydroxyl group in quantitative yield.

The signal of the α-O-4 substructure was not detected. A possible interpretation is that the α-O-4 bond may have been cleaved under the reaction conditions. However, the α-O-4 moiety was not cleaved in a separate model experiment with guaiacylglycerol-α,β-diguaiacyl ether under the same reaction conditions. The investigation for stability of the α-O-4 substructure under the present tosylation conditions is further required.

3.2.2.2 Thioetherification

New absorption bands of the alkyl group in the dodecylthioether moiety were distinctively observed at 2919 (ν CH) and 2846 (ν CH) cm^{-1} in the FT-IR spectrum of **DHP3** (Figure 3-2d). The intensities of the absorption bands of the Ts group at 1172, 811, 660, and 551 cm^{-1} decreased, but they are still present; probably, these are due to the Ts groups introduced into the phenolic hydroxyl groups, which cannot be substituted with Dod-SH.

In the ^{1}H-NMR spectrum, the signals of the Ts group at around 2.36 and 6.6–7.6 ppm decreased and signals of alkyl in dodecylthioether appeared at around 0.8–2.0 ppm. In the HSQC-NMR spectrum (Figure 3-3c), the Hγ/ Cγ signals in tosylated β-O-4 and β-5 substructures appeared at 4.07, 4.33/68.8, and 4.38/70.3 ppm, respectively, and disappeared completely after thioetherification reaction. In the spectrum of **DHP3**, these signals are shifted to a higher magnetic field, i.e., to 2.42, 2.77/32.0, and

2.87/35.6 ppm, respectively (see red and blue arrows in Figure 3-3c). The shift is the consequence of the shielding effect of the electron-donating dodecylthioether groups. There are few changes in the spectra apart from the Hγ/Cγ signals of the β-O-4 and β-5 and the β-β units.

The substitution reaction with Dod-SH proceeded selectively and quantitatively at the γ-position of the β-O-4 and β-5 substructures, whereas the remaining Ts groups are phenolic ones. These results are in agreement with those of the phenolic β-O-4 dimer model experiments, where the Ts groups at the γ-position were substituted with Dod-SH.

3.2.2.3 Sulfonylation (oxidation)

The FT-IR spectrum in Figure 3-2e reveals one sharp absorption band at 1124 cm^{-1} and another broad band as a shoulder in the range of 1329–1281 cm^{-1}, which correspond to 1160–1120 cm^{-1} (ν_s SO_2) and 1350–1300 cm^{-1} (ν_{as} SO_2) (Silverstein 1967).

In the HSQC-NMR spectrum (Figure 3-3d), the Hγ/Cγ signals in dodecylsulfone β-O-4 and β-5 substructures of **DHP3** appearing at 2.42, 2.77/32.0, and 2.87/35.6 ppm, respectively, disappeared completely after the oxidation reaction with oxone. Those signals in the **DHP4** are shifted to a lower magnetic field, such as 2.40/51.5, 3.59/52.7, and 3.00/51.3 ppm, respectively (red and blue arrows in Figure 3-3d), due to the deshielding effect of the electron-withdrawing dodecylsulfone groups. Also here, only Hγ/Cγ signals of the β-O-4 and β-5 substructures are modified and the other signals are not affected. Accordingly, only thioether groups in **DHP3** are quantitatively converted to the sulfone groups in **DHP4** by oxone oxidation.

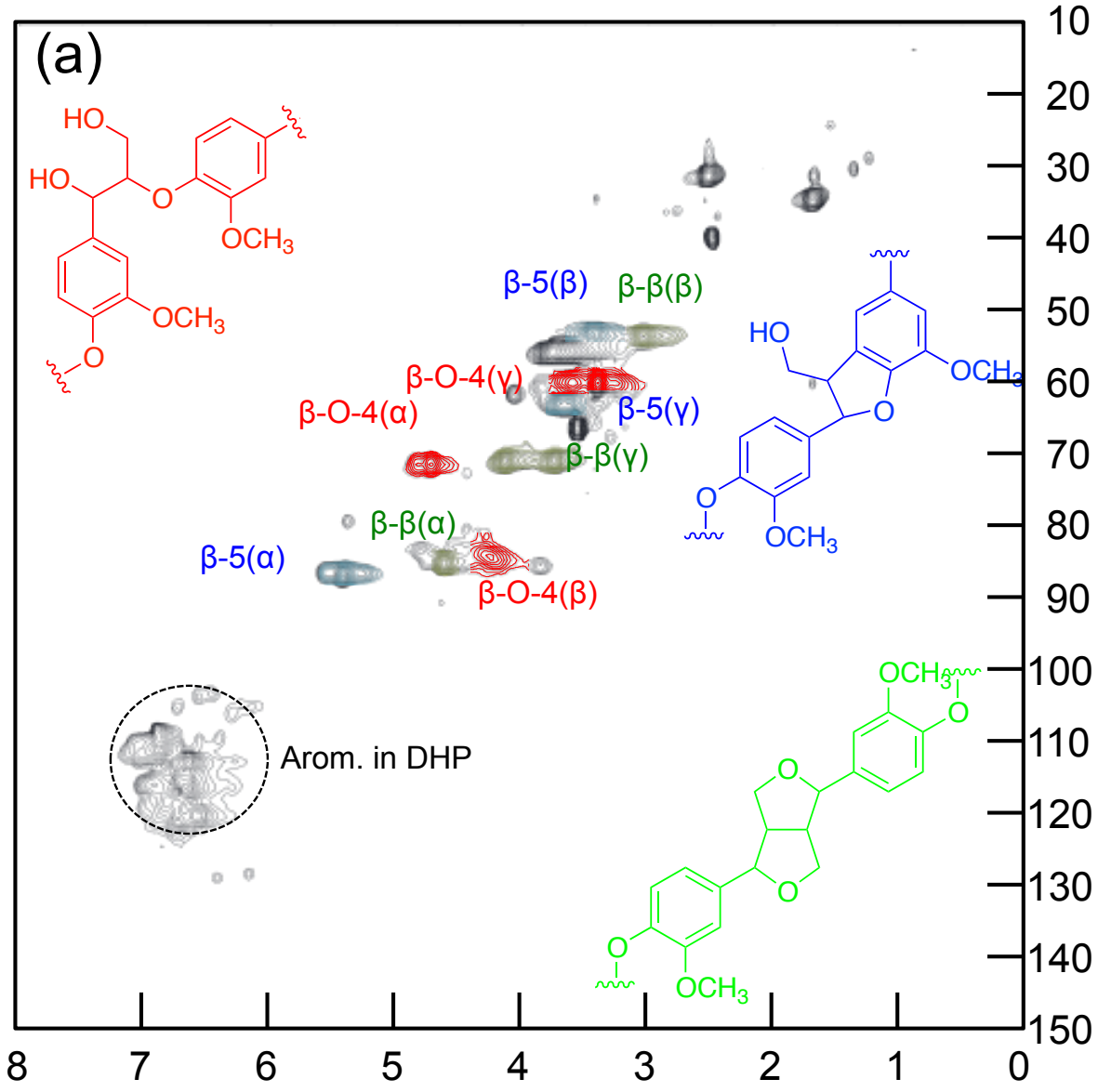

Figure 3-3 (a) HSQC-NMR spectrum of **DHP1**

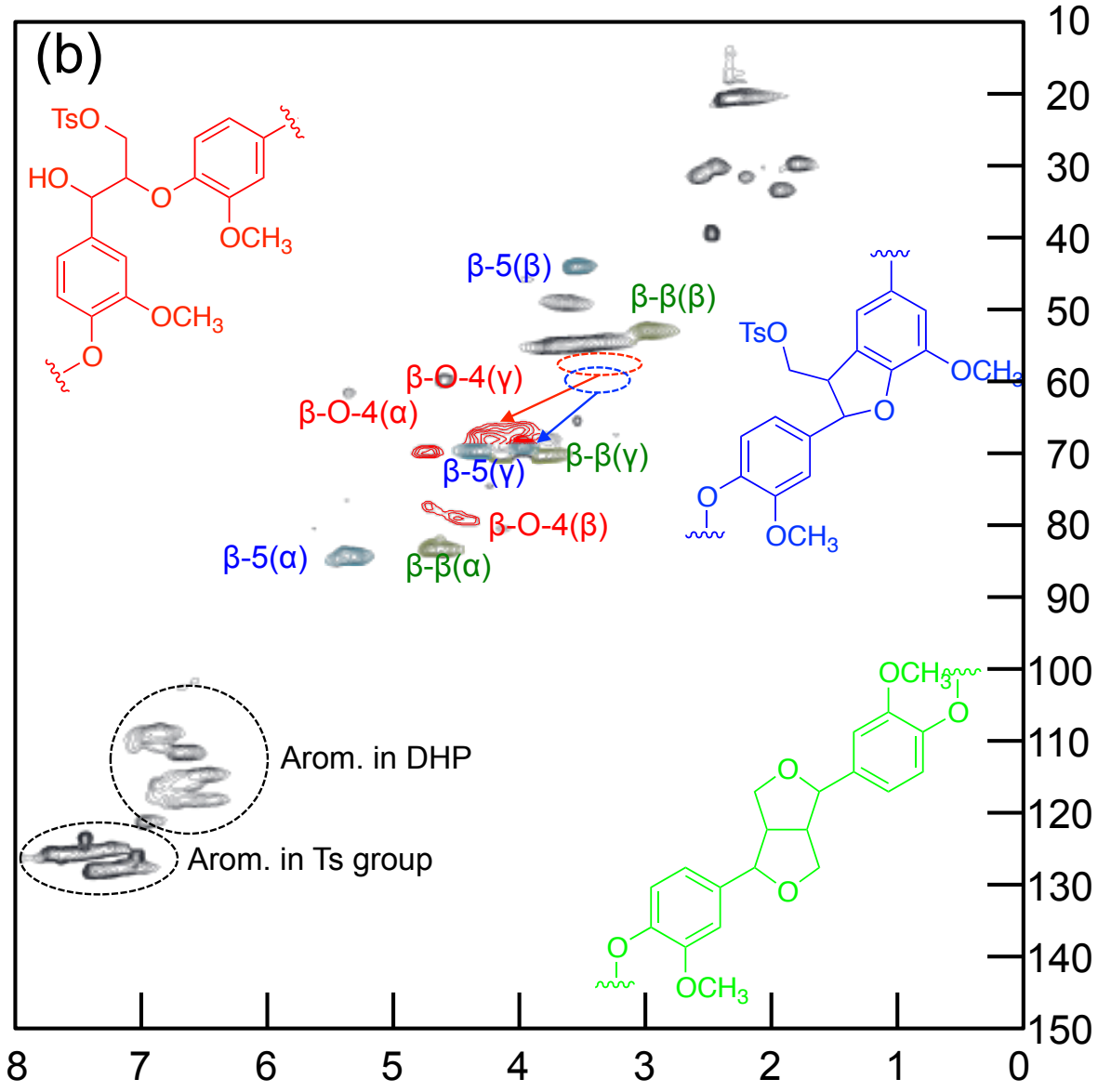

Figure 3-3 (b) HSQC-NMR spectrum of **DHP2**

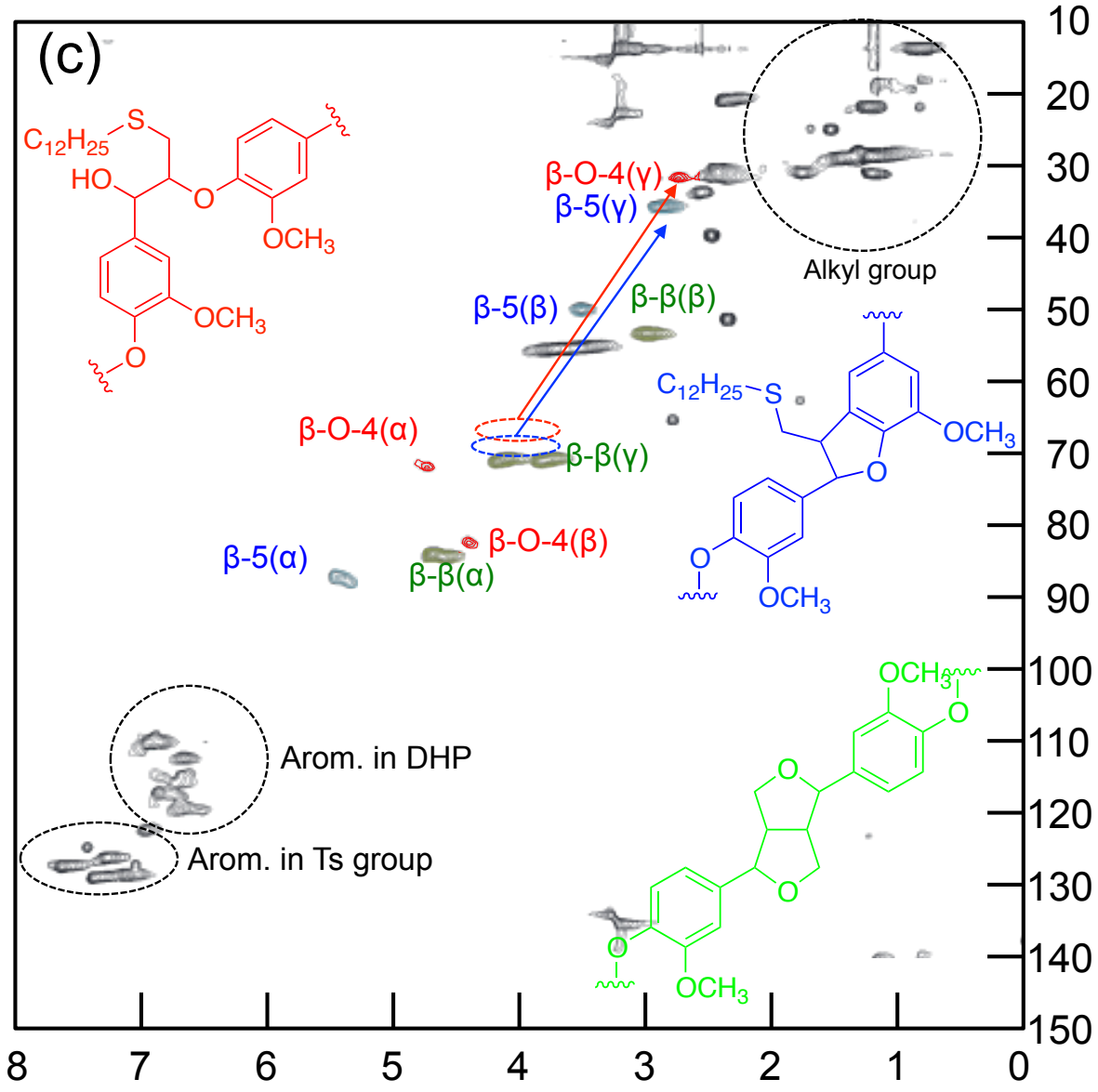

Figure 3-3 (c) HSQC-NMR spectrum of **DHP3**

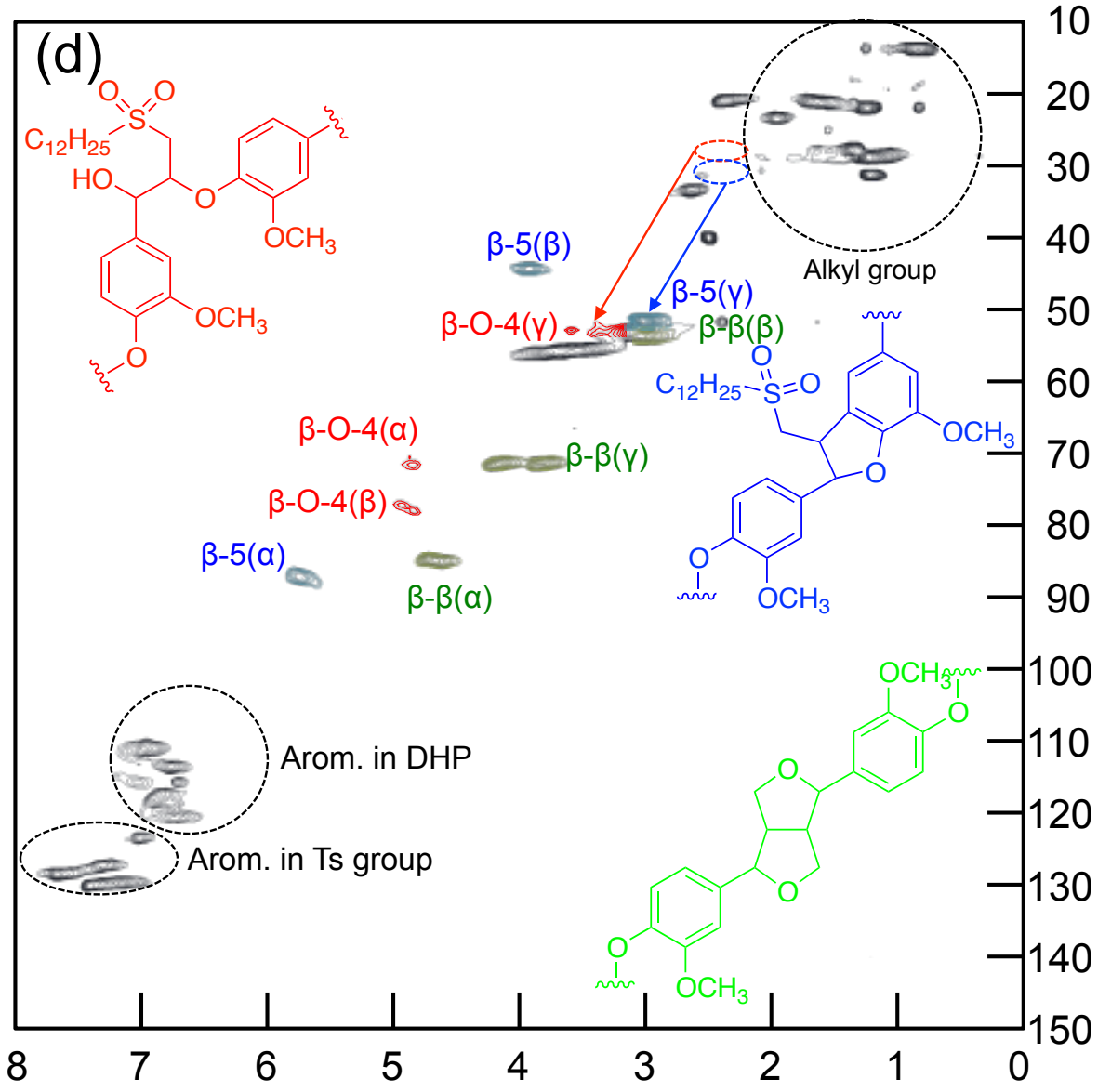

Figure 3-3 (d) HSQC-NMR spectrum of **DHP4**

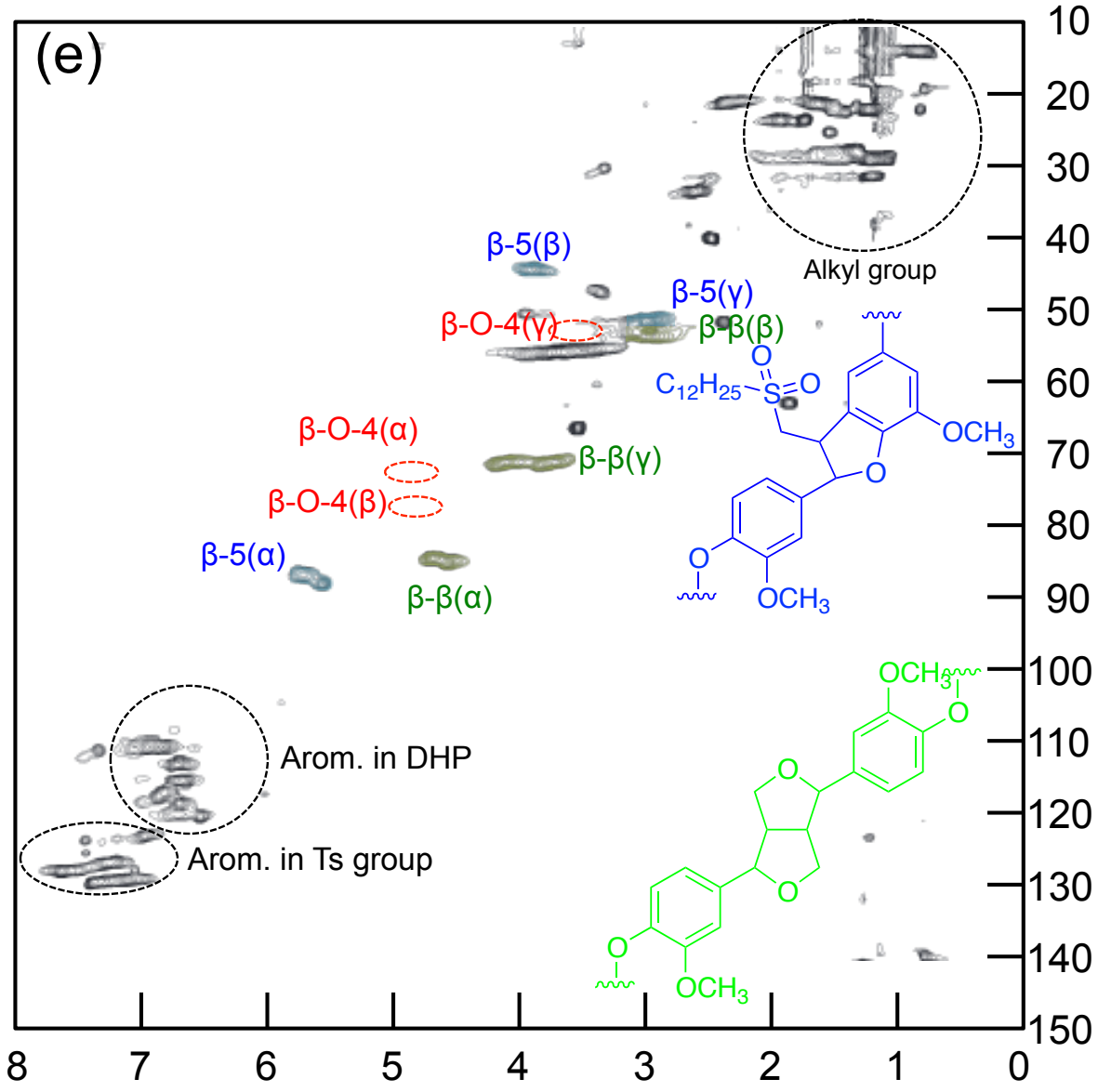

Figure 3-3 (e) HSQC-NMR spectrum of **DHP5**

Table 3-1 Assignments of $^{1}H/^{13}C$ correlation signals at α, β, and γ positions in the 2D-NMR spectra of the **DHPs 1–5**.

Assignment	DHP1	DHP2	DHP3	DHP4	DHP5
Hα/Cα(β-O-4)	4.75/71.2	4.76/71.3	4.78/72.3	4.88/71.8	-
		(***0.01***/***0.1***)	(***0.02***/***1.0***)	(***0.10***/**0.5**)	
Hβ/Cβ(β-O-4)	4.26/84.2	4.49/80.8	4.43/83.0	4.90/77.8	-
		(***0.23***/**3.4**)	(***0.06***/**2.8**)	(***0.47***/**5.2**)	
Hγ/Cγ(β-O-4)	3.41, 3.63 /59.9	4.07, 4.33 /68.8	2.42, 2.77/32.0	2.40/51.5, 3.59/52.7	-
		(***0.66***,***0.70***/***8.9***)	(**1.65**,**1.56**/**36.8**)	(**0.02**/***19.5***, ***0.82***/***20.7***)	
Hα/Cα(β-5)	5.45/86.6	5.34/85.3	5.45/87.5	5.73/86.8	5.75/86.5
		(**0.11**/**1.3**)	(***0.11***/***0.2***)	(***0.28***/**0.7**)	(***0.02***/**0.3**)
Hβ/Cβ(β-5)	3.45/53.2	3.58/44.3	3.53/49.9	3.92/44.0	3.90/43.9
		(***0.13***/**8.9**)	(**0.05**/***5.6***)	(***0.39***/**5.9**)	(**0.02**/**0.1**)
Hγ/Cγ(β-5)	3.68/62.8	4.38/70.3	2.87/35.6	3.00/51.3	3.00/51.3
		(***0.70***/***7.5***)	(**1.51**/**34.7**)	(***0.13***/***15.9***)	(0/0)
Hα/Cα(β-β)	4.51/82.9	4.72/84.1	4.71/84.2	4.72/84.3	4.71/84.2
		(***0.21***/***1.2***)	(**0.01**/***0.1***)	(***0.01***/***0.1***)	(**0.01**/**0.1**)
Hβ/Cβ(β-β)	3.04/53.4	3.00/53.4	3.00/53.5	3.10/53.0	3.08/52.7
		(**0.04**/0)	(0/***0.1***)	(***0.1***/**0.5**)	(**0.02**/**0.3**)
Hγ/Cγ(β-β)	3.75, 4.15 /70.8	3.86, 4.16 /71.0	3.84, 4.15 /71.1	3.84, 4.16 /71.1	3.79,4.14 /70.9
		(***0.11***,***0.01***/***0.2***)	(**0.02**,**0.01**/***0.1***)	(0, ***0.01***/0)	(**0.05**,**0.02**/**0.2**)
Hα/Cα(α-O-4)	5.41/79.1	-	-	-	-

*The bold and bold italic numbers indicate the shift to higher and lower magnetic fields, respectively.

3.2.2.4 Alkali treatment

In the FT-IR spectra (Figure 3-2f), a broad band of the phenolic hydroxyl group at 3680–3030 cm^{-1} is clearly visible as a result of the cleavage reaction of the β-O-4 linkages.

In the HSQC-NMR spectrum (Figure 3-3e), both Hα/Cα and Hβ/Cβ correlation signals of the β-O-4 substructures at 4.88/71.8 and 4.90/77.8 ppm completely disappeared in the spectrum of **DHP5**, whereas the Hα/Cα, Hβ/Cβ, and Hγ/Cγ signals of β-5 and β-β substructures in the **DHP4** are left

unaffected in the spectrum of **DHP5** with almost the same chemical shift. In the GPC of **DHP5$_{Ac}$** (Figure 3-4), a shoulder in the high molecular weight region (X region) in the **DHP4$_{Ac}$** is undoubtedly decreased, and a new peak in the low molecular weight region (Y region) appeared. This is a clear sign of the cleavage of β-O-4 linkages in **DHP4**.

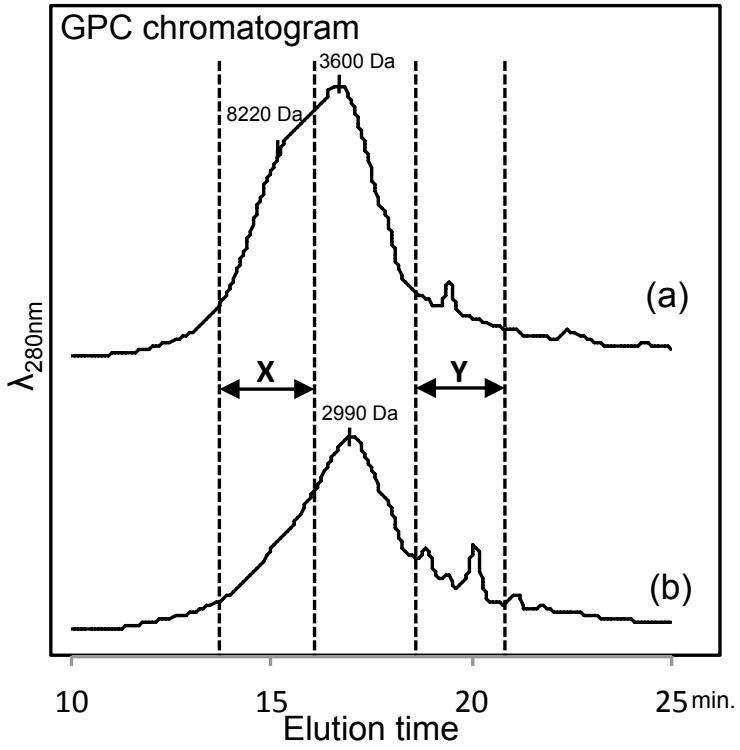

Figure 3-4 GPC chlomatograms of (a) **DHP4$_{Ac}$** and (b) **DHP5$_{Ac}$**

3.3 Summary

FT-IR and HSQC-NMR analyses of a lignin polymer model (DHP), submitted to the four-step γ-TTSA method consisting of γ-tosylation, thioetherification, sulfonylation, and mild alkali degradation, confirmed the results of similar experiments with a dimeric lignin model compound. After the first three steps, the β-O-4 and β-5 substructures in DHP were transformed to γ-sulfone derivatives without any side reaction. In the final step, the β-O-4 linkage was cleaved selectively. Accordingly, the

method could be useful for lignin polymer.

Chapter 4

Degradation of purified Milled Wood Lignin (pMWL) from *Eucalyptus globulus* by γ-TTSA method

4.1 Introduction

There are various lignins isolated from wood by some different methods. Milled wood lignin (MWL) of them has been used most widely as a chemically essentially unchanged lignin. In its preparation, the use of a preliminary, extensive grinding, followed by solvent extraction were introduced (Björkman 1956, 1957). It seems that MWL obtained in yields as high as 25% of the Klason lignin are fairly representative of the lignin in the wood examined. Indeed, it is reported that the substructures existing in MWL prepared from *Eucalyptus globulus* corresponds approximately to those of the lignin in the wood (Rencoret et al. 2008).

Eucalyptus globulus of tree species is an important source for pulp production and it belongs to the most investigated wood species until recently in terms of pulping and biorefinery (Patt et al. 2006; Leschinsky et al. 2008a,b; Brodin et al. 2009; Mendes et al. 2009; Dos Santos et al. 2011; Rodrígues-López et al. 2012; Nieminen and Sixta 2012; Vila et al. 2013). The lignin of *E. globulus* is well investigated and found to be rich in β-O-4 substructures (Rencoret et al. 2008; Guerra et al. 2008).

This is the reason why in this wood large amounts of LCCs can be assumed, which are linked by benzyl ether bonds to lignin in the neighborhood of β-O-4 linkages. Indeed, Li et al. (2011) fractionated and characterized LCCs from eucalyptus fibers.

To get an easy access to LCCs, an effective lignin degradation method is needed. The highly selective multi-step degradation method (the so called, γ-TTSA method, Figure 1) is a promising candidate to isolate cell wall moieties rich in LCC bonding sites. In Chapters 2 and 3, the author described a novel selective β-O-4 cleavage method with holding original α-substitution patterns in

lignin. In Chapter 2, the TTSA reaction sequence was examined with lignin β-O-4 dimeric model compounds. In Chapter 3, the reactivity of lignin polymer and the selective cleavage of β-O-4 linkages were investigated with artificial lignin (DHP). In this Chapter, the degradation of the native lignin, purified milled wood lignin (pMWL) from *Eucalyptus globulus*, by γ-TTSA method are described.

4.2 Results and discussion

The steps T, T, S, and A of the γ-TTSA reaction (steps *a* to *d* in Figure 4-1) procedure of **pMWL1** were qualitatively observed by FT-IR analysis (Figure 4-2) and the quantitative transformation processes were followed by HSQC-NMR spectroscopy (Figure 4-3a). The details and yields of the transformation process steps to **pMWL2** to **pMWL5** are presented in the Experimental.

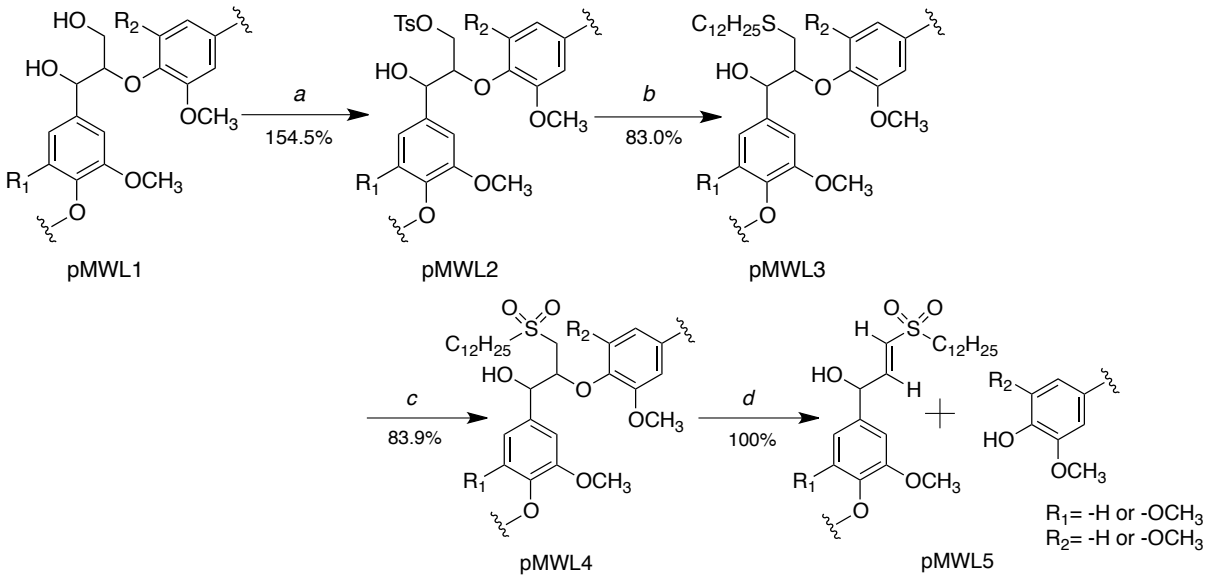

[a] TsCl/pyridine/r.t./5 h; [b] $C_{12}H_{25}SH/K_2CO_3$/ DMF/70°C/ 20 h; [c] oxone/dioxane:H_2O = 9:1/r.t./2 h; [d] 0.03 N NaOH (dioxane:H_2O = 9:1)/25°C/2 h.

Figure 4-1 γ-TTSA method applied to **pMWL1** of *E. globulus*

4.2.1 Preparation of pMWL

The purified MWL, named as **pMWL1**, was prepared from the wood (from 8-years-old *E. globulus*) by the Björkman's method (1956). The GPC analysis of the acetylated **pMWL1** of *E. globulus* revealed a M_n = 3853 and a dispersivity of M_w/M_n = 2.08. The HSQC-NMR spectrum of **pMWL1** is presented in Figure 4-3a. Cross-signals were assigned on the basis of published data (Ralph et al. 2004, Rencoret et al. 2008). The main side-chain assignments are listed in Table 4-1. The Hα/Cα, Hβ/Cβ, and Hγ/Cγ signals of the β-O-4 substructure are at 4.84/71.5, 4.09/85.5, and 3.40, 3.65/58.8 ppm, respectively. Then, the Hα/Cα, Hβ/Cβ, and Hγ/Cγ signals of the β-β substructure are observable at 4.63/84.5, 3.07/53.1 and 3.79, 4.17/70.8 ppm, respectively. Therefore, the **pMWL1** was found to be a macromolecule consisting mainly of β-O-4 and β-β substructures.

4.2.2 Application of γ-TTSA method to pMWL

4.2.2.1 γ-Tosylation

In the FT-IR spectrum of the **pMWL2** (Figure 4-2b), the absorption bands at 1359 (ν_{as} SO_2), 1172 (ν_s SO_2), 811 (ν SO), 663 (ν SO), and 551 (ν SO) cm^{-1}, attributable to the tosyl (Ts) groups, are prominent. In the HSQC-NMR spectrum of the **pMWL2** (Figure 4-3b, Table 4-1), the H/C correlation signals of the methyl group and the aromatic ring in the Ts group are observed at 2.40/21.2 ppm and 7.26/129.1, 7.43/126.2 ppm, respectively. The Hγ/Cγ signals in β-O-4 substructures of the **pMWL1**, which appeared at 3.40, 3.65/58.8 ppm, disappeared completely after tosylation, and these signals were newly observed in the **pMWL2** at lower magnetic fields, i.e. at 4.29, 4.38/68.7 ppm, as shown in Figure 4-3b. On the other hand, the chemical shifts of the Hα/Cα and Hβ/Cβ signals of the β-O-4 substructure scarcely changed after tosylation (Table 4-1), indicating that the tosylation was found to proceed exclusively on the primary hydroxyl group at γ-position and not at the secondary one at α-position.

4.2.2.2 Thioetherification

New absorption bands of the alkyl group in the dodecylthioether moiety were distinctively observed at 2918 (ν CH) and 2852 (ν CH) cm^{-1} in the FT-IR spectrum of **pMWL3** (Figure 4-2c). The intensities of the absorption bands of the Ts group at 1359, 1172, 811, 663, and 551 cm^{-1} decreased, but they are still present after the complete γ-thioetherification as in the DHP experiments (Chapter 3); these are due to the Ts groups introduced into the phenolic hydroxyl groups, which cannot be substituted with Dod-SH.

In the HSQC-NMR spectrum (Figure 4-3c, Table 4-1), the Hγ/Cγ signals in tosylated β-O-4 substructure appeared at 4.29, 4.38/68.7 ppm, disappeared completely after thioetherification. In the spectrum of **pMWL3**, these signals are shifted to a higher magnetic field, i.e. to 2.61, 2.76/31.4 ppm. These shifts are the consequence of the shielding effect of the electron-donating dodecylthioether groups.

It can be stated that the substitution reaction with Dod-SH proceeded selectively and quantitatively at the γ-position of the β-O-4 substructure, while the remaining Ts groups are phenolic ones. These results are in agreement with those of the experiments with phenolic β-O-4 dimer model and DHPs (Chapter 2, Chapter3).

4.2.2.3 Sulfonylation (oxidation)

The FT-IR spectrum in Figure 4-2d reveals one sharp absorption band at 1124 cm^{-1} and another broad band as a shoulder in the range of 1329-1281 cm^{-1}, which correspond to 1160-1120 cm^{-1} (ν_s SO_2) and 1350-1300 cm^{-1} (ν_s SO_2) (Silverstein 1967).

In the HSQC-NMR spectrum (Figure 4-3d), the Hγ/Cγ signals in dodecylsulfone β-O-4 substructure of the **pMWL3** appearing at 2.61, 2.76/31.4 ppm, disappeared completely after the oxidation reaction with oxone. Those signals in the **pMWL4** are shifted to a lower magnetic field, such as 2.93, 3.53/53.2 ppm in the **pMWL4**, respectively, due to the deshielding effect of the

electron-withdrawing dodecylsulfone groups. Also here, only Hγ/Cγ signals of the β-O-4 substructure are modified and the other signals are not affected. Accordingly, only thioether groups in **pMWL3** are quantitatively converted to the sulfone groups in **pMWL4** by oxone oxidation.

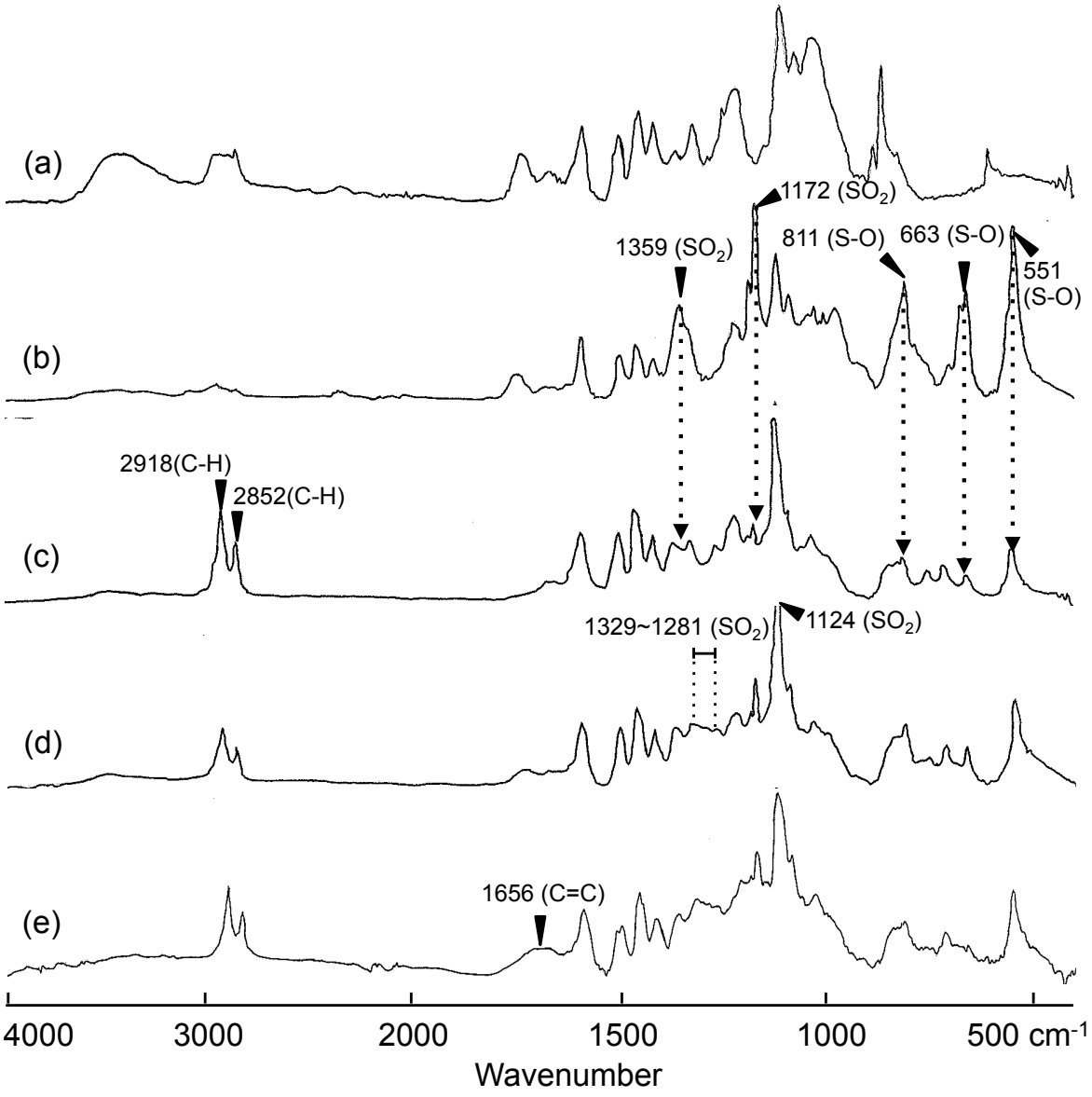

Figure 4-2 FT-IR spectra of (a) **pMWL1** (initial material), (b) **pMWL2**, (c) **pMWL3**, (d) **pMWL4** and (e) **pMWL5** as the results of the four step γ-TTSA method

4.2.2.4 Alkali treatment

In the FT-IR spectra (Figure 4-2e), a band of the double bond at about 1656 cm^{-1} is visible as a result of the β-O-4 cleavage.

In the HSQC-NMR spectrum (Figure 4-3e), both Hα/Cα and Hβ/Cβ correlation signals of the β-O-4 linkages at 4.76/71.9 and 4.79/80.1 ppm (Figure 4-3d) are disappeared almost in the spectrum of **pMWL5**, although these weak signals are detectable at lower contour level (Figure 4-3f). The β-O-4/β-β ratios of **pMWL4** and **pMWL5** were 1.94 and 0.35, calculated from the Hα/Cα correlation peak area of each linkage. The β-O-4/β-β ratio becomes a parameter of the amount of β-O-4 linkages because β-β substructures remain intact under the γ-TTSA method. As a result, 82 %(100-(0.35/1.94×100) = 82.0 ≈ 82) of all β-O-4 linkages in **pMWL4** were cleaved by the alkali treatment. Then, new signals appeared at 5.41/72.9, 6.96/148.3 and 6.73/127.2 ppm, corresponding Hα/Cα, Hβ/Cβ and Hγ/Cγ signals of the (*E*) β-γ unsaturated sulfone structure that was the result of the cleavage of the β-O-4 linkages.

Consequently, the β-O-4 linkages in the **pMWL1** are almost decomposed by the mild alkaline treatment to give olefinic degradation products as expected from our results reported previously.

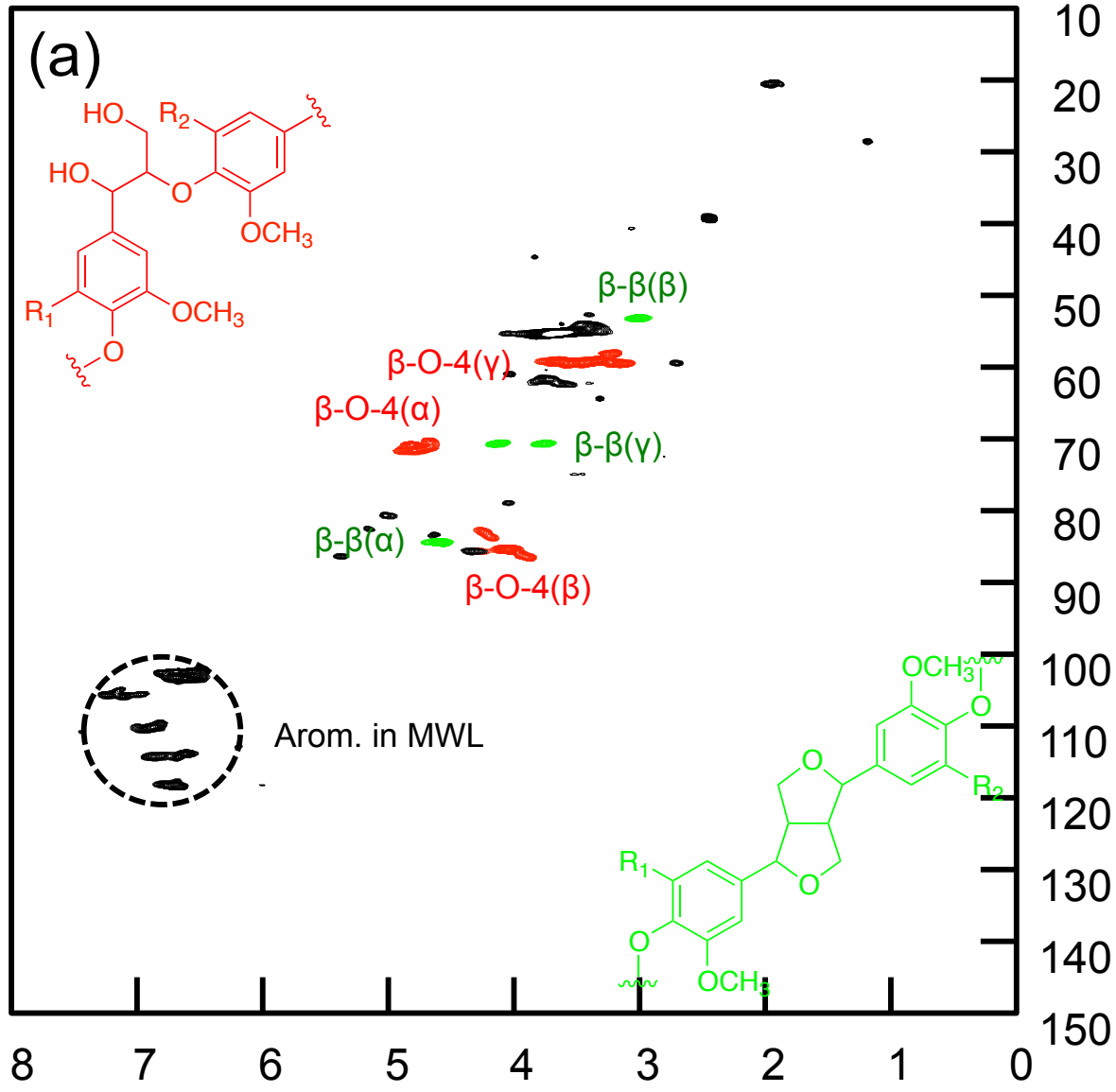

Figure 4-3 (a) HSQC-NMR spectrum of **pMWL1**

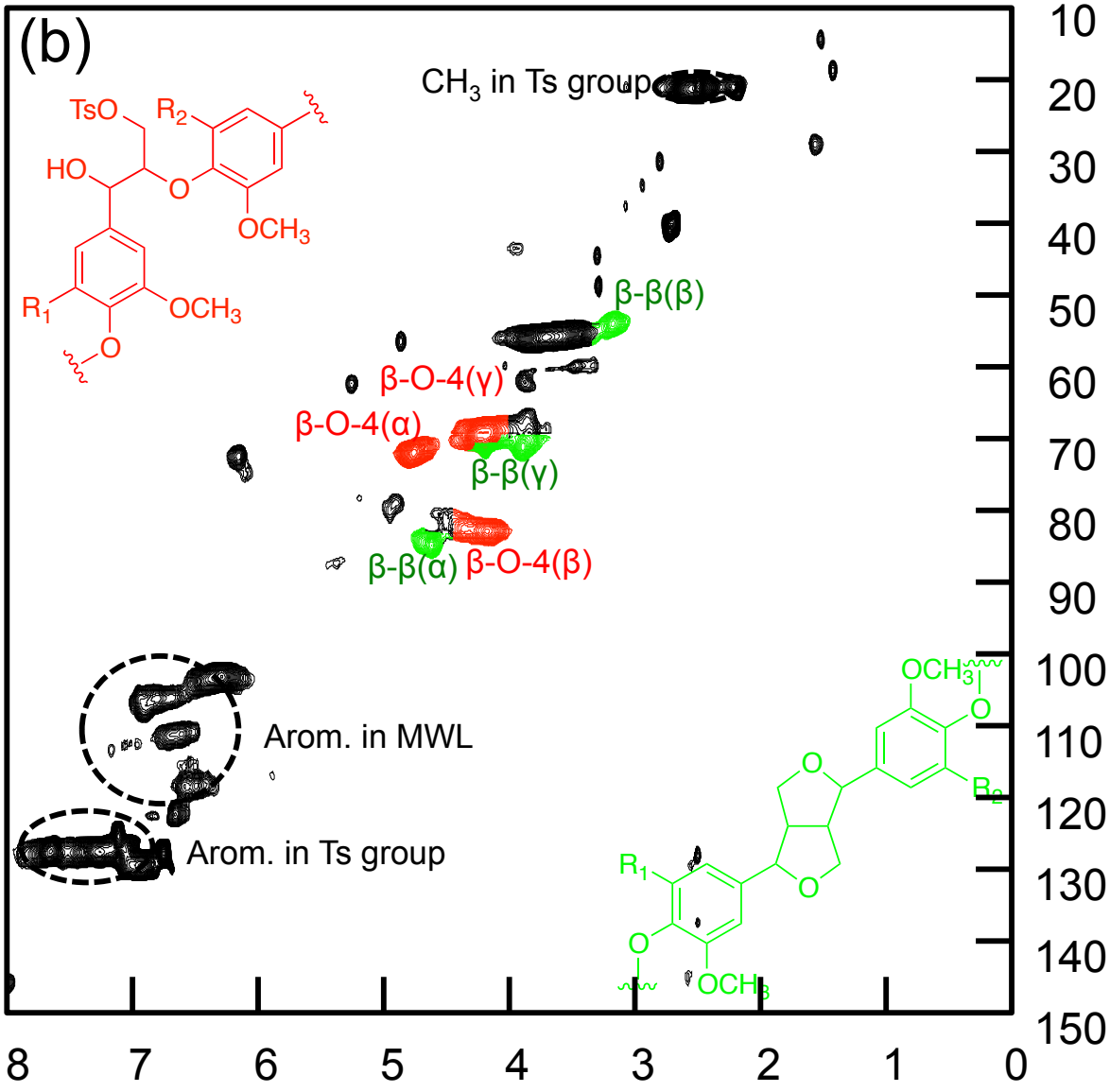

Figure 4-3 (b) HSQC-NMR spectrum of **pMWL2**

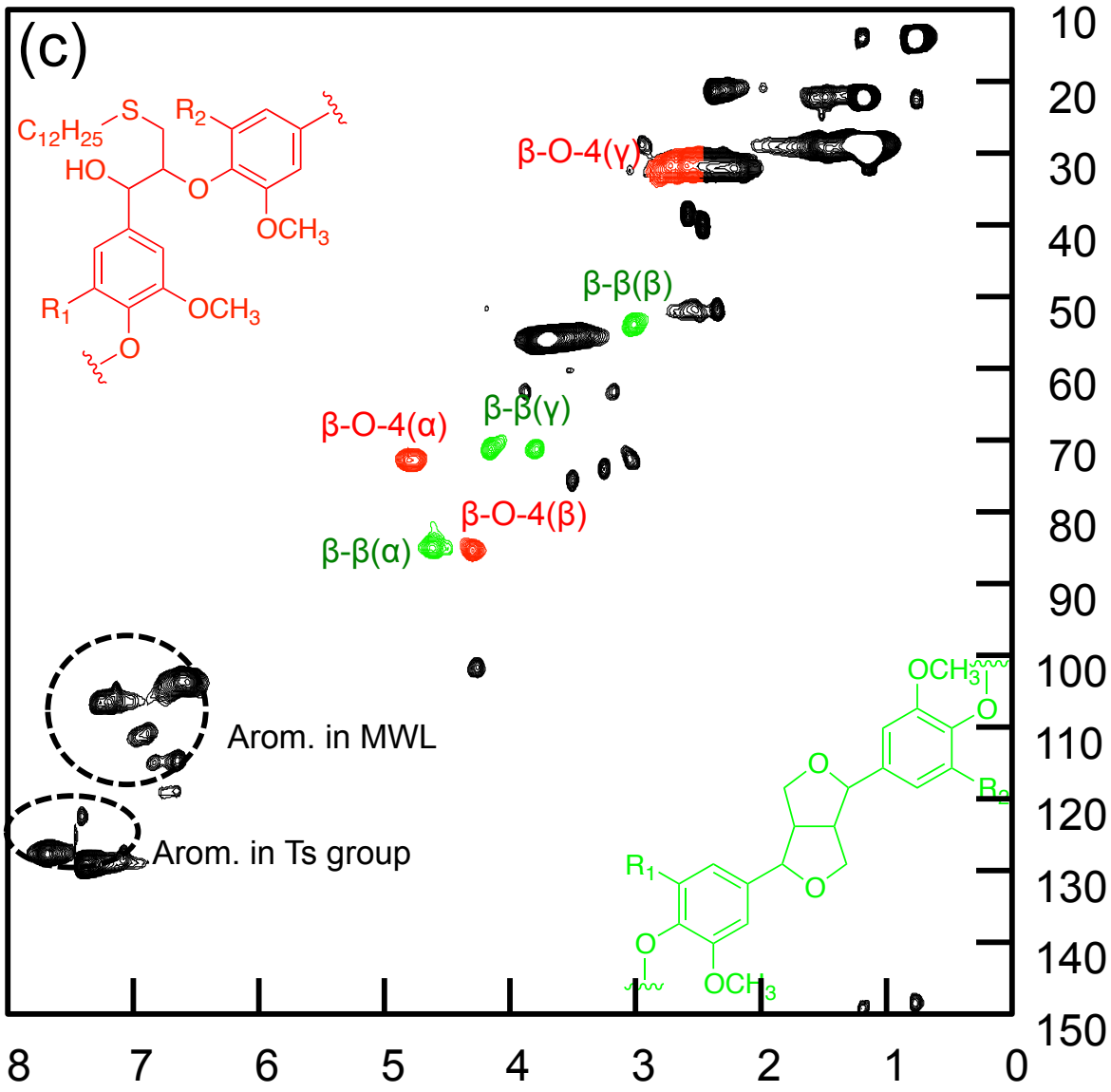

Figure 4-3 (c) HSQC-NMR spectrum of **pMWL3**

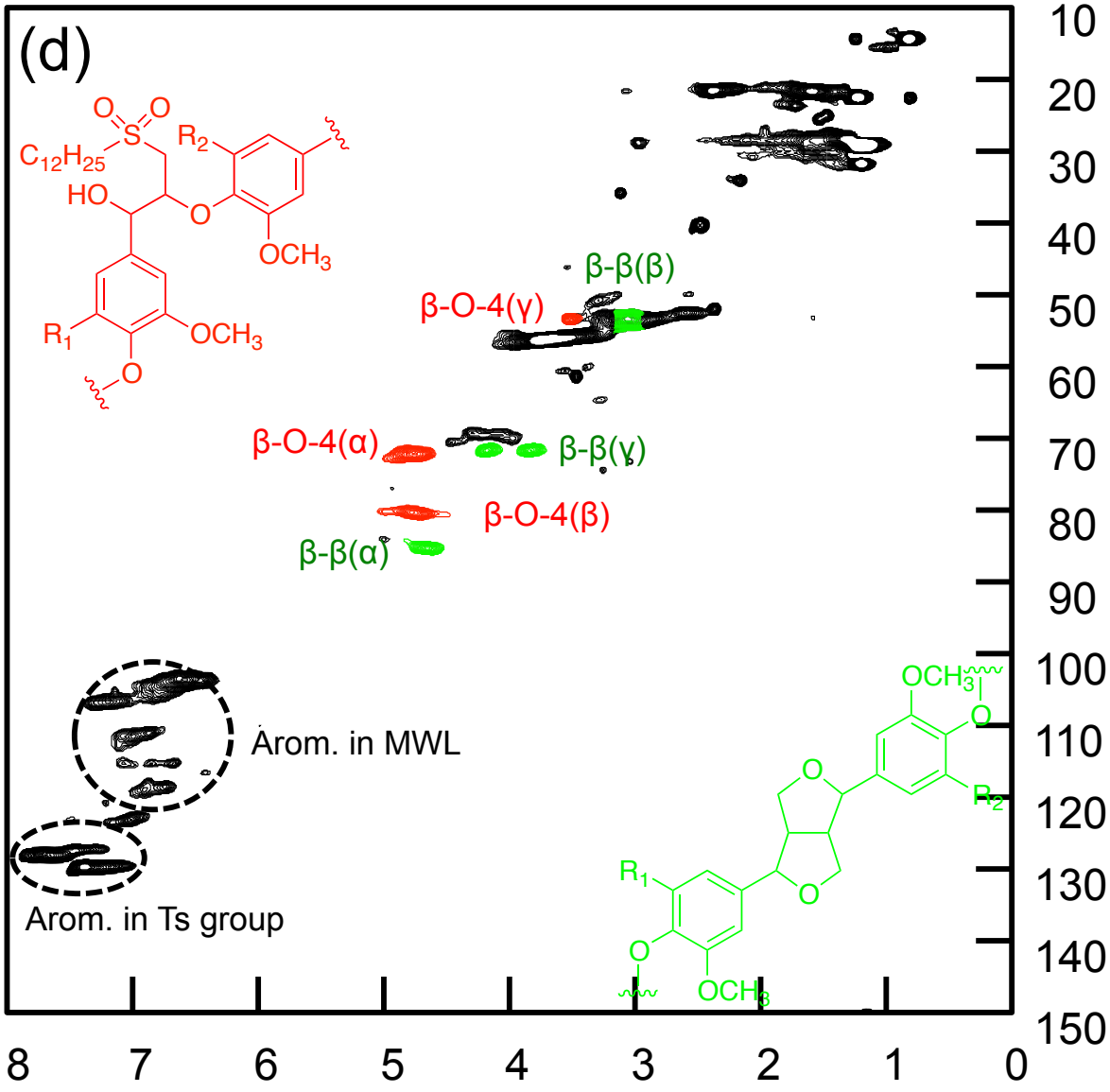

Figure 4-3 (d) HSQC-NMR spectrum of **pMWL4**

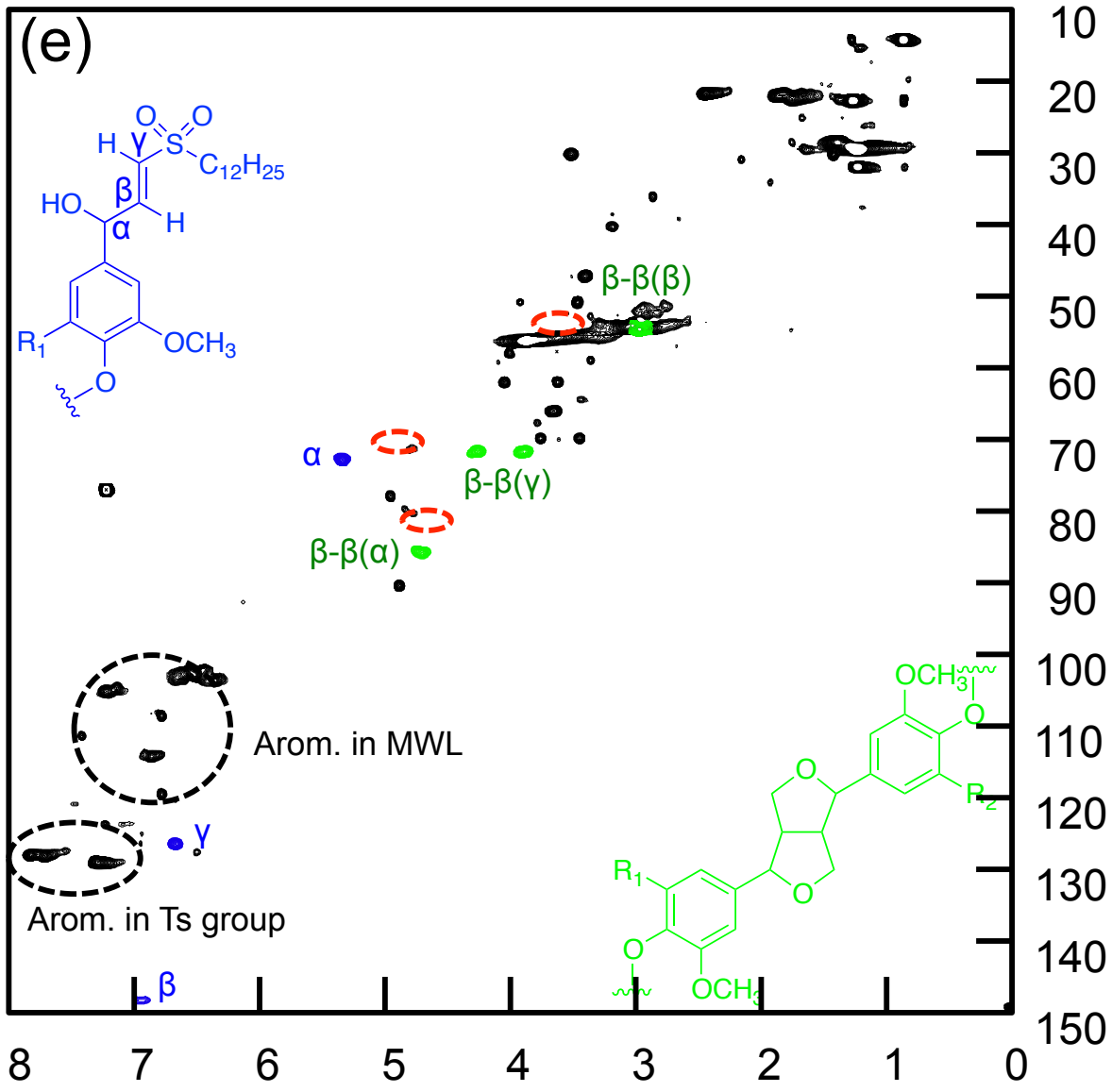

Figure 4-3 (e) HSQC-NMR spectrum of **pMWL5**

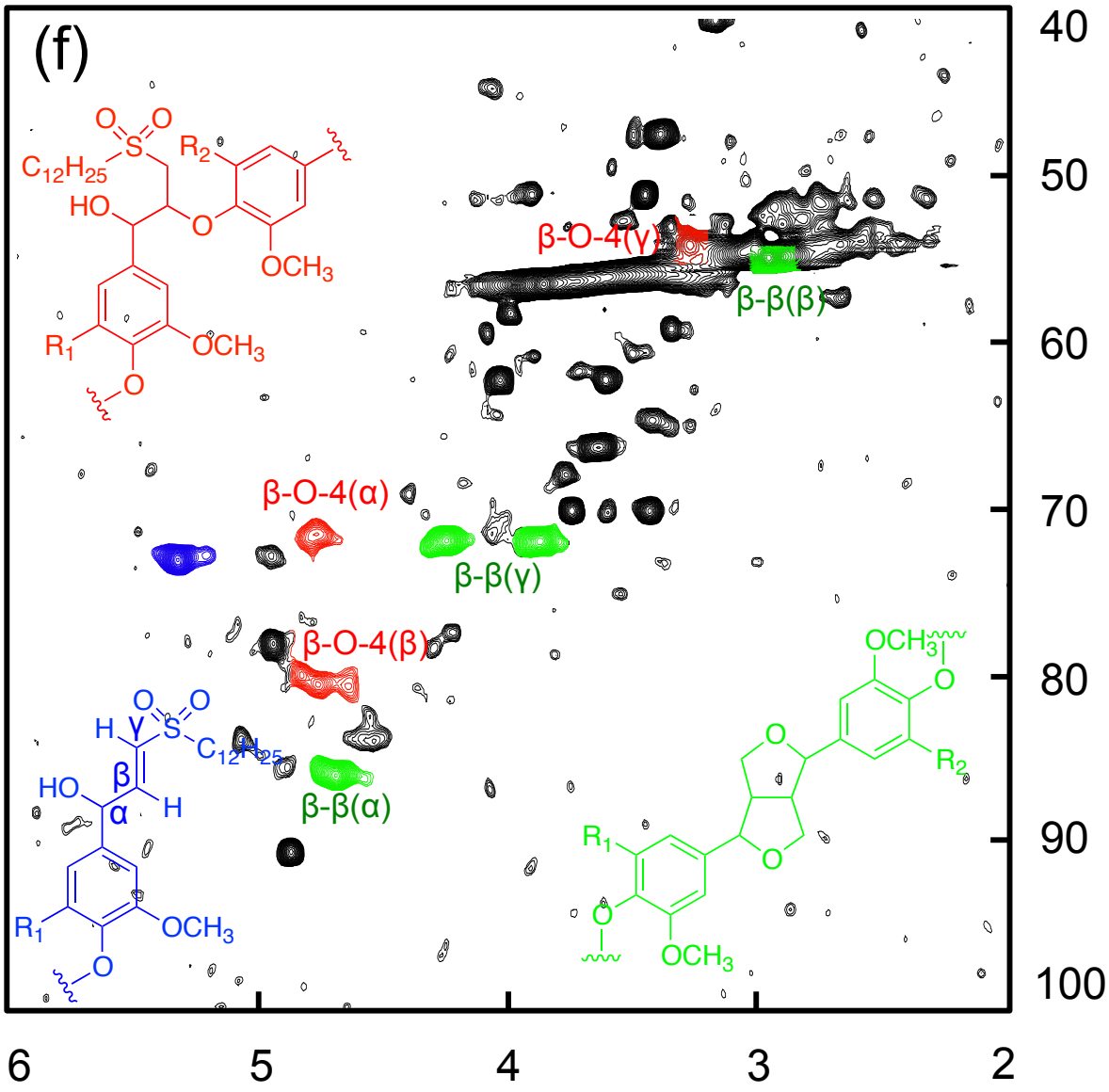

Figure 4-3 (f) HSQC-NMR spectrum of **pMWL5** (at low contour level)

Table 4-1 Assignments of $^{1}H/^{13}C$ correlation signals at α, β and γ positions in the 2D-NMR spectra of the **pMWLs 1-5**

Assignment	pMWL1	pMWL2	pMWL3	pMWL4	pMWL5
Hα/Cα(β-O-4)	4.84/71.5	4.85/71.6	4.84/73.1	4.76/71.9	-
		(***0.01***/***0.1***)	(**0.01**/***1.5***)	(**0.08**/**1.2**)	
Hβ/Cβ(β-O-4)	4.09/85.5	4.29/82.5	4.33/85.8	4.79/80.1	-
		(***0.20***/**3.0**)	(***0.04***/***3.3***)	(***0.46***/**5.7**)	
Hγ/Cγ(β-O-4)	3.40, 3.65 /58.8	4.29, 4.38 /68.7	2.61, 2.76/31.4	2.93, 3.53/53.2	-
		(***0.89***, ***0.73***/***9.9***)	(**1.68**, **1.62**/**37.3**)	(***0.32***, ***0.77***/***21.8***)	
Hα/Cα(β-β)	4.63/84.5	4.68/84.5	4.63/85.2	4.68/84.4	4.71/85.7
		(***0.05***/0)	(**0.05**/***0.8***)	(***0.05***/**0.8**)	(***0.03***/***1.3***)
Hβ/Cβ(β-β)	3.07/53.1	3.03/53.7	3.02/53.3	3.10/52.6	3.03/53.8
		(**0.04**/***0.6***)	(**0.01**/**0.4**)	(***0.08***/**0.7**)	(**0.07**/***1.2***)
Hγ/Cγ(β-β)	3.79, 4.17 /70.8	3.85, 4.23/71.0	3.80, 4.20/71.4	3.85, 4.19/71.0	3.89, 4.26/71.5
		(***0.06***, ***0.06***/***0.2***)	(**0.05**,**0.03**/***0.4***)	(***0.05***, **0.01**/**0.4**)	(***0.04***,***0.07***/***0.5***)

*The bold and bold italic numbers indicate the shift to higher and lower magnetic fields, respectively.

4.2.3 Effects of the γ-TTSA method on the β-β substructures

The Hα/Cα, Hβ/Cβ and Hγ/Cγ signals of β-β substructure in the **pMWL1** appeared at 4.63/84.5, 3.07/53.1 and 3.79, 4.17/70.8, respectively. These signals appeared almost at the same chemical shifts with small deviations in all TTSA-reaction steps, namely at 0.04~0.06/0~0.6, 0.01~0.05/0.4~0.8, 0.01~0.08/0.4~0.8, and 0.03~0.07/0.5~1.3, respectively (Figures 4-3a~4-3e, Table 4-1). That is, these peaks still remain intact after TTSA-treatment, indicating that the presented γ-TTSA degradation is really substructure-selective, the effect of which is limited to β-O-4 linkages.

4.2.4 Effects of the γ-TTSA method on the molecular weight distribution of Lignin

As indicated above, the β-O-4 linkages in the **pMWL1** were cleaved almost after the γ-TTSA treatment (Figure 4-3e). The variation of *Mw* as a function of β-O-4 cleavage was checked by

GPC analysis. The GPC chromatograms of the acetylated pMWLs before and after the γ-TTSA treatment (**pMWL1$_{Ac}$** and **pMWL5$_{Ac}$**) are presented in Figures 4-4a and 4-4b. The maximum of **pMWL1$_{Ac}$** is centered near 5000 Da as an average *Mw*. On the other hand, **pMWL5$_{Ac}$** gives two peaks at 1260 Da and 570 Da; these are in the low molecular weight region and correspond to oligomers and monomers. Especially, the peak at 570 Da corresponds to the expected degradation product after mild alkali treatment (Figure 4-4c), that is prepared from γ-dodecylsulfone derivative of 4-benzyloxy-3,5-dimethoxyphenylglycerol-β-syringyl ether via three step reactions (catalytic reduction, alkali treatment and acetylation). Accordingly, the *Mw* of **pMWL1** is decreased indicating the break down of the macromolecule to oligomers or monomers, when almost all β-O-4 linkages are cleaved. Holtman et al. (2003) described similar observations as lignin was degraded by the modified DFRC and thioacidolysis.

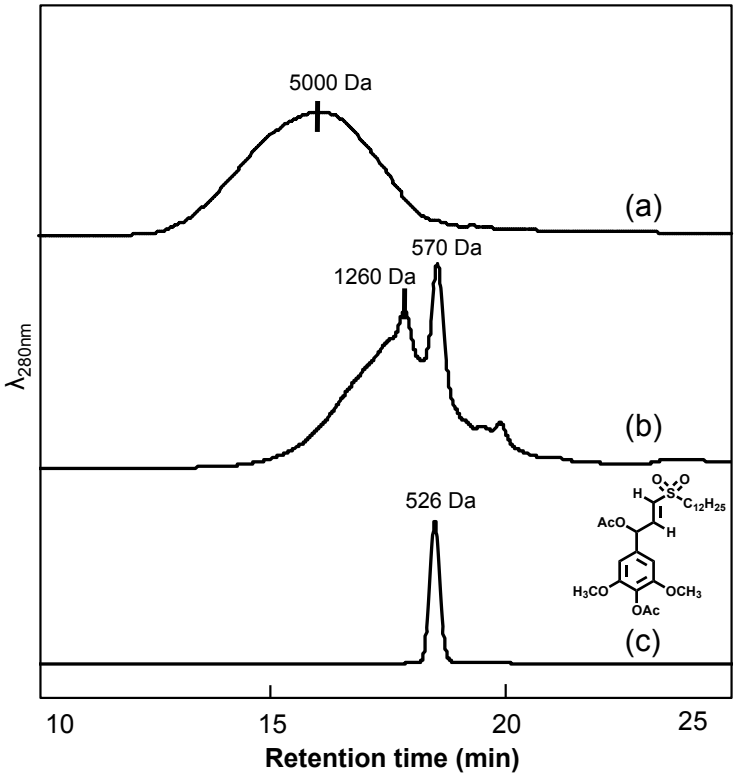

Figure 4-4 GPC chromatograms of (a) **pMWL1$_{Ac}$**, (b) **pMWL5$_{Ac}$**, and (c) degradation product of a dimeric model compound

4.3 Summary

The γ-TTSA method was applied to the **pMWL1** from *E. globulus* that contains many of the β-O-4 and β-β substructures. After the first three steps, the β-O-4 substructure was transformed to γ-sulfone derivatives without any side reaction, and the following alkali treatment cleaved almost the β-O-4 linkages selectively. As a consequence, natural lignin can be degraded by the γ-TTSA method without modifying the α-position.

Chapter 5

Selective degradation of lignin in crude Milled Wood Lignin (cMWL) from *Eucalyptus globulus* by γ-TTSA method

5.1 Introduction

Regarding LCCs, many researches have been conducted by various approaches such as solvent extraction, NMR spectroscopy etc. The fractionation of various LCC fragments from biomaterial of wood and pulp, were reported (Lawoko et al. 2003, 2005, 2006). It was considered that lignin and hemicellulose are closely interacted rather than lignin and cellulose in wood biomass (Henriksson et al. 2007; Du et al. 2013; Li et al. 2011; Leskinen et al. 2011, 2013; Choi et al. 2007). The new findings of the complicated LCC structures have been obtained by the combination of conventional methods and latest analytical techniques. Recently, it was reported the characterization of various LCC fractions with high-sensitivity NMR spectroscopy (Balakshin et al. 2007, 2011; Nicholson et al. 2012; Salanti et al. 2012; Yuan et al. 2011 ; Miyagawa et al. 2013).

However, little evidence has been reported on the direct isolation and chemical structure determination of LCC bonding sites in native woods. The problem is that the content of LCC bonding sites seems to be too small in LCC fractions. No matter how hard we purify LCC fragment from raw materials, the proportion of bonding site in one molecule of LCC is very low probability because LCC is a complex polymer that contains lignin and carbohydrate such as cellulose and hemicellulose. So, it is difficult to get the newer information concerning LCC bonding sites with only purification than ever.

In the author's strategy for the isolation of the LCC bonding sites, first only lignin, especially β-O-4 substructure unit, is degraded by the selective degradation method without any secondary condensation reaction to give a LCC with small lignin-moiety. Then, the LCC thus obtained is degraded by the enzymatic treatment with cellulase or hemicellulase that permits the selective degradation of car-

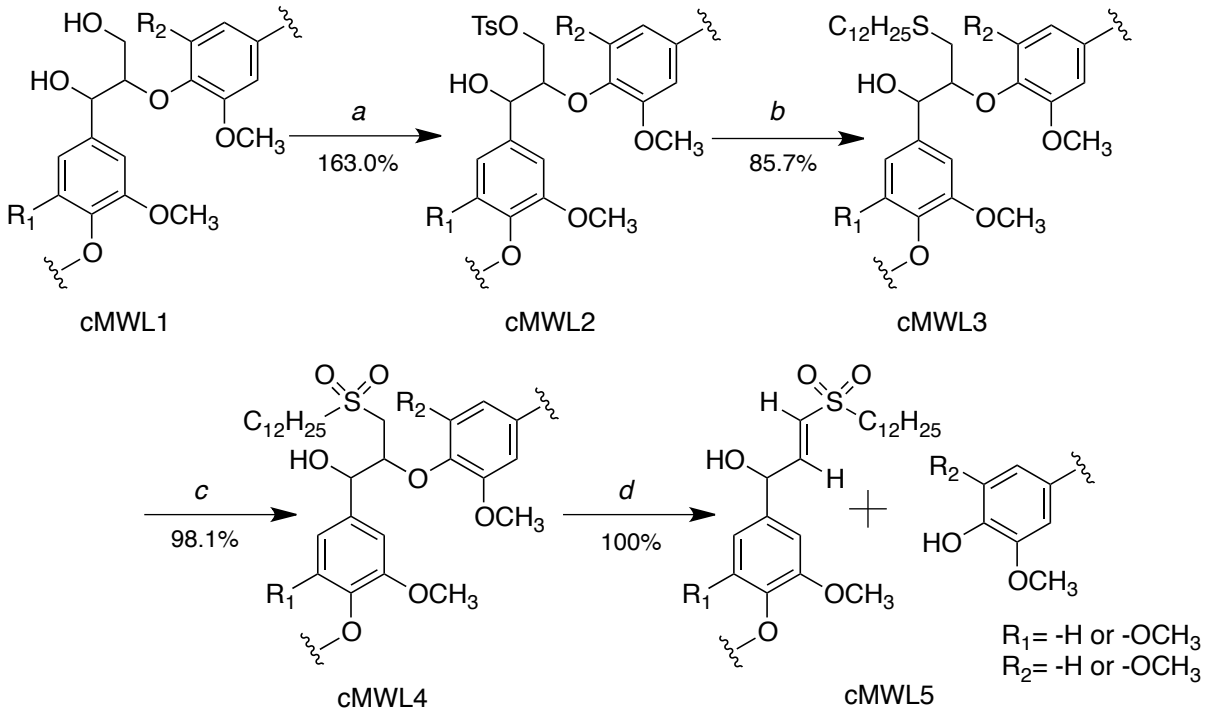

[a]TsCl/pyridine/r.t./5h; [b]$C_{12}H_{25}SH/K_2CO_3$/DMF/70°C/20 h; [c]oxone/dioxane:H_2O = 9:1/r.t./2 h; [d]0.03 N NaOH (dioxane:H_2O = 9:1)/25°C/2 h.

Figure 5-1 γ-TTSA method applied to **cMWL1** of *E. globulus*

bohydrate to give low-molecular weight compounds consisting of monosaccharides and low-molecular weight fraction with LCC bonding sites. Unfortunately, there is no suitable lignin degradation method for this strategy until now.

Thus, the author developed of the novel selective lignin degradation method, called γ-TTSA method, for LCC analysis in Chapter 2 and 3. Moreover, β-O-4 linkages in purified MWL were cleaved by γ-TTSA method to decompose into low molecular degradation products in Chapter 4. In this Chapter, the author describes to degrade selectively lignin in crude MWL by using γ-TTSA method to get some LCC fractions. The chemical structures of these fractions were analyzed by spectroscopies.

5.2 Results and discussion

It is known that crude Milled Wood Lignin (cMWL) consists of a small amount of carbohydrate (Hirosawa et al. 2002; Fruno et al. 2006; Balakshin et al. 2007, 2011). Therefore, crude MWL obtained from *Eucalyptus globulus* was selected as an LCC sample for this research.

The γ-TTSA method is a lignin degradation method by the selective cleavage of β-O-4 linkages that consist of four-step reaction (TTSA reaction sequence). It is expected that the only γ-hydroxyl group of the β-O-4 substructure is reacted with *p*-toluene sulfonyl chloride in the first step, followed by the subsequent reactions as well as previous chapters (Chapter 2~4) and β-O-4 linkages are cleaved selectively without changing other substructures in crude MWL to obtain a new LCC fraction.

5.2.1 Preparation of cMWL

The crude MWL, named as **cMWL1**, was prepared from the wood (from 8-years-old *E. globulus*) by the Björkman's method (1956). The GPC analysis of the acetylated **cMWL1** of *E. globulus* revealed a M_n = 4760 and a dispersivity of M_w/M_n = 10.8. The HSQC-NMR spectrum of **cMWL1** is presented in Figure 5-3a. Cross-signals were assigned on the basis of published data (Ralph et al. 2004, Rencoret et al. 2008). The Hα/Cα, Hβ/Cβ, and Hγ/Cγ signals of the β-O-4 substructure are at 4.84/72.3, 4.11/86.2, and 3.39, 3.70/59.9 ppm, respectively. Then, the Hα/Cα, Hβ/Cβ, and Hγ/Cγ signals of the β-β substructure are observable at 4.65/85.1, 3.05/53.8 and 3.82, 4.18/71.4 ppm, respectively. Moreover, H_1/C_1, H_2/C_2, H_2/C_2(acetylated), H_3/C_3, H_3/C_3(acetylated), H_4/C_4 and H_5/C_5 signals of xylan are observed at 4.17/103.4, 3.04/73.0, 4.49/73.5, 3.22/74.2, 4.77/75.1, 3.51/75.9 and 3.26, 3.91/63.2 ppm, respectively. Therefore, the **cMWL1** was found to be a macromolecule consisting mainly of β-O-4 and β-β substructures and xylan.

5.2.2 Application of γ-TTSA method to cMWL

5.2.2.1 γ-Tosylation

In the FT-IR spectrum of the **cMWL2** (Figure 5-2b), the absorption bands (1362 (ν_{as} SO_2), 1174 (ν_s SO_2), 815 (ν SO), 664 (ν SO), and 551 (ν SO) cm^{-1}) of the tosyl (Ts) groups are prominent. The **cMWL2** was analysed with HSQC-NMR spectroscopy after acetylation because the **cMWL2** did not dissolve well in DMSO-*d6*. The HSQC-NMR spectrum of acetylated **cMWL2** (**cMWL2$_{Ac}$**) is shown in Figure 5-3b. The H/C correlation signals of the Ts group are observed at 2.41/21.5 ppm (the methyl group) and 7.28/129.6, 7.63/ 127.7 ppm (the aromatic ring), respectively.

In case of β-O-4 substructures, the Hγ/Cγ signal at 3.39, 3.70/59.9 ppm were shifted to at 4.16, 4.32/ 67.4 ppm after tosylation. On the other hand, the Hα/Cα signal at 4.84/72.3 ppm was shifted to at 5.94/73.4 ppm which correspond to the acetylated β-O-4 model compound and the chemical shifts of the Hβ/Cβ signal of the β-O-4 substructure changed scarcely. Concerning β-β substructures, the Hα/Cα, Hβ/Cβ and Hγ/Cγ signals are not changed almost after tosylation. Concerning xylan, H_1/C_1, H_2/C_2, H_3/C_3, H_4/C_4 and H_5/C_5 signals of acetylated xylan are observed at 4.45/99.7, 4.70/70.5, 5.02/71.2, 3.56/75.1 and 3.29,3.89/62.2 ppm by acetylation before NMR analysis.

The above results supported that tosylation was proceeded selectively with the primary hydroxyl groups at the γ-position of β-O-4 substructures without changing β-β substructures and xylan in **cMWL1**.

5.2.2.2 Thioetherification

Absorption bands (2923 (ν CH) and 2851 (ν CH) cm^{-1}) of the alkyl group in the dodecylthioether moiety were distinctively observed in the FT-IR spectrum of **cMWL3** (Figure 5-2c). The absorption bands of the Ts group (1362, 1174, 815, 664, and 551 cm^{-1}) are still present after the complete γ-thioetherification of DHP prepared from a coniferylalcohol and purified MWL from *E.*

globulus as in the previous Chapters; these are due to the Ts groups introduced into the phenolic hydroxyl groups, which cannot be substituted with Dod-SH.

Moreover, each substructure is checked by using HSQC-NMR analysis. About a β-O-4 substructure, the Hγ/Cγ signals at 4.16, 4.32/ 67.4 ppm are shifted to at 2.59, 2.73/31.4 ppm after thioetherification in HSQC-NMR spectrum (Figure 5-3c). The other signals (Hα/Cα and Hβ/Cβ) nearly correspond to previous data in the previous Chapter. Regarding β-β substructure, the Hα/Cα, Hβ/Cβ and Hγ/Cγ signals are not changed almost after the reaction. On the other hand, xylan was deacetylated under the reaction condition and H_1/C_1, H_2/C_2, H_3/C_3, H_4/C_4 and H_5/C_5 signals of xylan are observed at 4.27/101.9, 3.06/72.9, 3.27/74.2, 3.52/75.6 and 3.19,3.88/63.3 ppm.

It can be stated that the reaction proceeded selectively and quantitatively at the γ-position of the β-O-4 substructure and acetyl groups in xylan were eliminated under the reaction condition.

5.2.2.3 Sulfonylation (oxidation)

One sharp absorption band at 1125 cm^{-1} and another broad band as a shoulder in the range of 1329-1281 cm^{-1} are found in the FT-IR spectrum of **cMWL4** (Figure 5-2d). These bands correspond to 1160-1120 cm^{-1}(ν_s SO_2) and 1350-1300 cm^{-1}(ν_s SO_2) (Silverstein 1967).

In the HSQC-NMR spectrum (Figure 5-3d), the Hγ/Cγ peaks at 2.59, 2.73/31.4 ppm are shifted to at 3.18, 3.52/53.2 ppm after oxidation, meanwhile the Hα/Cα and Hβ/Cβ peaks are scarcely affected. These signals correspond to the previous data of γ-sulfone lignin derivative (Chapter 2~4). Also here, the other substructures are not modified and the signals of those are undergo very little change.

It suggested that sulfone structures were formed at the γ-postiion of β-O-4 substructures by the selective oxidation of sulfur with oxone.

5.2.2.4 Alkali treatment

As expected, β-β substructure and xylan remain intact by the alkali treatment. In the HSQC-NMR spectrum of **cMWL5** (Figure 5-3e), the Hα/Cα, Hβ/Cβ and Hγ/Cγ signals of the β-β substructure are observed at 4.60/85.6, 3.06/53.6 and 3.75,4.15/71.4 ppm and H_1/C_1, H_2/C_2, H_3/C_3, H_4/C_4 and H_5/C_5 signals of xylan are observed at 4.25/102.1, 3.03/73.0, 3.25/74.4, 3.49/75.7 and 3.16,3.86/63.5 ppm. Concerning the β-O-4 substructure, Hγ/Cγ signal at 3.52/53.2 ppm and Hβ/Cβ signal at 4.77/80.3 ppm are disappeared almost. Signal at 4.80/72.5 ppm, corresponded with Hα/Cα signal of the γ-derivatized β-O-4 substructure, still remains. However, this peak is probably different from Hα/Cα signal in light of the intensity of the other signals (Hα/Cα and Hβ/Cβ). Moreover, the Hα/Cα, Hβ/Cβ and Hγ/Cγ signals of the β-γ unsaturated γ-sulfone structure derived from the β-O-4 cleavage are appeared at 5.25/71.2, 6.71/150.2, 6.71/126.3 ppm. It found that the *Mw* of **cMWL1$_{Ac}$** is definitely decreased by the cleavage of β-O-4 linkages to give the low molecular weight products as shown in the latter section (Figure 5-5).

Consequently, the β-O-4 linkages in the **cMWL1** are almost cleaved selectively by the mild alkaline treatment to give degradation products (**cMWL5**) that consist of β-β substructures in lignin and xylan structure in hemicellulose.

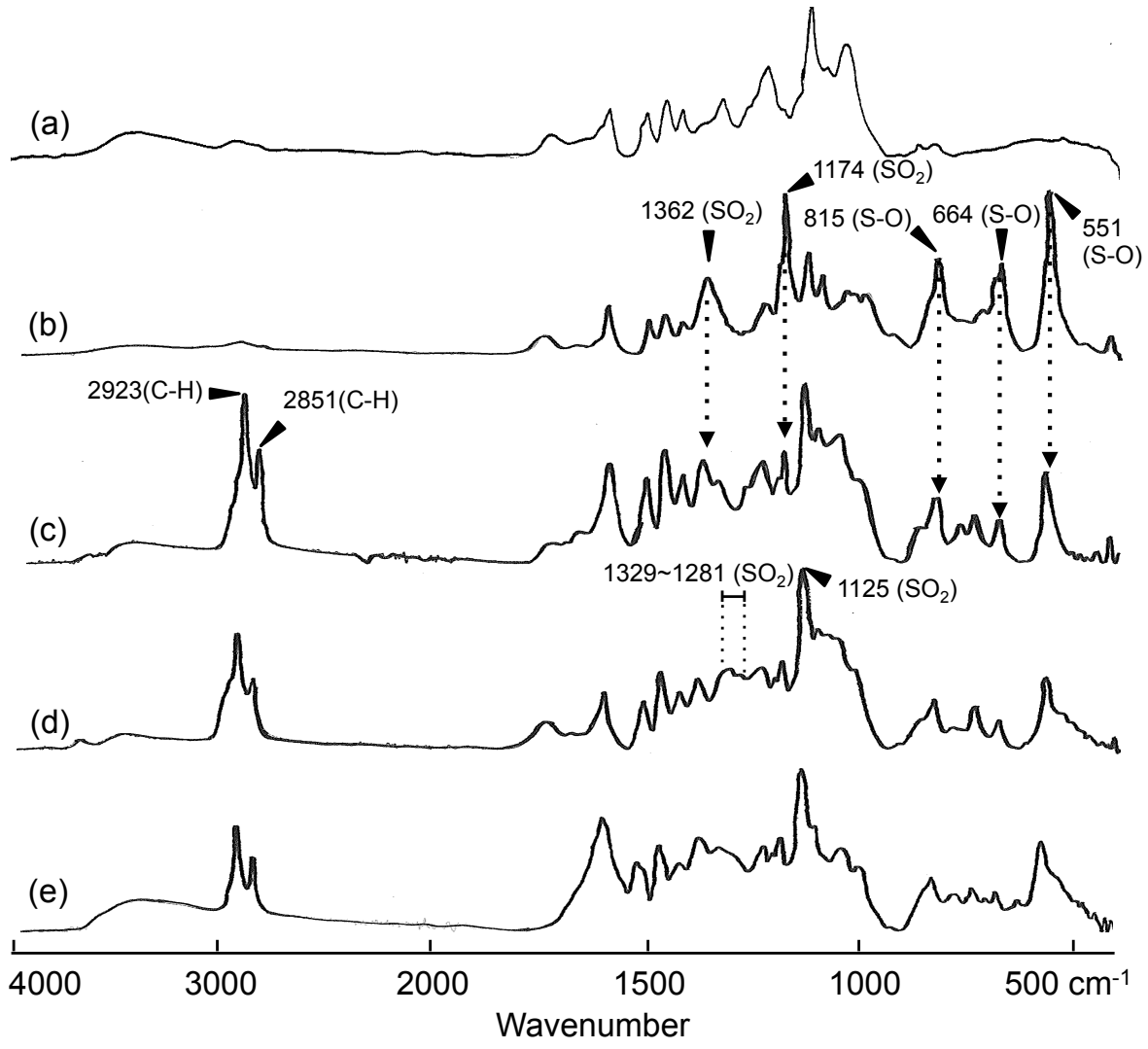

Figure 5-2 FT-IR spectra of (a) **cMWL1**, (b) **cMWL2**, (c) **cMWL3**, (d) **cMWL4** and (e) **cMWL5**

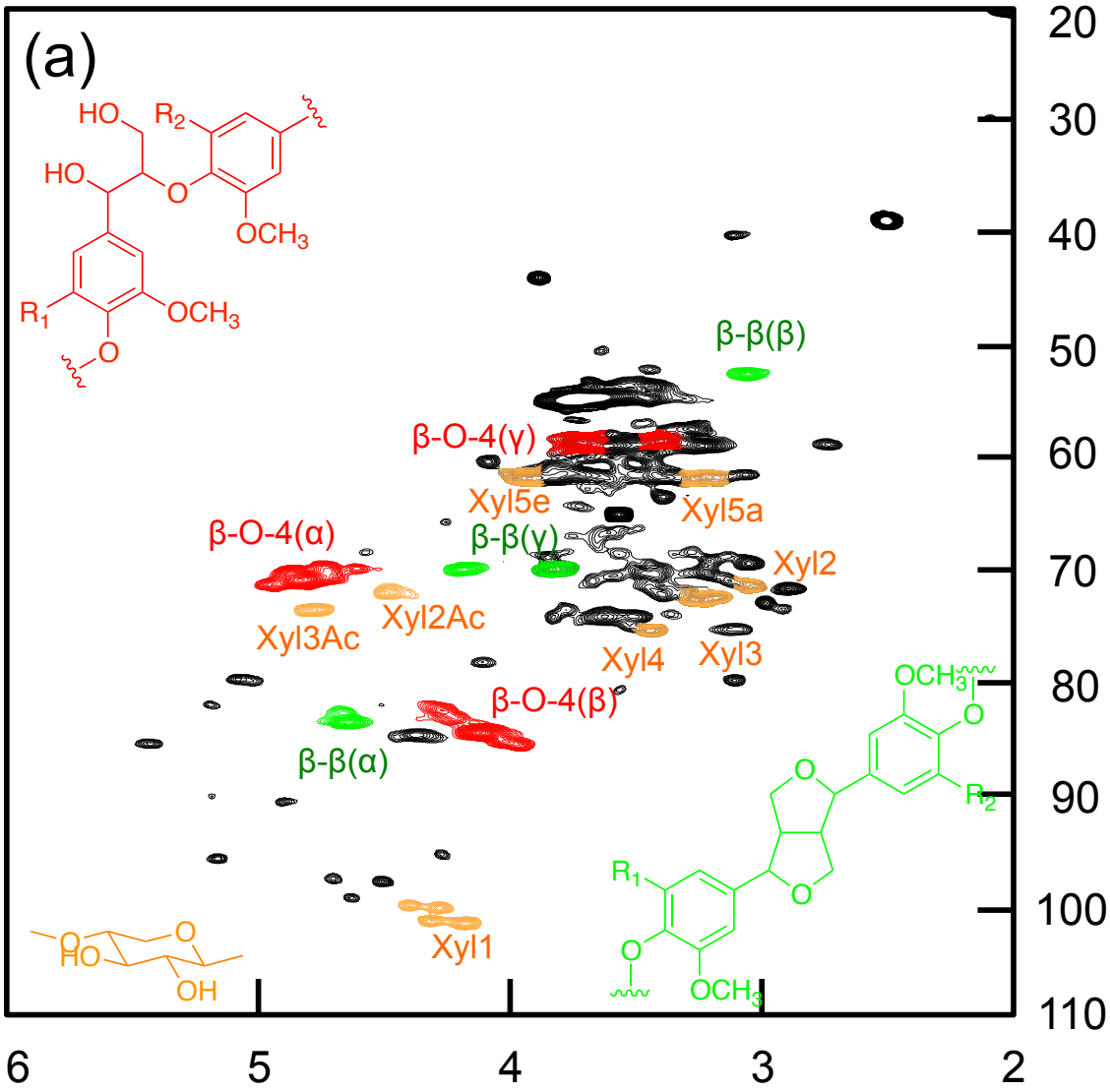

Figure 5-3 (a) HSQC-NMR spectrum of **cMWL1**

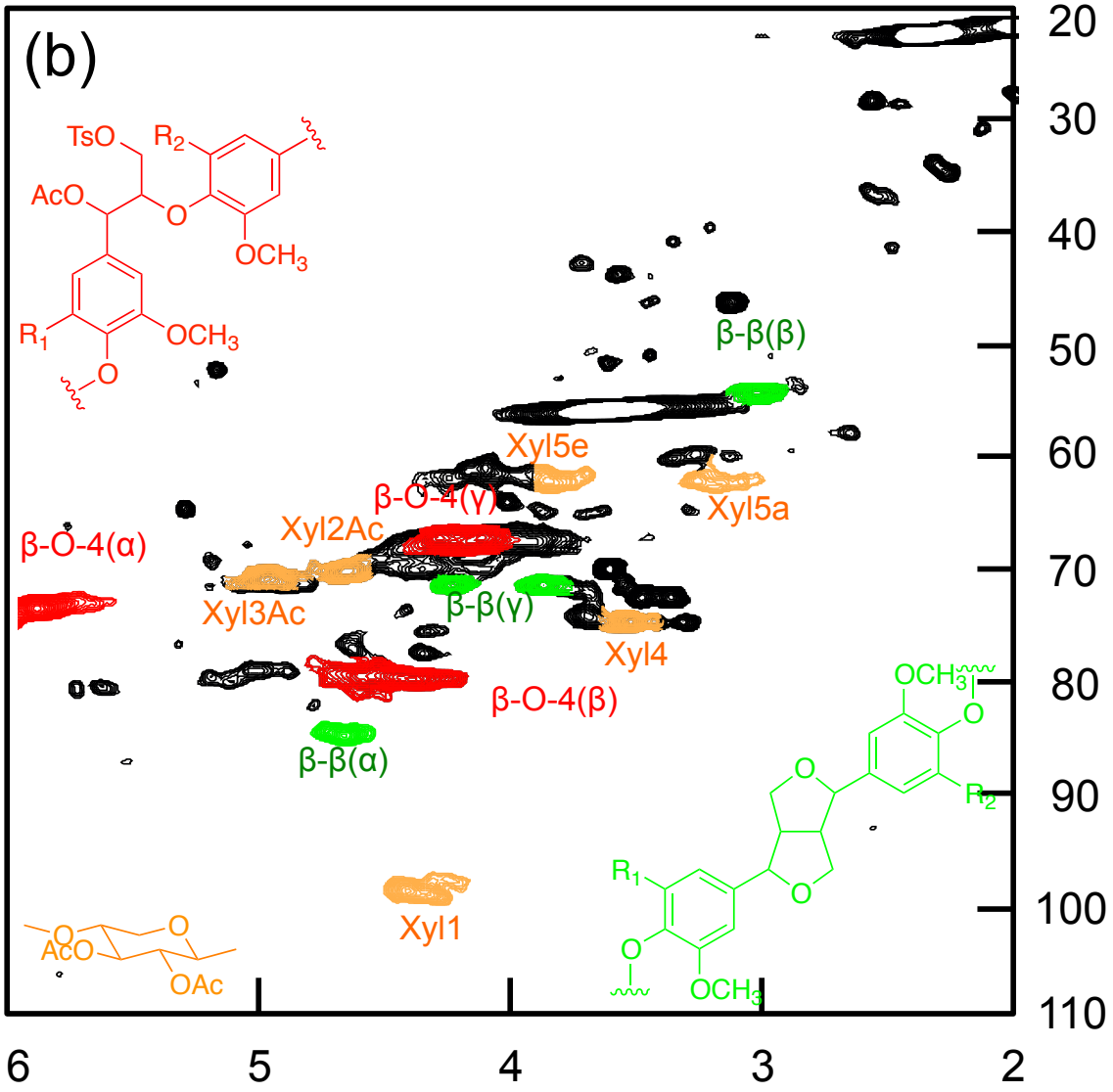

Figure 5-3 (b) HSQC-NMR spectrum of **cMWL2**

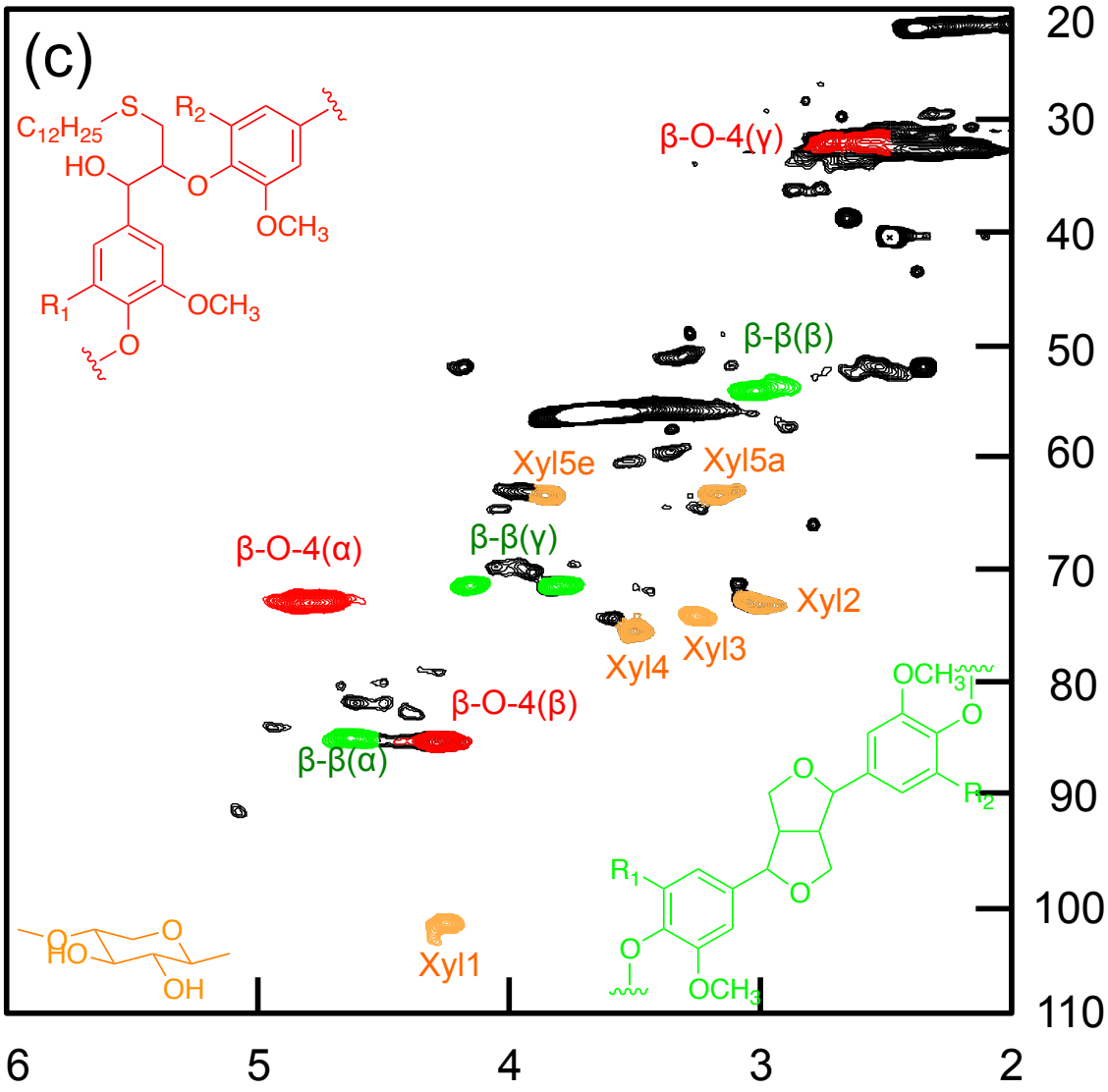

Figure 5-3 (c) HSQC-NMR spectrum of **cMWL3**

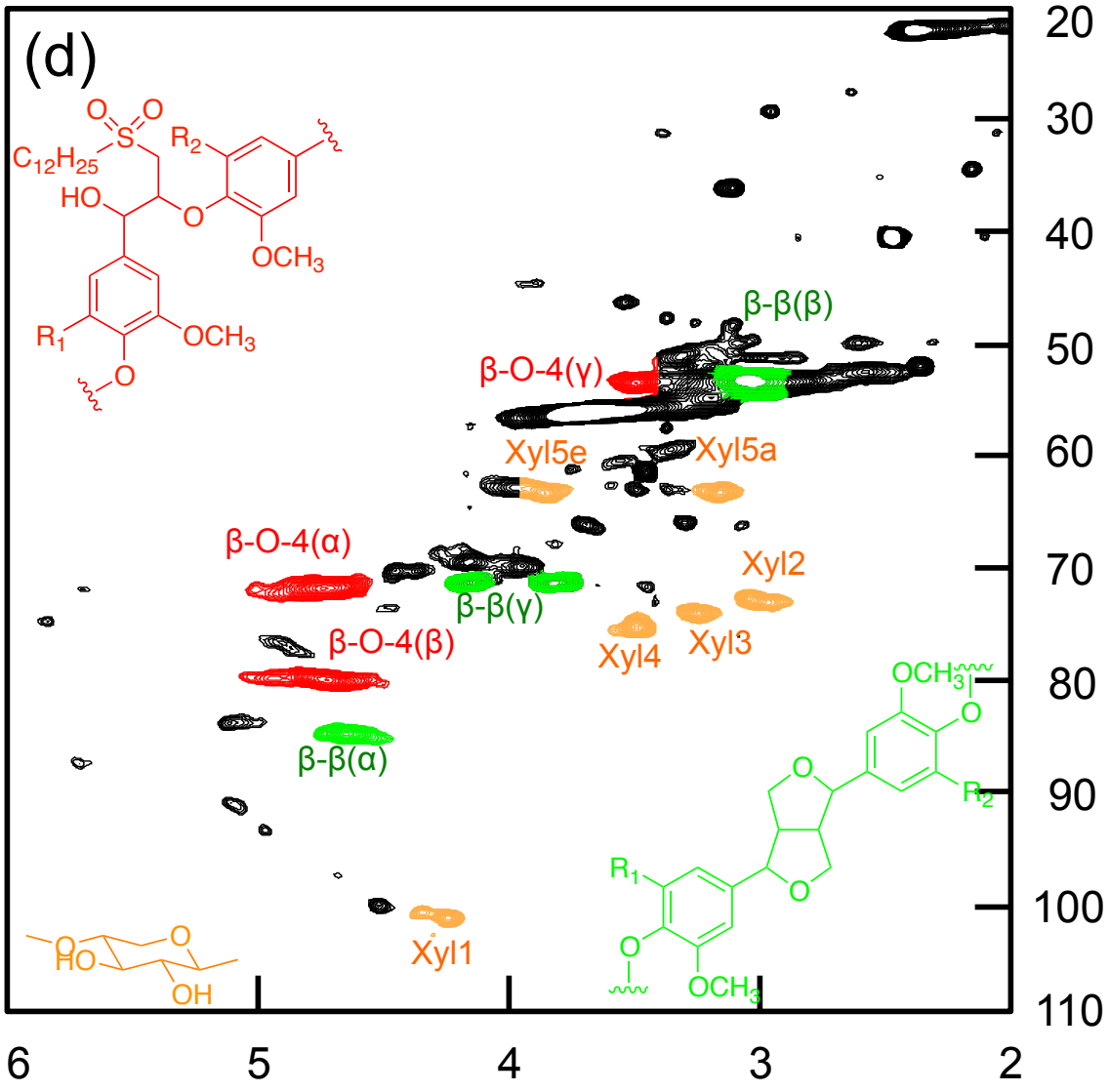

Figure 5-3 (d) HSQC-NMR spectrum of **cMWL4**

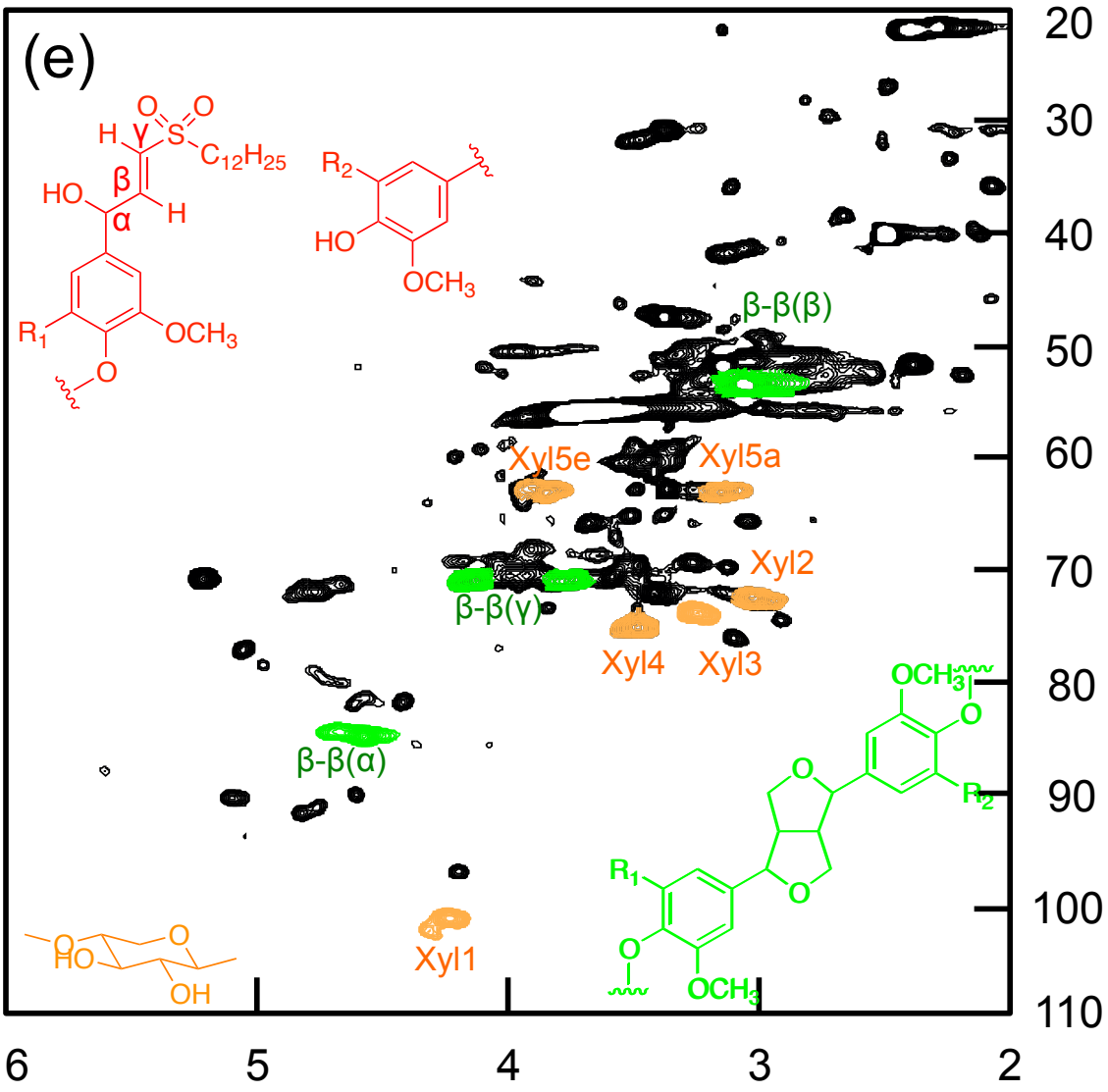

Figure 5-3 (e) HSQC-NMR spectrum of **cMWL5**

5.2.3 Fractionation of lignin degradation product (cMWL5)

The **cMWL5** was fractionated with some organic solvents for the removal of lignin degradation products. Three solvents, Et_2O (δ=15.8 $(MPa)^{1/2}$), EtOAc (δ=18.1 $(MPa)^{1/2}$) and THF (δ=19.4 $(MPa)^{1/2}$) were selected based on the different solvent polarity (Hansen's parameter (Hansen 1969)). The **cMWL5** was extracted with Et_2O, EtOAc and THF in series to get extractives (**cMWL5-1**, **cMWL5-2** and **cMWL5-3**) and the residue (**cMWL5-4**) in the yield of 40%, 19%, 16% and 25%, respectively (Figure 5-4). Each fraction was characterized by GPC (Figure 5-5) and HSQC-NMR analysis (Figure 5-6 and 5-7). The S/G ratio and the β-β substructure/xylan ratio were calculated from the volume of the aromatic peaks, and Hα/Cα peak of β-β substructure and H1/C1 of xylan for a qualitative evaluation.

The GPC chromatogram of the **cMWL5-1$_{Ac}$** shows two peaks at 530 and 1200 Da (Figure 5-5b). In the HSQC-NMR spectrum of **cMWL5-1** (Figure 5-6a), correlation signals (Hα/Cα, Hβ/Cβ and Hγ/Cγ) of β-β substructure appeared at 4.60/85.6, 3.06/53.6, 3.75,4.15/71.4 ppm, respectively. Then, the Hα/Cα, Hβ/Cβ and Hγ/Cγ signals of the β-γ unsaturated γ-sulfone structure derived from the β-O-4 cleavage are appeared at 5.25/71.3, 6.71/150.1, 6.70/126.4 ppm. The signals of G- and S-type lignin were observed in the aromatic region (Figure 5-7a) and the ratio of S/G was 2.6. H/C correlation signals from S and G units were used to estimate the S/G ratio. However, there are no signals of xylan in the spectrum (Figure 5-6a). It was found that **cMWL5-1** was a fraction of some low molecular lignin degradation products such as monomer and oligomer and 40% of **cMWL5** was removed as lignin degradation products.

In the GPC chromatogram of **cMWL5-2$_{Ac}$**, the maximum are centered near 2000 Da as an average *Mw* (Figure 5-5c). In the HSQC-NMR spectrum of **cMWL5-2** (Figure 5-6b), correlation signals of β-β substructure (Hα/Cα=4.61/85.6, Hβ/Cβ=3.05/53.6, Hγ/Cγ=3.79, 4.16/71.5 ppm) and xylan (H_1/C_1=4.25/102.2, H_2/C_2=3.02/73.2, H_3/C_3=3.24/74.4, H_4/C_4=3.50/75.9, H_5/C_5=3.18, 3.83/63.2

ppm) appeared. Then, the β-β substructure/xylan ratio, was about 3/2. The signals of G- and S-type lignin were observed in the aromatic region (Figure 5-7b). The S/G ratio was 6.4. As a result, the **cMWL5-2** was a LCC fraction. It is considered that hydrophobic lignin moiety give the solubility of **cMWL5-2** to EtOAc, although this fraction contains xylan that is insoluble in EtOAc. Then, S-type lignin is abundant in the contained lignin moiety.

In the GPC chromatogram of **cMWL5-3$_{Ac}$**, the maximum are centered near 2550 Da as an average *Mw* (Figure 5-5d). In the HSQC-NMR spectrum of **cMWL5-3** (Figure 5-6c), correlation signals of β-β substructure (Hα/Cα=4.60/85.5, Hβ/Cβ=3.06/53.6, Hγ/Cγ=3.76, 4.15/71.4 ppm) and xylan (H_1/C_1=4.25/102.1, H_2/C_2=3.02/73.0, H_3/C_3=3.24/74.4, H_4/C_4=3.49/75.8, H_5/C_5=3.16, 3.86/63.4 ppm) appeared. The β-β substructure/xylan ratio was about 2/3. Moreover, $H_{2,6}/C_{2,6}$ signals of S-type lignin were mainly observed at 6.59/103.9 and 7.26/106.4 ppm in the aromatic region (Figure 5-7c) and the S/G ratio was 6.5. It was found that the **cMWL5-3** was a LCC fraction that was soluble in THF owing to hydrophobic lignin moiety despite the xylan's insolubility to THF. Then, lignin moiety of this fraction was almost S-type as is the case in **cMWL5-2**, although lignin-content was lower than **cMWL5-2**.

In the GPC chromatogram of **cMWL5-4$_{Ac}$** (Figure 5-5e), the maximum are centered near 3120 Da as an average *Mw*. In the HSQC-NMR spectrum of **cMWL5-4** (Figure 5-6c), correlation signals of β-β substructure (Hα/Cα=4.60/85.3, Hβ/Cβ=3.06/53.5, Hγ/Cγ=3.78, 4.15/71.4 ppm) and xylan (H_1/C_1=4.25/102.0, H_2/C_2=3.02/73.0, H_3/C_3=3.24/74.3, H_4/C_4=3.49/75.6, H_5/C_5=3.16, 3.86/63.4 ppm) appeared. The β-β substructure/xylan ratio was about 1/4. Moreover, the S/G ratio was 9.9 and $H_{2,6}/C_{2,6}$ signals of S-type lignin were observed at 6.58/103.9 and 7.21/106.3 ppm in the aromatic region although signals of G-type lignin were very few (Figure 5-7d). The obtained **cMWL5-4** was a highest xylan content LCC fraction compared with **cMWL5-2** and **cMWL5-3**. Then, lignin moiety of this fraction was almost S-type more than the other LCC fractions (**cMWL5-2** and **cMWL5-3**).

Based on the results, it was capable to remove 40 % of **cMWL5** as low *Mw* lignin degradation products by Et_2O extraction. Then, soluble different LCC fractions (**cMWL5-2** ~ **cMWL5-4**) were obtained by EtOAc and THF extractions. In these LCC fractions, the lignin content decreased in the order of **cMWL5-2**, **cMWL5-3** and **cMWL5-4**. On the other hand, S-type lignin content of lignin moiety in each fraction increased. Then, if the β-β substructure is not linked between lignin and xylan, β-β substructure in lignin moiety should be provided as a syringaresinol after the degradation. But the lignin moiety of any fraction contained the β-β substructure. These results strongly suggest that the β-β substructure plays an important role for linking between lignin and xylan. It is indicated that a phenyl glycoside bond is a prime candidate as the bond between the β-β substructure and xylan in light of the fact that the highest xylan-content **cMWL5-4** contains syringaresinol-type β-β substructures. In future, the bonding site may be obtained by the enzymatic treatment of these fractions although we need detailed researches.

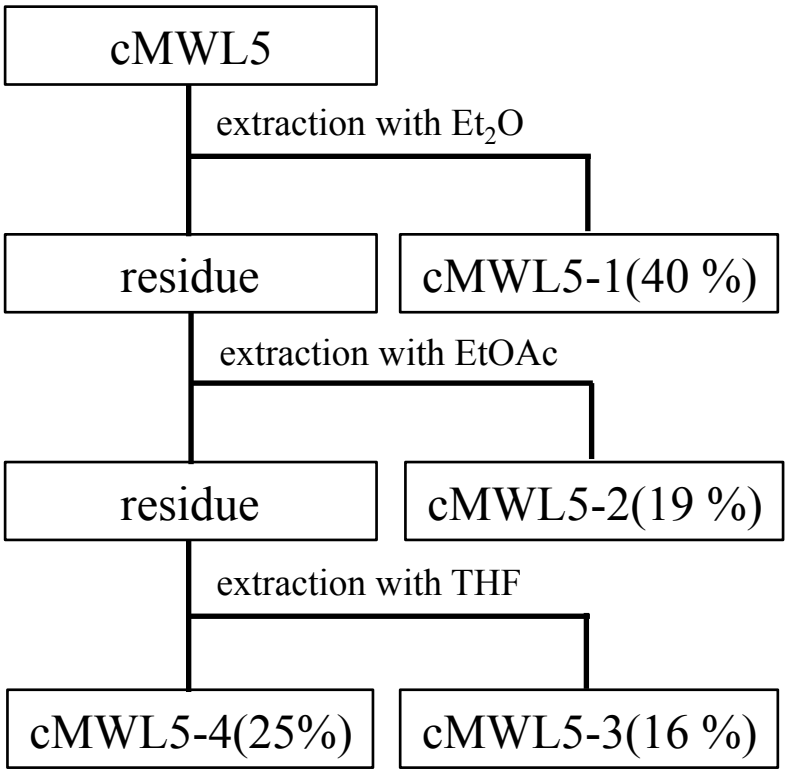

Figure 5-4 Fractionation of **cMWL5** with solvents

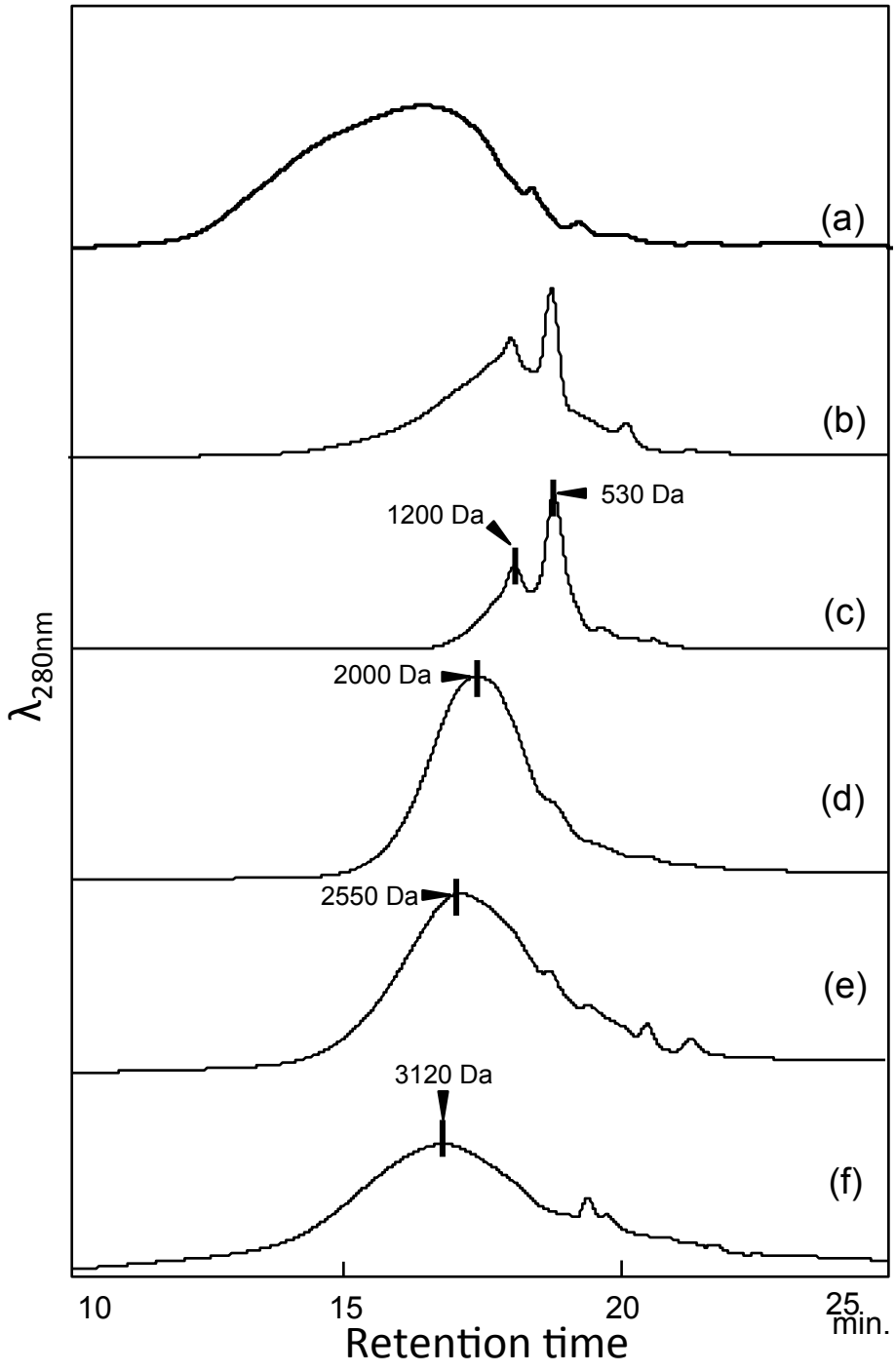

Figure 5-5 GPC chromatograms of (a) **cMWL1$_{Ac}$**, (b) **cMWL5$_{Ac}$**, (c) **cMWL5-1$_{Ac}$**, (d) **cMWL5-2$_{Ac}$**, (e) **cMWL5-3$_{Ac}$** and (f) **cMWL5-4$_{Ac}$**

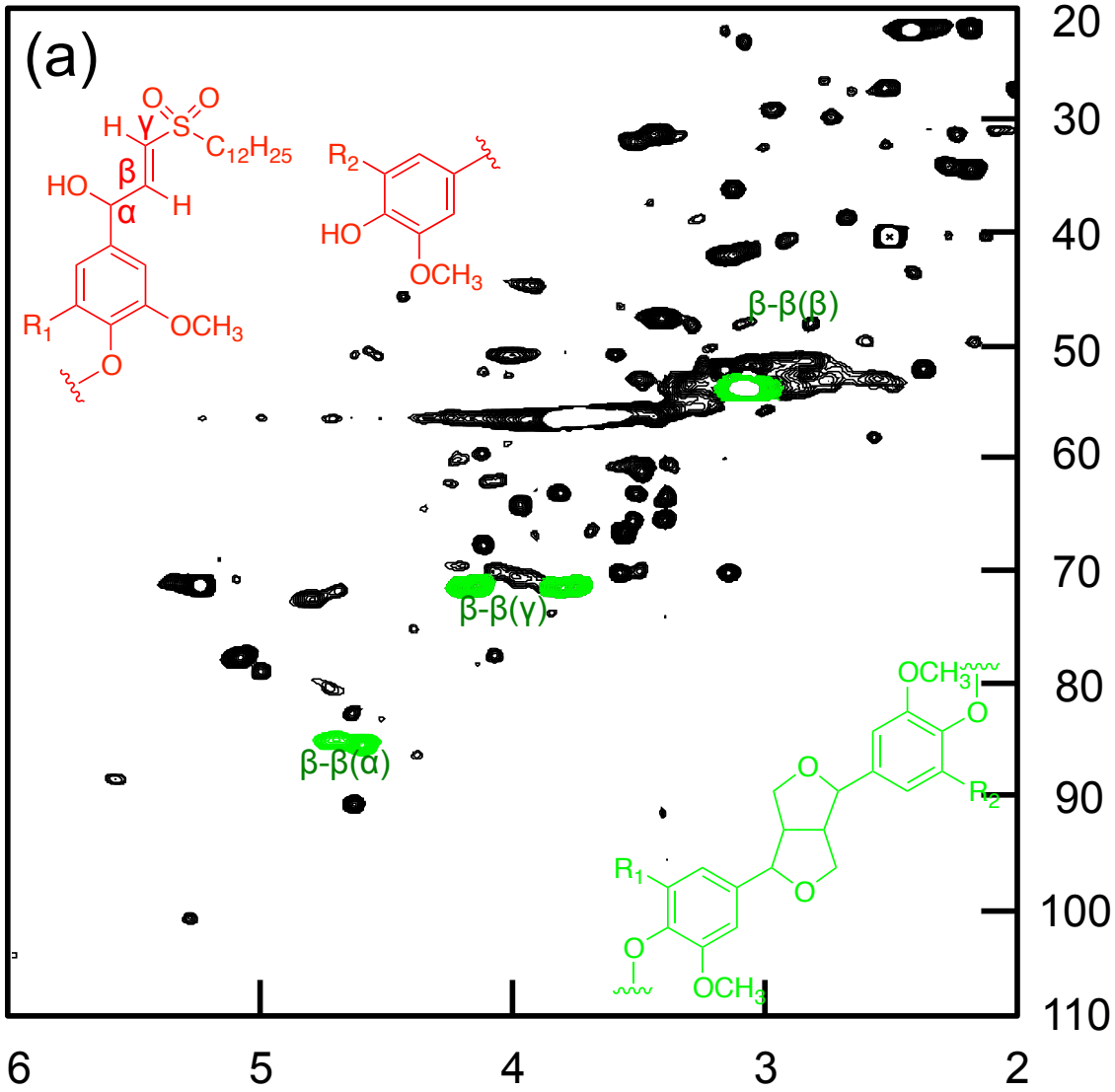

Figure 5-6 (a) HSQC-NMR spectrum (aliphatic region) of **cMWL5-1**

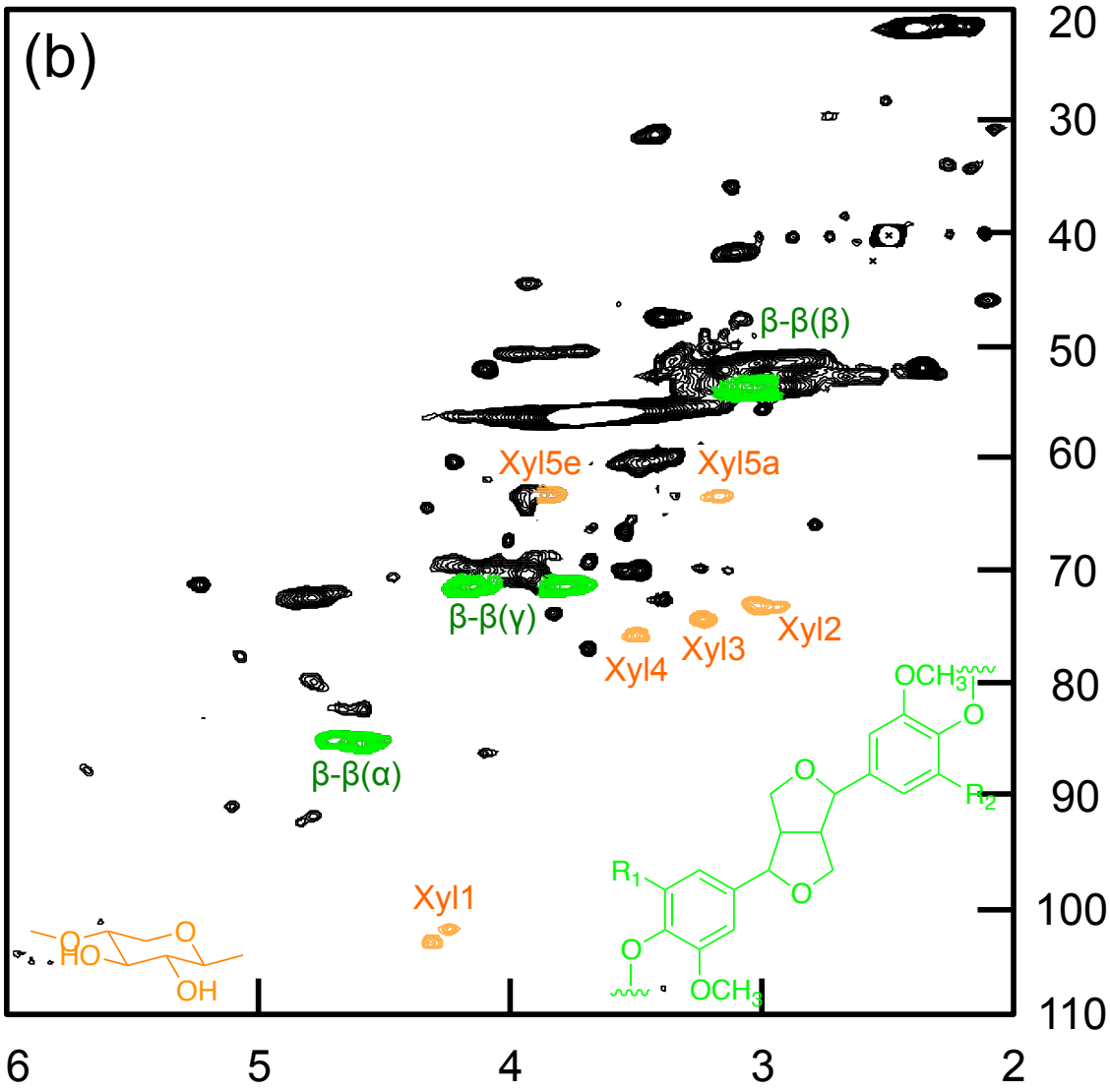

Figure 5-6 (b) HSQC-NMR spectrum (aliphatic region) of **cMWL5-2**

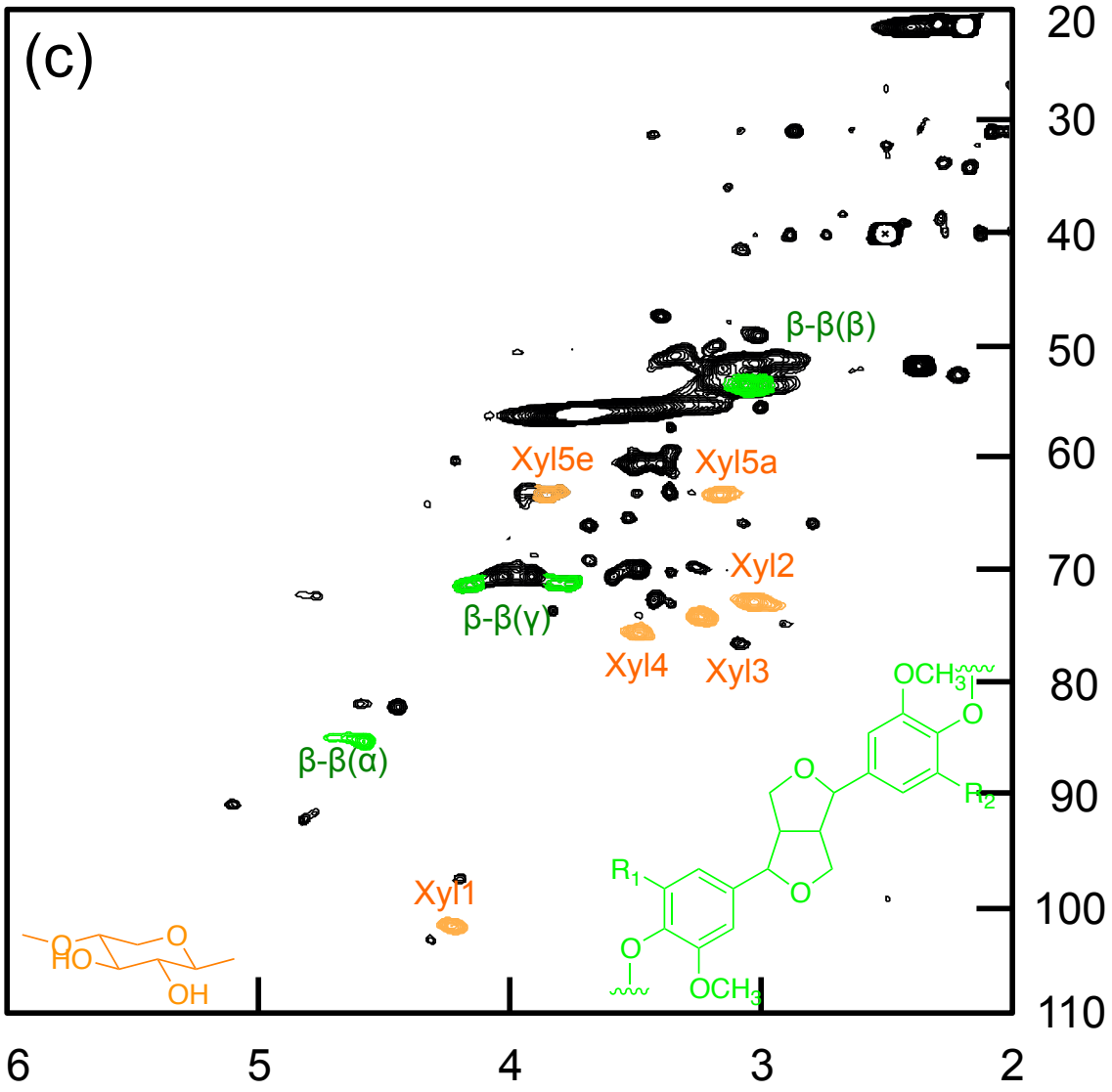

Figure 5-6 (c) HSQC-NMR spectrum (aliphatic region) of **cMWL5-3**

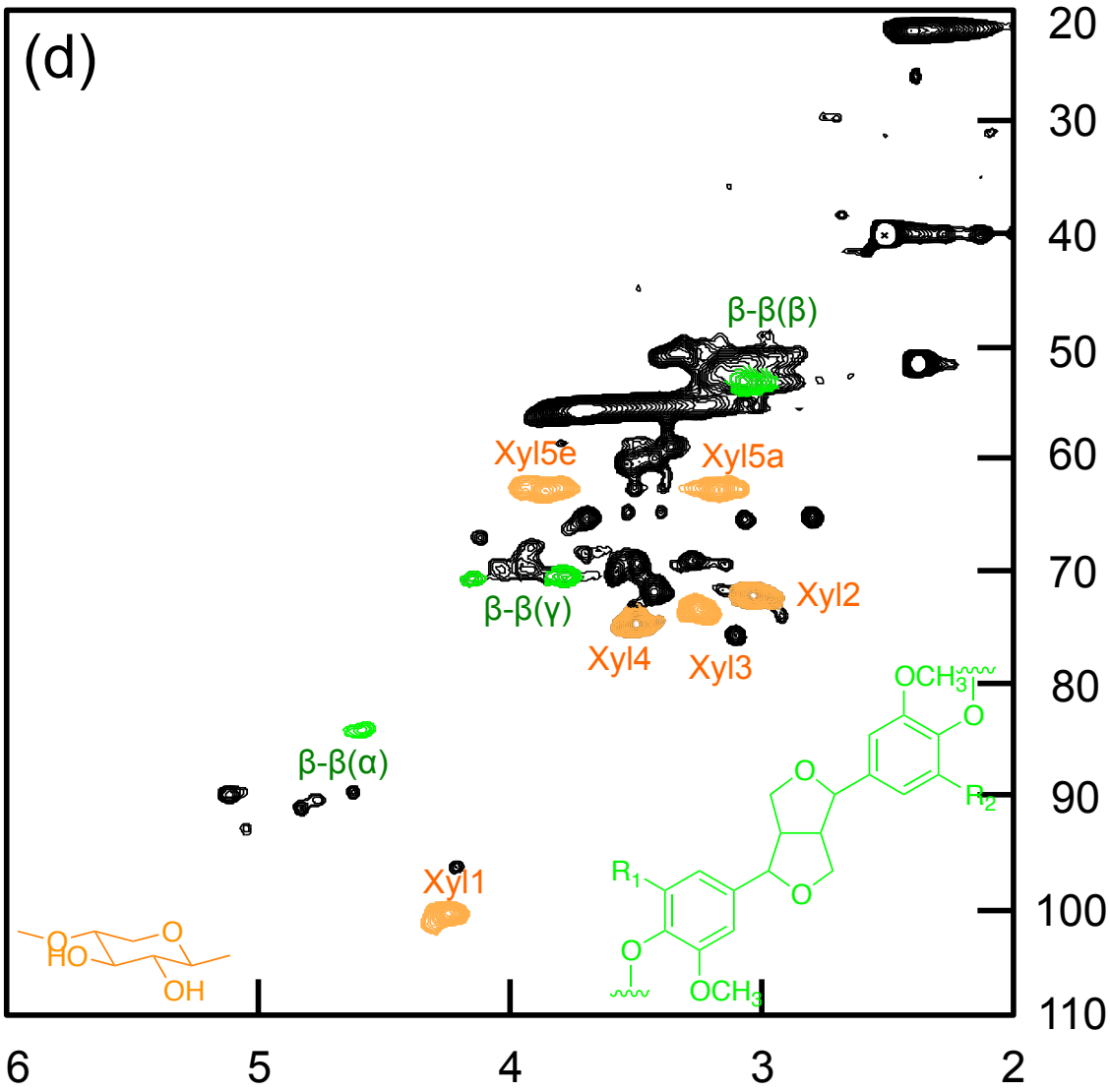

Figure 5-6 (d) HSQC-NMR spectrum (aliphatic region) of **cMWL5-4**

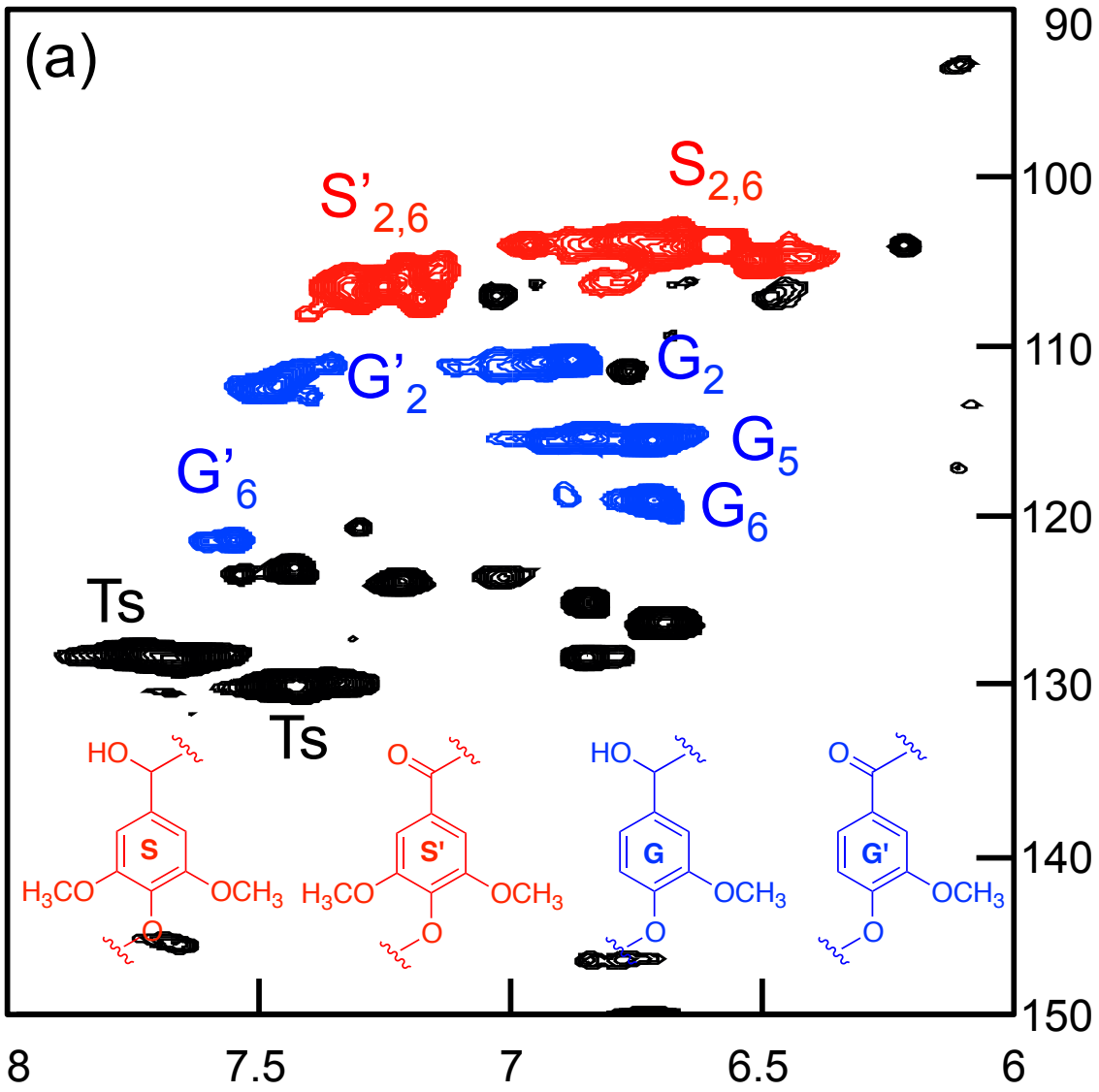

Figure 5-7 (a) HSQC-NMR spectrum (aromatic region) of **cMWL5-1**

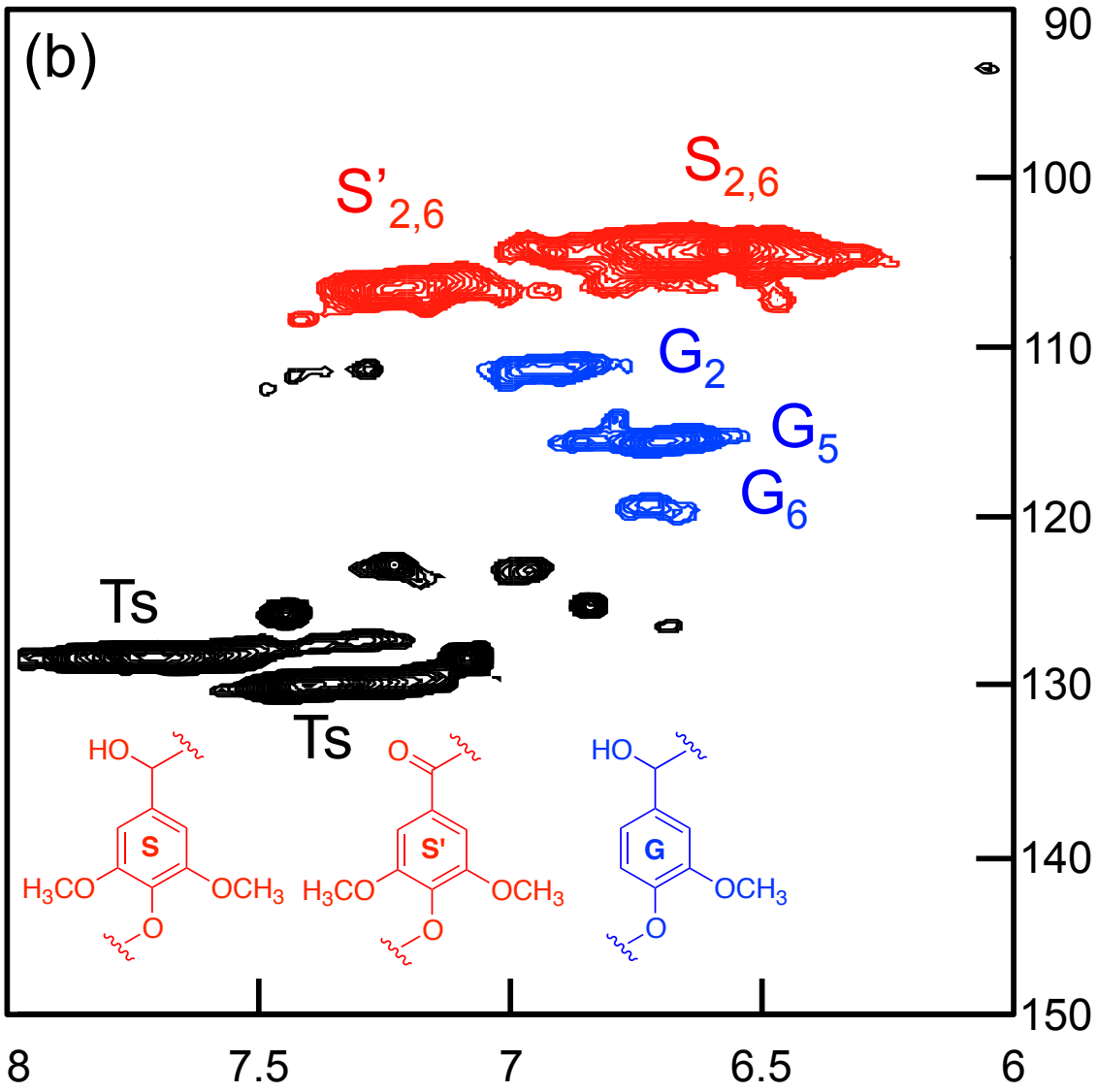

Figure 5-7 (b) HSQC-NMR spectrum (aromatic region) of **cMWL5-2**

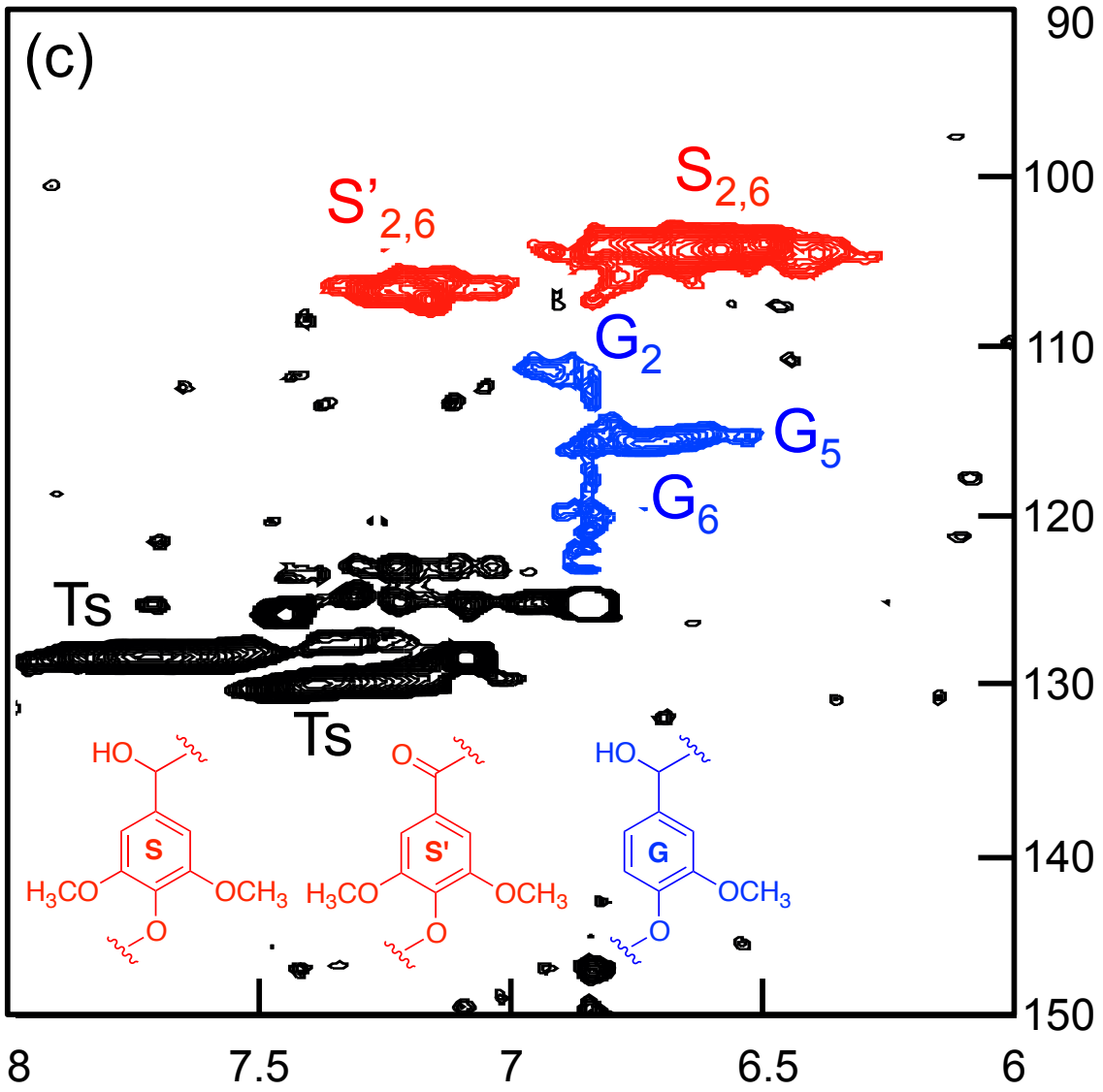

Figure 5-7 (c) HSQC-NMR spectrum (aromatic region) of **cMWL5-3**

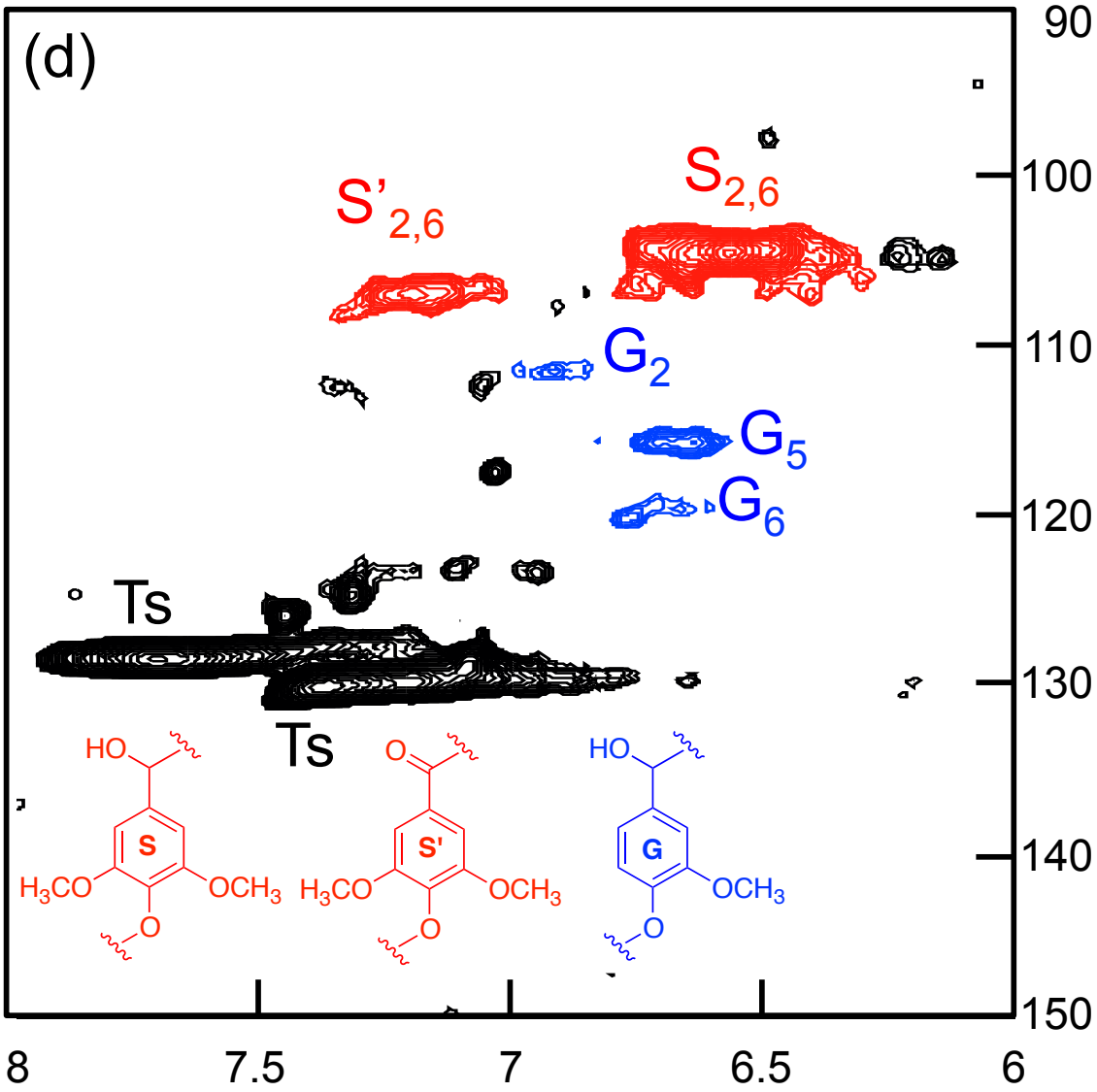

Figure 5-7 (d) HSQC-NMR spectrum (aromatic region) of **cMWL5-4**

5.2.4 Appearance of new peaks in cMWL5

Some new peaks in **cMWL5** were appeared after the alkali treatment. There are five existing area of these new peaks (A: 3.00-4.12/30.0-51.3 ppm, C: 3.24-3.74/61.9-68.1 ppm, B: 4.38-5.15/70.0-82.5 ppm, D: 2.86-3.74/68.1-76.9 ppm, E: 4.12-5.15/89.4-97.5 ppm), shown in Figure 5-8. In **cMWL5-1** and **cMWL5-2** that are high lignin-content fractions, peaks of A~C regions are observed (Figure 5-6a and 5-6b). On the other hand, peaks of D~E regions are observed in **cMWL5-3** and **cMWL5-4** that are high xylan-content fractions (Figure 5-6c and 5-6d). Thus, it is considered that three (A~C) regions derived from lignin moiety and two (D and E) regions derived from xylan moiety. In future, these peaks maybe clear by the more detailed research of the degradation products with various analyses such as HPLC and GC analyses.

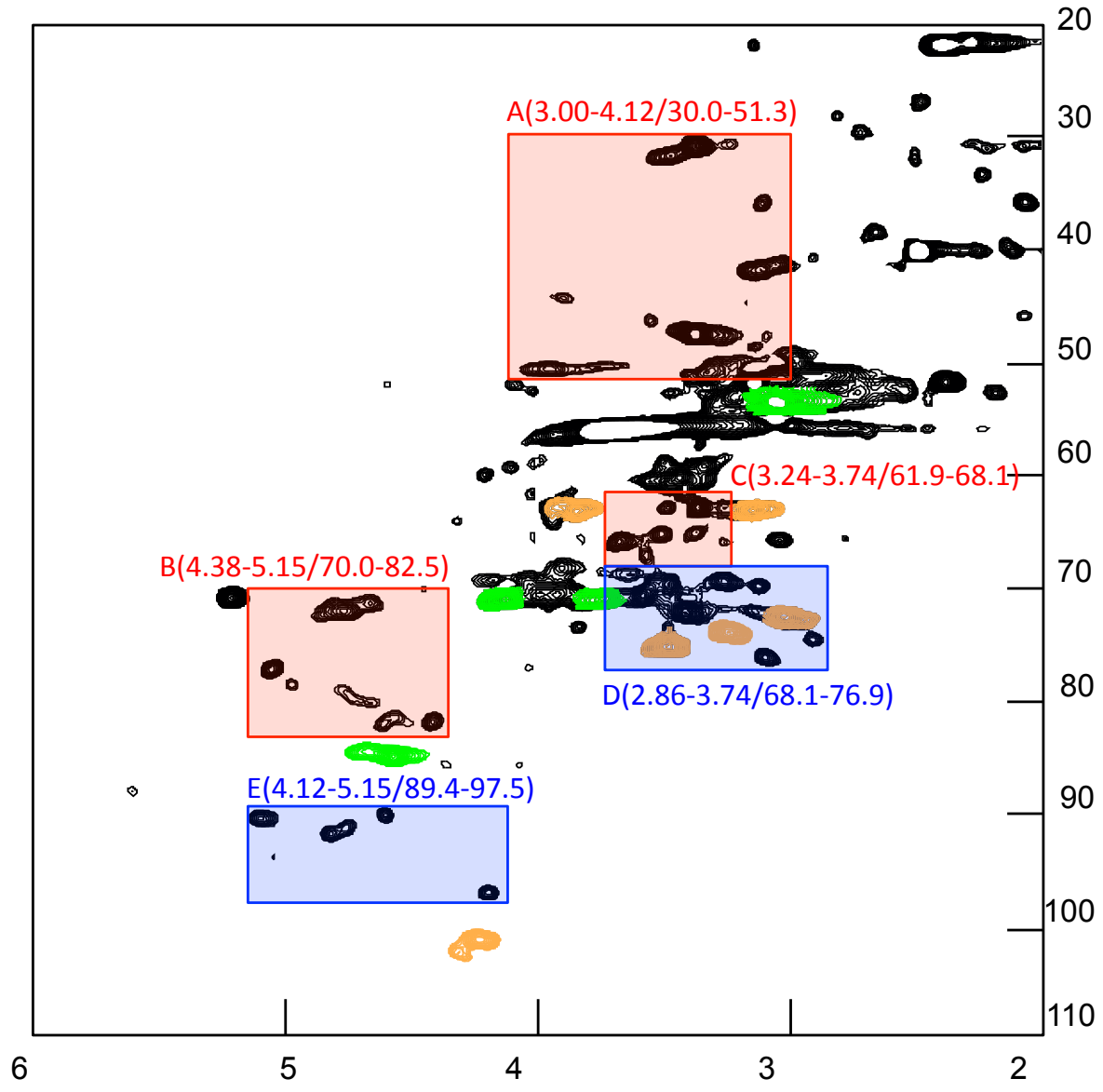

Figure 5-8 Five peak areas in HSQC-NMR spectrum of **cMWL5** (A, B, C, D and E)

5.3 Summary

Lignin in crude MWL from *Eucalyptus globulus* was degraded selectively by γ-TTSA method. Under γ-TTSA reaction sequence, β-O-4 linkages are transformed to γ-sulfone derivatives and finally cleaved without damaging other structures such as β-β substructures and xylan. The obtained degradation products, named as **cMWL5**, were fractionated with some organic solvent to afford four fractions. One was the fraction of low molecular lignin degradation products (**cMWL5-1**) and others were soluble different LCC fractions (**cMWL5-2**, **cMWL5-3** and **cMWL5-4**). These LCC fractions contain abundant S-type lignin, contained β-β substructure. Especially, the contained lignin in **cMWL5-4** consists of β-β substructure almost all. These results show that the syringaresinol-type β-β substructure plays an important role for linking between lignin and xylan. In future, the bonding site may be obtained by the enzymatic treatment of these fractions although we need detailed researches.

Conclusions

In the thesis, the author has demonstrated the development and the usefulness of γ-TTSA method for the structural analysis of LCCs. α-TSA reaction seaquence, named as α-TSA method, was established. It demonstrated that the cleavage of β-O-4 linkage proceeded under mild alkali treatment without side reactions by the existence of a sulfone group at a neighboring carbon of the β-O-4 linkage (Chapter 1). Based on this result, γ-TTSA reaction sequence, named as γ-TTSA method for LCC anlaysis, was established in dimer model experiment. In γ-TTSA method, the structures at α-position in lignins, such as benzyl ether-type LCC bonding site, are retained (Chapter 2). In polymer model experiment, it was demonstrated that each reaction proceeded without any difficulty and β-O-4 linkages were cleaved selectively (Chapter 3). Indeed, when γ-TTSA method was applied to purified MWL, β-O-4 linkages were cleaved without damaging the other structure and its molecular weight decreased (Chapter 4). Accordingly, it was demonstrated that γ-TTSA method was useful for lignin degradation. Finally, lignin in crude MWL containing xylan was degraded by γ-TTSA method and fractionated by solvent extraction to obtain some LCC fractions. The new knowledge of LCC that the β-β substructure plays an important role for linking between lignin and xylan was obtained by the chemical structural analysis of the fractions (Chapter 5). From these results, it was insisted that γ-TTSA method was a useful lignin degradation method for LCC analysis. In the future, the information obtained by γ-TTSA method will contribute to investigate the chemical structures about LCC bonding sites. The following is summarized results.

In Chapter 1, the author described the development of a novel lignin degradation method named as α-TSA method. This method consists of three steps; α-thioetherification (T) at the α-position, sulfonylation by oxidation (S) and alkali treatment (A). β-O-4 linkage was quantitatively cleaved by α-TSA method in the application to guaiacyl type lignin dimer model compound to obtain *E*- and *Z*- α-β

unsaturated sulfone compounds. The β-O-4 cleavage reaction proceeded with a mild alkali treatment without side reactions unlike conventional methods (acidolysis, thioacidolysis and DFRC etc.) with strong acid and high temperature conditions. Thus, it was demonstrated that β-elimination of sulfone compound was able to cleave the β-O-4 linkage under the mild condition without side reactions and then the α-TSA method was useful for the chemical structural analysis of lignin.

In Chapter 2, the author described the development of a novel lignin degradation method for the analysis of LCCs, named as γ-TTSA method. The method consists of four steps; tosylation (T) of a primary hydroxyl group at γ-position, subsequent thioetherification (T) (substitution reaction with Dod-SH), sulfonylation (S) by oxidation with oxone and the cleavage of β-O-4 linkage by mild alkali treatment (A). In three non-phenolic β-O-4 lignin dimer model compounds guaiacyl, syringyl and *p*-hydoxylphenyl type, the β-O-4 linkages were quantitatively cleaved by γ-TTSA method to afford γ-β olefinic sulfone compounds. The β-O-4 cleavage initiated from the γ-position retains some information about the α-linkage. Thus, it was demonstrated that γ-TTSA method was useful for isolation of LCC bonding sites, where the α-position of lignin is involved in linkages to polysaccharides.

In Chapter 3, the author described the influence of other substructures except β-O-4 substructure and the reactivity of polymer in TTSA reaction sequence using artificial lignin, a so-called dehydrogenation polymer (DHP). The obtained DHP according to the Zutropf method consists of β-O-4, β-5 and β-β substructures. Each reaction step of the method was followed by FT-IR and HSQC-NMR analyses. Tosylation proceeded selectively at the primary hydroxyl groups at γ-position of β-O-4 and β-5 substructures. Subsequent thioetherification and sulfonylation proceeded quantitatively. The β-O-4 and β-5 substructures in DHP were transformed to γ-sulfone derivatives without any side chain. Then, β-O-4 linkages were cleaved selectively by mild alkali treatment. On the other hand, β-5

and β-β linkages were intact after γ-TTSA treatment. In GPC analysis, it was found that molecular weight was decreased after γ-TTSA method. It is reconfirmed that γ-TTSA method is useful for the degradation of lignin polymer.

In Chapter 4, the author described the degradation of purified MWL (**pMWL1**) from *Eucalyptus globulus* by γ-TTSA method. The MWL consist of β-O-4 and β-β substructures mainly. β-O-4 substructures in **pMWL1** were transformed to γ-sulfone derivatives without any side chain. In final step, the β-O-4 linkages were cleaved selectively without side reactions unlike the conventional methods. The reaction sequence was followed by HSQC-NMR analysis. Moreover, the peak at 570 Da of the expected degradation product and the peak at 1260 Da of degradation oligomer were found in GPC chromatogram of the obtained degradation product (**pMWL5**). The *Mw* of **pMWL1** is decreased indicating the break down of the macromolecule to oligomers or monomers. As a consequence, natural lignin can be degraded by γ-TTSA method without the transformation of the structure at α-position.

In Chapter 5, the author described that lignin in crude MWL (**cMWL1**) from *Eucalyptus globulus* was selectively degraded by γ-TTSA method. The **cMWL1** contains β-O-4 and β-β substructures in lignin moiety and xylan in polysaccharide. Tosylation proceeded selectively at γ-position of β-O-4 substructure. For this, β-O-4 substructures in **cMWL1** were transformed to γ-sulfone derivatives without the transformation of the other structures and the following alkali treatment cleaved almost the β-O-4 linkages selectively. Then, the obtained degradation products were extracted with three organic solvents (Et_2O, EtOAc and THF) to afford the four fractions (**cMWL5-1**, **cMWL5-2**, **cMWL5-3** and **cMWL5-4**). Three of these fractions were LCC fractions containing xylan. The extraction with solvents was useful for the removal of low molecular lignin degradation products. Especially, the highest xylan-content **cMWL5-4**, that is extractive residue, contains mainly

syringaresinol-type β-β substructure as lignin moiety. This fact suggests that the β-β substructure plays an important role for linking between lignin and xylan.

Experimental Section

Chapter 1

Materials and methods

The guaiacyl lignin dimer model compound (**1G**) was synthesized by the modified method described in the literature (Nakatsubo et al. 1975). Preparative thin-layer choromatography (P-TLC) was performed on silica gel plates [Kieselgel 60 F_{254}; Merck (Darmstadt, Germany) 2 mm×20 cm×20 cm]. 1-Dodecane thiol (Dod-SH) was purchased from Tokyo Chemical Industry Co. (Tokyo, Japan). Other reagents were purchased from Nacalai Tesque (Kyoto, Japan) and used as received.

Mesurements

The instrument for ^{1}H- and ^{13}C-nuclear magnetic resonance (NMR) spectroscopy was a Varian INOVA 300 FT-NMR (Varian, Santa Clara, CA, USA) (300 MHz) spectrometer; samples were dissolved in $CDCl_3$ with tetramethylsilane(TMS) as an internal standard. Proton signals were assigned by 2D NMR (gCOSY) experiments and carbonsignals by 2D NMR (gHSQC) experiments. Chemical shifts (δ) and coupling constants (*J*) are given in δ-values (ppm) and Hz, respectively. Matrix-assisted laser desorption/ionization times-of-flight mass spectropy (MALDI-TOF MS) spectra were recorded with a Bruker MALDI-TOF MS Reflex III (Bruker, Billerica, MA, USA) in the positive ion and reflector modes. For ionization, a nitrogen laser was used. All spectra were measured in the reflector mode using external calibration. 2,5-Dihydroxybenzoic acid (DHB) served as a matrix. A Perkin Elmer Spectrum Fourier transforminfrared (FT-IR) spectrometer (Perkin Elmer, Boston, MA, USA) was used. The attenuated total reflectance (ATR) technique was applied.

α-thioetherification

To a solution of compound **1G** (only *erythro* isomer) (121.2 mg, 0.295 mmol) dissolved in 5

ml of dichloromethane, Dod-SH (141 μl, 0.591 mmol) and boron trifluoride etherate (10 μl, 0.0810 μmol) were added. The reaction mixture was kept at room temperature (r.t.) for 1 h and then diluted with ethyl acetate, washed with brine, dried over Na_2SO_4, concentrated *in vacuo* to give a colorless syrup, which was purified by P-TLC developed with ethyl acetate / *n*-hexane (1:2, v/v) to give compound **2G** (*erythro*/*threo* = 3/2) as colorless syrup (143.3 mg, 81.3 % yield).

Compound 2G

^{1}H NMR δ ($CDCl_3$): 0.88 (3H, t *J*=6.9, C*H*$_3$(CH$_2$)$_{11}$S), 1.25 (18H, broad , CH$_3$(C*H*$_2$)$_9$CH$_2$CH$_2$S), 1.50 (2H, m, CH$_3$(CH$_2$)$_9$C*H*$_2$CH$_2$S), 2.37 (2H, m, CH$_3$(CH$_2$)$_9$CH$_2$C*H*$_2$S), 3.30 (H, dd *J*=2.7, 12.6, Hγ), 3.52 (H, dd *J*=2.4, 12.6, Hγ), 3.78, 3.86, 3.87, 3.89 (6H, s, H$_3$CO), 3.95 (H, dd *J*=4.2, 12.0, Hγ), 4.18 (Hα), 4.25 (Hβ), 4.28 (Hβ), 4.35(Hα) (4H, m), 5.14 (2H, s, C*H*$_2$C$_6$H$_5$), 6.62-7.45 (12H, m, H in arom.),

^{13}C NMR δ ($CDCl_3$): 14.1, 22.7, 28.8, 28.9, 29.2, 29.3, 29.5, 29.6, 29.6, 29.6, 31.6, 31.8, 31.9 (C$_{12}$H$_{25}$S), 50.6, 50.9(Cα), 55.7, 55.9, 56.0, 56.1 (CH$_3$O), 61.3, 62.3 (Cγ), 71.0 (CH$_2$C$_6$H$_5$), 87.0, 88.1 (Cβ), 111.6, 111.9, 112.0, 112.1, 113.4, 113.6, 120.4, 121.0, 121.1, 121.2, 121.3, 121.6, 123.6, 124.0, 127.3, 127.8, 127.8, 128.0, 128.4, 128.5, 128.6, 132.0, 133.1, 137.0, 137.2, 147.3, 147.4, 147.5, 147.6, 149.5, 149.7, 151.1, 151.5 (C in arom.)

MALDI-TOF MS: m/z $[M+Na]^+$ calculated for $C_{36}H_{50}O_5S$: 617.84 ; found:617.43

Sulfonylation (oxidation)

To a solution of compound **2G** (116.1 mg, 0.195 mmol) dissolved in 3 ml of dioxane/H_2O (9/1, v/v), oxone (358.3 mg, 0.584 mmol) was added. The reaction mixture was stirred for 3h at r.t., and then diluted with ethyl acetate, washed with brine, dried over Na_2SO_4 and then concentrated *in vacuo* to give compound **3G** (*erythro*/*threo* = 3/2) as colorless syrup (119.5 mg, 99.3 % yield). A part of compound **3G** was separated by P-TLC developed with dichloromethane to give *erythro*-**3G** (Rf-value:

0.06) and *threo*-**3G** (Rf-value: 0.21).

Compound *erythro*-3G

^{1}H NMR δ ($CDCl_3$): 0.88 (3H, t *J*=6.6, C*H*$_3$C$_{11}$H$_{22}$SO$_2$), 1.20, 1.24 (18H, broad, CH$_3$C$_9$*H*$_{18}$C$_2$H$_4$SO$_2$), 1.71 (2H, broad,C$_{10}$H$_{21}$C*H*$_2$CH$_2$SO$_2$), 2.77 (2H, m, C$_{11}$H$_{23}$C*H*$_2$SO$_2$), 3.76 (3H, s, H$_3$CO), 3.84 (1H, dd *J*=4.2, 12.3, Hγ), 3.87 (3H, s, H$_3$CO), 4.00 (1H, dd *J*=3.9, 12.3, Hγ), 4.53 (1H, d *J*=6.3, Hα), 5.06 (1H, m, Hβ), 5.17 (2H, s, C*H*$_2$C$_6$H$_5$),6.82-7.44 (12H, m, H in arom.)

^{13}C NMR δ ($CDCl_3$): 14.1, 21.1, 22.7, 28.4, 29.0, 29.2, 29.3, 29.5, 29.6, 31.9, 51.7, (C$_{12}$H$_{25}$SO$_2$), 55.7, 56.0 (CH$_3$O), 61.9 (Cγ), 69.0 (Cα), 70.8 (*C*H$_2$C$_6$H$_5$), 80.1 (Cβ), 112.0, 113.4, 113.6, 119.2, 121.3, 123.6, 123.7, 127.3, 128.0, 128.6, 136.7, 146.5, 148.8, 149.5, 150.9 (C in arom.)

Compound *threo*-3G

^{1}H NMR δ ($CDCl_3$): 0.88 (3H, t *J*=6.3, C*H*$_3$C$_{11}$H$_{22}$SO$_2$), 1.22 (18H, broad, CH$_3$C$_8$*H*$_{16}$C$_3$H$_6$SO$_2$), 1.38 (2H, broad,C$_{10}$H$_{19}$C*H*$_2$CH$_2$CH$_2$SO$_2$), 1.91 (2H, m, C$_{10}$H$_{21}$C*H*$_2$CH$_2$SO$_2$), 3.05 (2H, d *J*=12.6, Hγ), 3.27 (2H, m, C$_{11}$H$_{23}$C*H*$_2$SO$_2$), 3.57 (2H, d *J*=12.3, Hγ), 3.89 (3H, s, H$_3$CO), 3.90 (3H, s, H$_3$CO), 4.70 (2H, s, Hα Hβ), 5.15 (2H, s, C*H*$_2$C$_6$H$_5$), 6.88-7.50 (12H, m, H in arom.)

^{13}C NMR δ ($CDCl_3$): 14.1, 22.1, 22.7, 28.5, 29.0, 29.2, 29.3, 29.5, 29.6, 29.6, 31.9, 56.2, (C$_{12}$H$_{25}$SO$_2$), 55.9, 56.1 (CH$_3$O), 59.6 (Cγ), 68.2 (Cα), 70.9 (*C*H$_2$C$_6$H$_5$), 84.4 (Cβ), 112.0, 112.7, 113.9, 122.1, 122.2, 122.6, 125.1, 127.3, 127.9, 128.6, 136.8, 145.5, 149.0, 149.9, 152.0 (C in arom.)

MALDI-TOF MS: m/z $[M+Na]^+$ calculated for $C_{36}H_{50}O_7S$: 649.83 ; found:649.05

Mild alkali treatment

To a solution of compound **3G**(46.7 mg, 0.0755 mmol), consisting of *erythro* and *threo* isomers (*erythro*/*threo* = 3/2), dissolved in 4.50 ml of dioxane, 1M NaOH aqueous solution (0.50 ml) was added.

The reaction mixture was stirred for 12 h at r.t. and then diluted with ethyl acetate, washed with brine, dried over Na_2SO_4 and then concentrated *in vacuo* to give a colorless syrup. This syrup was purified by P-TLC developed with ethyl acetate /n-hexane (1/3, v/v) four times to give *Entgegen*(*E*)-**4G** (20.7 mg, 54.6 % yield) (Rf-value: 0.38) and *Zusammen*(*Z*)-**4G** (12.2 mg, 32.9 % yield) (Rf-value: 0.46).

Compound *E*-4G

^{1}H NMR δ ($CDCl_3$): 0.88 (3H, t *J*=6.3, C*H*$_3$C$_{11}$H$_{22}$SO$_2$), 1.22 (18H, broad, CH$_3$C$_9$*H*$_{18}$C$_2$H$_4$SO$_2$), 1.67 (2H, m, C$_{10}$H$_{21}$C*H*$_2$CH$_2$SO$_2$), 2.75 (2H, m, C$_{11}$H$_{23}$C*H*$_2$SO$_2$), 3.89 (3H, s, H$_3$CO), 4.24 (2H, d *J*=6.0, Hγ), 5.18 (2H, s, C*H*$_2$C$_6$H$_5$), 6.79 (1H, dd *J*=2.1, 8.2, H6 in arom.), 6.91 (1H, d *J*=8.7, H5 in arom.), 7.02 (1H, d *J*=2.1, H2 in arom.),7.08 (1H, t *J*=6.0, Hβ), 7.32-7.46 (5H, m, C$_5$ *H*$_6$CH$_2$)

^{13}C NMR δ ($CDCl_3$): 14.1, 22.1, 22.7, 28.2, 29.0, 29.2, 29.3, 29.4, 29.6, 31.9, 51.4 (C$_{12}$H$_{25}$SO$_2$), 56.1 (CH$_3$O), 59.7 (Cγ), 70.9 (*C*H$_2$C$_6$H$_5$), 140.9 (Cβ), 113.1, 113.4, 122.6, 122.7, 127.2, 128.1, 128.6, 136.5, 141.0, 149.3, 149.6 (C in arom.)

MALDI-TOF MS: m/z $[M+Na]^+$ calculated for $C_{29}H_{42}O_5S$: 525.70 ; found: 525.03

Compound *Z*-4G

^{1}H NMR δ ($CDCl_3$): 0.88 (3H, t *J*=6.3, C*H*$_3$C$_{11}$H$_{22}$SO$_2$), 1.24, 1.21 (18H, broad, CH$_3$C$_9$*H*$_{18}$C$_2$H$_4$SO$_2$), 1.67 (2H, m, C$_{10}$H$_{21}$C*H*$_2$CH$_2$SO$_2$), 2.77 (2H, m, C$_{10}$H$_{21}$CH$_2$C*H*$_2$SO$_2$), 3.90 (3H, s, H$_3$CO), 4.77 (2H, d *J*=5.7, Hγ), 5.17 (2H, s, C*H*$_2$C$_6$H$_5$), 6.47 (1H, t *J*=5.4, Hβ), 6.87 (1H,d *J*=8.1, H5 in arom.), 6.96 (1H,dd *J*=2.1, 8.1, H6 in arom.), 7.12 (1H,d *J*=2.1, H2 in arom.), 7.31-7.45 (5H, m, C$_5$ *H*$_6$CH$_2$)

^{13}C NMR δ ($CDCl_3$): 14.1, 21.9, 22.6, 28.2, 29.0, 29.2, 29.3, 29.4, 29.6, 31.9, 53.2 (C$_{12}$H$_{25}$SO$_2$), 56.1 (CH$_3$O), 59.1 (Cγ), 70.9 (*C*H$_2$C$_6$H$_5$), 145.7 (Cβ), 112.5, 113.3, 121.8, 127.2, 127.3, 128.0, 128.6, 136.6, 139.5, 149.1, 149.3 (C in arom.)

MALDI-TOF MS: m/z $[M+Na]^+$ calculated for $C_{29}H_{42}O_5S$: 525.70 ; found: 525.10

Monitoring of the β-elimination reaction

Compound **3G** (4.8 mg, 0.00767 mmol) was dissolved in dioxane (1.080 ml). The degradation was initiated by adding 1M NaOH aqueous solution (0.120 ml) at r.t. to the solution. An aliquot of the reaction mixture (100 μl) was sequentially sampled at 0.16, 0.5, 1, 2, 3, 6 and 12 h and mixed with 100 μl of 0.1M AcOH (dioxane/water = 9/1) solution. The mixture was subjected to high-performance liquid chromatography (HPLC) on Shimazu LC-20AT with a PDA detector (SPD-M20A, monitoring at 280 nm) (Kyoto, Japan) under the following conditions. Column: Cosmosil 5C18-MS (4.6×150 mm; Nacalai Tesque, Kyoto, Japan); eluent: H_2O/MeOH [initially H_2O/MeOH: 80/20 (v/v), linear gradient over 10 min to H_2O/MeOH: 20/80 (v/v), held isocratically at H_2O/MeOH: 20/80 (v/v) for 50min: flow rate: 1.0 ml min^{-1}].

Chapter 2

Mesurements

The instrument for ^{1}H- and ^{13}C-NMR spectroscopy was a Varian INOVA 300 FT-NMR (Varian, Santa Clara, CA, USA) (300 MHz) spectrometer; samples were dissolved in chloroform-*d* with TMS as an internal standard. Proton signals were assigned by 2D NMR (gCOSY) experiments and carbon signals by 2D NMR (gHSQC) experiments. Chemical shifts (δ) and coupling constants (*J*) are given in δ-values (ppm) and Hz, respectively. MALDI-TOF MS spectra were recorded with a Bruker MALDI-TOF MS Reflex III (Bruker, Billerica, MA, USA) in the positive ion and reflector modes. For ionization, a nitrogen laser was used. All spectra were measured in the reflector mode using external calibration. DHB served as a matrix. A Perkin Elmer Spectrum FT-IR spectrometer (Perkin Elmer, Boston, MA, USA) was used.

Materials and reagents

The guaiacyl (**1G**), syringyl (**1S**), and *p*-hydroxyphenyl (**1H**) lignin model compounds were synthesized by the modified method described in the literature (Nakatsubo et al. 1975). Only the *erythro* isomer of **1G**, and a mixture consisting of *erythro*/*threo* isomers (5:3) of **1S** and **1H** were investigated in the present study. P-TLC was performed on silica gel plates [Kieselgel 60 F_{254}; Merck (Darmstadt, Germany) 2 mm×20 cm×20 cm]. Dod-SH was purchased from Tokyo Chemical Industry Co. (Tokyo, Japan). Other reagents were purchased from Nacalai Tesque (Kyoto, Japan) and used as received.

γ-Tosylation

Tosyl chloride (TsCl) (124.0 mg, 0.645 mmol) was added to a stirred solution of **1G** (53.1 mg, 0.129 mmol) dissolved in 4 ml of dry pyridine. The reaction mixture was kept at room temperature (r.t.) for 3 h and then diluted with ethyl acetate, washed with brine, dried over Na_2SO_4, and then concentrated *in vacuo* to give a colorless syrup, which was purified by P-TLC developed with ethyl acetate/n-hexane (1:2, v/v) to give **5G** as a colorless syrup (63.1 mg, 86.4% yield). **1S** (241.2 mg, 0.513 mmol) and **1H** (109.3 mg, 0.312 mmol) were treated in the same manner to give **5S** (228.7 mg, 71.0% yield) and **5H** (131.0 mg, 83.2% yield), respectively.

Compound 5G

^{1}HNMR δ ($CDCl_3$) of *erythro* isomer: 2.40(3H, s, $CH_3C_6H_4$), 3.67(H, d, *J*=3.6, αOH), 3.83 (3H, s, OCH_3), 3.85 (3H, s, OCH_3), 4.07 (H, dd, *J*=10.2, 2.1, Hγ), 4.31 (H, dd, *J*=17.7, 7.5, Hγ), 4.38 (H, m, Hβ), 4.84 (H, t, *J*=3.6, Hα), 5.14 (2H, s, $CH_2C_6H_5$), 6.68–7.66 (12H, m, aromatic H), 7.23(2H, d, *J*=8.1, aromatic H of tosyl group), 7.64 (2H, d, *J*=8.1, aromatic H of tosyl group)

^{13}CNMR δ ($CDCl_3$) of *erythro* isomer: 21.6 ($H_3CC_6H_4$), 55.9 (OCH_3), 55.7 (OCH_3), 68.5 (Cγ), 70.9 ($CH_2C_6H_5$), 71.5 (Cα), 84.4 (Cβ), 109–151 (109.5, 112.1,113.6, 118.2, 121.0, 121.5, 124.3, 127.2,

127.8, 127.9, 128.5, 129.7, 131.4, 132.5, 137.0, 144.7, 146.4, 147.5, 149.6, 151.4) (aromatic C)

MALDI-TOF MS: m/z $[M+Na]^+$ calculated for $C_{36}H_{50}O_5S$: 587.68 ; found:587.00

Compound 5S

^{1}HNMR δ ($CDCl_3$) of *erythro*/*thereo* (5/3) mixture: 2.40 (3H, s, $CH_3C_6H_4$), 3.77 (3H, s, OCH_3), 3.78 (3H, s, OCH_3), 3.87 (6H, s, OCH_3), 3.92 (0.4H, dd, *J*=10.2, 2.4, Hγ), 3.98 (0.6H, dd, *J*=11.1, 3.3, Hγ), 4.03 (0.4H, dd, *J*=10.2, 2.4, Hγ), 4.37 (0.6H, dd, *J*=10.2, 2.4, Hγ), 4.50 (0.6H, m, Hβ), 4.52 (0.4H, m, Hβ), 4.82 (0.6H, d, *J*=3.0, Hα), 4.97 (0.4H, s, Hα), 5.00 (2H, s, $CH_2C_6H_5$), 6.50–7.75 (14H, m, aromatic H)

^{13}CNMR δ ($CDCl_3$) of *erythro* isomer: 21.6 ($H_3CC_6H_4$), 55.9 (OCH_3), 56.1 (OCH_3), 56.2 (OCH_3), 68.6 (Cγ), 71.6 (Cα), 75.0 ($CH_2C_6H_5$), 83.4 (Cβ), 102–154 (102.8, 103.9, 105.2, 105.4, 124.6, 127.8, 127.9, 128.1, 128.5, 129.6, 152.6, 153.4, 153.5, 153.6) (aromatic C)

MALDI-TOF MS: m/z $[M+Na]^+$ calculated for $C_{36}H_{50}O_5S$: 647.20 ; found:647.31

Compound 5H

^{1}HNMR δ ($CDCl_3$) of *erythro*/*thereo* (5/3) mixture: 2.41 (3H, s, $CH_3C_6H_4$), 3.93 (0.4H, dd, *J*=10.8, 4.5, Hγ), 4.21 (0.4H, dd, *J*=10.8, 3.9, Hγ), 4.22 (0.6H, dd, *J*=10.8, 3.0, Hγ), 4.34 (0.6H, dd, *J*=10.8, 5.7, Hγ), 4.43 (0.4H, m, Hβ), 4.49 (0.6H, m, Hβ), 4.89 (0.4H, d, *J*=6.3, Hα), 4.94 (0.6H, d, *J*=5.1, Hα), 5.04 (2H, s, $CH_2C_6H_5$), 6.74–7.68 (18H, m, aromatic H)

^{13}CNMR δ ($CDCl_3$) of *erythro* isomer: 21.6 ($H_3CC_6H_4$), 67.2 (Cγ), 68.0 (Cγ), 70.0 ($CH_2C_6H_5$), 72.2 (Cα), 72.4 (Cα), 80.2 (Cβ), 80.3 (Cβ), 114–159 (114.8, 115.0, 116.6, 116.7, 122.1, 122.3, 127.4, 127.6, 127.9, 127.9, 128.0, 128.6, 129.5, 129.6, 129.7, 129.8, 131.4, 132.5, 136.8, 144.8, 144.9, 157.9, 158.6, 158.8) (aromatic C)

MALDI-TOF MS: m/z $[M+Na]^+$ calculated for $C_{36}H_{50}O_5S$: 527.16 ; found:527.18

Thioetherification

K_2CO_3 (63.1 mg, 0.112 mmol) and Dod-SH (107 ml, 0.447 mmol) were added to a stirred solution of **5G** (63.1 mg, 0.112 mmol) dissolved in 10 ml of acetone. The reaction mixture was refluxed over-night, then filtrated with ethyl acetate to remove excess K_2CO_3, and washed with ethyl acetate. The combined filtrate and washings were washed with brine, dried over Na_2SO_4, and then concentrated in *vacuo* to give a colorless syrup, which was purified by P-TLC developed with ethyl acetate/*n*-hexane (1:2, v/v) to give **6G** as a colorless syrup (61.0 mg, 91.8% yield). **5S** (228.7 mg, 0.366 mmol) and **5H** (103.5 mg, 0.205 mmol) were treated in the same manner to give **6S** (215.6 mg, 89.9% yield) and **6H** (104.2 mg, 95.0% yield), respectively.

Compound 6G

^{1}H NMR δ ($CDCl_3$): 0.89 (3H, t, *J*=6.9, C*H*$_3$(CH$_2$)$_{11}$S), 1.25 (18H, broad , CH$_3$(C*H*$_2$)$_9$CH$_2$CH$_2$S), 1.47 (2H, m, CH$_3$(CH$_2$)$_9$C*H*$_2$CH$_2$S), 2.49 (2H, m, CH$_3$(CH$_2$)$_9$CH$_2$C*H*$_2$S), 2.61 (H, dd *J*=14.0, 5.7, Hγ), 2.79 (H, dd, *J*=14.0, 4.5, Hγ), 3.86 (3H, s, OCH$_3$), 3.88 (3H, s, OCH$_3$), 4.22 (H, dd, *J*=12.0, 5.7, Hβ), 4.90 (H, d *J*=6.0, Hα), 5.14 (2H, s, C*H*$_2$C$_6$H$_5$), 6.81-7.43 (12H, m, aromatic H)

^{13}C NMR δ ($CDCl_3$): 14.1, 22.7, 28.8, 29.2, 29.3, 29.5, 29.6, 29.6, 31.9, 33.1 (C$_{12}$H$_{25}$SO$_2$), 33.2 (Cγ), 55.7, 55.9 (OCH$_3$), 70.9 (*C*H$_2$C$_6$H$_5$), 75.5 (Cα), 87.8 (Cβ), 110.4, 112.0, 113.7, 119.6, 119.7, 121.4, 123.4, 127.2, 127. 8, 128.5, 133.0, 137.0, 147.8, 148.1, 149.6, 150.6 (C in arom.)

MALDI-TOF MS: m/z $[M+Na]^+$ calculated for $C_{36}H_{50}O_5S$: 617.84 ; found:617.62

Compound 6S

^{1}H NMR δ ($CDCl_3$): 0.88 (3H, t, *J*=6.3, C*H*$_3$(CH$_2$)$_{11}$S), 1.24 (18H, broad , CH$_3$(C*H*$_2$)$_9$CH$_2$CH$_2$S), 1.50 (2H, m, CH$_3$(CH$_2$)$_9$C*H*$_2$CH$_2$S), 2.50 (1.2H, t, *J*=7.2, CH$_3$(CH$_2$)$_9$CH$_2$C*H*$_2$S), 2.56 (0.8H, t, *J*=7.2, CH$_3$(CH$_2$)$_9$CH$_2$C*H*$_2$S), 2.47 (0.4H, dd *J*=14.1, 3.9, Hγ), 2.62 (0.6H, dd, *J*=13.5, 2.7, Hγ), 3.02 (0.6H, dd, *J*=13.8, 7.8, Hγ), 3.20 (0.4H, dd, *J*=14.1, 6.0, Hγ), 3.79 (3H, s, OCH$_3$), 3.80 (3H, s, OCH$_3$), 3.85 (3H, s, OCH$_3$), 3.90 (3H, s, OCH$_3$), 4.24 (0.4H, m, Hβ), 4.40 (0.6H, m, Hβ), 4.83 (0.4H, s, Hα), 4.99 (2H, s,

$CH_2C_6H_5$), 5.07 (0.6H, d *J*=6.6, Hα), 6.57-7.48 (10H, m, aromatic H)

^{13}C NMR δ ($CDCl_3$): 14.1, 22.7, 28.9, 29.0, 29.3, 29.3, 29.5, 29.6, 29.6, 29.6, 29.8, 31.9, 32.6, 33.5 ($C_{12}H_{25}SO_2$), 30.9, 33.8 (Cγ), 55.9, 56.0, 56.1, 56.2 (OCH_3), 74.9 ($CH_2C_6H_5$), 72.6 (Cα), 85.2, 87.5 (Cβ), 103.2, 103.7, 105.1, 105.4, 123.8, 124.2, 127.7, 128.5, 128.5, 128.7, 134.9, 135.0, 135.8, 136.6, 137.8, 152.7, 153.2, 153.4, 153.7 (C in arom.)

MALDI-TOF MS: m/z $[M+Na]^+$ calculated for $C_{36}H_{50}O_5S$: 677.36 ; found:677.44

Compound 6H

^{1}H NMR δ ($CDCl_3$): 0.88 (3H, t, *J*=6.6, $CH_3(CH_2)_{11}S$), 1.25 (18H, broad , $CH_3(CH_2)_9CH_2CH_2S$), 1.47 (2H, m, $CH_3(CH_2)_9CH_2CH_2S$), 2.46 (0.8H, t, *J*=6.3, $CH_3(CH_2)_9CH_2CH_2S$), 2.49 (1.2H, t, *J*=7.2, $CH_3(CH_2)_9CH_2CH_2S$), 2.56 (0.4H, dd *J*=14.1, 6.0, Hγ), 2.66 (0.6H, dd, *J*=13.8, 4.5, Hγ), 2.86 (0.4H, dd, *J*=14.1, 6.0, Hγ), 2.88 (0.6H, dd, *J*=13.8, 6.6, Hγ), 4.49 (0.4H, m, Hβ), 4.56 (0.6H, m, Hβ), 5.03 (0.4H, s, Hα), 5.05 (2H, s, $CH_2C_6H_5$), 5.07 (0.6H, s, Hα), 6.94-7.44 (14H, m, aromatic H)

^{13}C NMR δ ($CDCl_3$): 14.1, 22.7, 28.8, 29.2, 29.3, 29.5, 29.6, 29.6, 31.8, 31.9 ($C_{12}H_{25}SO_2$), 31.2, 33.0 (Cγ), 70.0 ($CH_2C_6H_5$), 73.6, 74.1 (Cα), 82.4 (Cβ), 114.7, 114.8, 116.3, 116.6, 118.3, 121.7, 127.4, 127.8, 128.0, 128.2, 128.6, 129.6 (C in arom.)

MALDI-TOF MS: m/z $[M+Na]^+$ calculated for $C_{36}H_{50}O_5S$: 557.32 ; found:557.34

Sulfonylation (Oxidation)

Thioether **6G** (65.0 mg, 0.109 mmol) was dissolved in 5 ml of dioxane/H_2O (9/1, v/v), and then *m*-chloroperbenzoic acid (MCPBA) (73.8 mg, 0.428 mmol) was added. After stirring at r.t. overnight, the reaction mixture was diluted with ethyl acetate, washed with brine, dried over Na_2SO_4 and then concentrated *in vacuo* to give a colorless syrup, which was purified by P-TLC developed with ethyl acetate/*n*-hexane (1:2, v/v) to give **7G** as a colorless syrup (67.3 mg, 98.2% yield). **6S** (213.2 mg, 0.326 mmol) and **6H** (85.3 mg, 0.160 mmol) were treated in the same manner to give **7S** (168.7 mg, 75.4%

yield) and **7H** (84.6 mg, 93.6% yield), respectively.

Compound 7G

^{1}H NMR δ ($CDCl_3$): 0.88 (3H, t, *J*=6.9, C*H*$_3$C$_{11}$H$_{22}$SO$_2$), 1.24 (16H, broad, CH$_3$CH$_2$C$_8$*H*$_{16}$CH$_2$CH$_2$SO$_2$), 1.37 (2H, m, CH$_3$C*H*$_2$C$_{10}$H$_{20}$SO$_2$), 1.84 (2H, m, C$_{10}$H$_{21}$C*H*$_2$CH$_2$SO$_2$), 2.76 (1H, d *J*=15.0,Hγ), 3.14 (2H, m, C$_{11}$H$_{23}$C*H*$_2$SO$_2$), 3.65 (1H, dd *J*=15.3, 10.8, Hγ), 3.87 (3H, s, OC*H*$_3$), 3.92 (3H, s, OC*H*$_3$), 4.63 (1H, m *J*=11.4, Hβ), 4.88 (1H, d *J*=3.0, Hα), 5.13 (2H, s, C*H*$_2$C$_6$H$_5$), 6.65-7.44 (12H, m, H in arom.)

^{13}C NMR δ ($CDCl_3$): 14.1, 21.7, 22.7, 28.4, 29.0, 29.2, 29.3, 29.5, 29.5, 29.6, 31.9, 55.3 (C$_{12}$H$_{25}$SO$_2$), 51.4 (Cγ), 55.9, 56.0 (OCH$_3$), 70.7 (Cα), 71.1 (*C*H$_2$C$_6$H$_5$), 83.8 (Cβ), 108.8, 111.9, 114.1, 117.6, 122.1, 122.2, 125.3, 127.2, 127.8, 128.5, 130.3, 136.9, 145.3, 147.6, 149.9, 152.0 (C in arom.)

MALDI-TOF MS: m/z $[M+Na]^+$ calculated for C$_{36}$H$_{50}$O$_7$S : 649.83 ; found:649.52

IR (cm^{-1}): 3491, 2923, 2853, 2342, 2095, 1729, 1592, 1501, 1455, 1420, 1380, 1252, 1219, 1177, 1122, 1079, 1023, 913, 853, 808, 741, 696, 510, 462

Compound 7S

^{1}H NMR δ ($CDCl_3$): 0.88 (3H, t, *J*=7.2, C*H*$_3$C$_{11}$H$_{22}$SO$_2$), 1.24 (16H, broad, CH$_3$CH$_2$C$_8$*H*$_{16}$CH$_2$CH$_2$SO$_2$), 1.38 (2H, dd, *J*=14.7, 7.5, CH$_3$C*H*$_2$C$_{10}$H$_{20}$SO$_2$), 1.87 (2H, m, C$_{10}$H$_{21}$C*H*$_2$CH$_2$SO$_2$), 2.85 (1H, d *J*=15.6,Hγ), 3.13 (0.8H, m, C$_{11}$H$_{23}$C*H*$_2$SO$_2$), 3.36 (1.2H, m, C$_{11}$H$_{23}$C*H*$_2$SO$_2$), 3.61 (1H, dd *J*=15.1, 9.3, Hγ), 3.77 (3H, s, OC*H*$_3$), 3.80 (3H, s, OC*H*$_3$), 3.86 (3H, s, OC*H*$_3$), 3.93 (3H, s, OC*H*$_3$), 4.74 (0.4H, m, Hβ), 4.86 (0.6H, s, Hβ), 4.85 (0.6H, s, Hα), 4.98 (2H, s, C*H*$_2$C$_6$H$_5$), 5.14 (0.4H, d, *J*=5.4, Hα), 6.46-7.49 (10H, m, H in arom.)

^{13}C NMR δ ($CDCl_3$): 14.1, 21.5, 22.7, 28.5, 29.0, 29.0, 29.2, 29.3, 29.5, 29.5, 29.6, 31.9, 53.8 (C$_{12}$H$_{25}$SO$_2$), 52.4 (Cγ), 55.8, 56.0, 56.1 (OCH$_3$), 71.3 (Cα), 74.5, 74.9 (*C*H$_2$C$_6$H$_5$), 80.5 (Cβ), 102.5, 103.4, 104.9, 105.1, 105.2, 127.8, 128.1, 128.5, 128.5, 132.6, 133.2, 136.0, 137.7, 152.2, 153.2, 153.7,

153.7 (C in arom.)

MALDI-TOF MS: m/z $[M+Na]^+$ calculated for $C_{36}H_{50}O_7S$: 709.35 ; found:709.50

IR (cm^{-1}): 3500, 2921, 2850, 1595, 1494, 1480, 1464, 1455, 1417, 1378, 1336, 1296, 1258, 1228, 1187, 1150, 1124, 1088, 1069, 1016, 1000, 896, 873, 843, 812, 792, 773, 751, 734, 718, 698, 645, 622, 530, 512, 457, 438

Compound 7H

^1H NMR δ ($CDCl_3$): 0.88 (3H, t, *J*=6.9, $CH_3C_{11}H_{22}SO_2$), 1.23 (18H, broad, $CH_3CH_2C_8H_{16}CH_2CH_2SO_2$), 1.71 (0.8H, m, $C_{10}H_{21}CH_2CH_2SO_2$), 1.78 (1.2H, m, $C_{10}H_{21}CH_2CH_2SO_2$), 2.89 (1.2H, m, $C_{11}H_{23}CH_2SO_2$), 2.97 (0.8H, m, $C_{11}H_{23}CH_2SO_2$), 3.14 (0.4H, dd, *J*=15.0, 8.4,Hγ), 3.30 (0.4H, dd *J*=15.3, 3.3, Hγ), 3.61 (0.6H, dd *J*=15.3, 9.6, Hγ), 4.94 (0.4H, t, *J*=2.4, Hβ), 4.97 (0.6H, t, *J*=2.4, Hβ), 5.02 (0.4H, d, *J*=4.8, Hα), 5.09 (0.6H, d, *J*=2.7, Hα), 5.08 (2H, s, $CH_2C_6H_5$), 6.94-7.44 (14H, m, H in arom.)

^{13}C NMR δ ($CDCl_3$): 14.1, 21.7, 21.8, 22.7, 28.3, 28.3, 28.9, 28.9, 29.2, 29.3, 29.5, 29.5, 29.6, 31.9, 54.7, 54.9 ($C_{12}H_{25}SO_2$), 51.5, 53.1 (Cγ), 72.9, 78.7 (Cα), 70.0 ($CH_2C_6H_5$), 72.0, 76.0 (Cβ), 114.8, 115.1, 115.8, 117.0, 122.3, 122.9, 126.9, 127.4, 127.9, 128.0, 128.6, 129.9, 130.2, 130.3, 131.0, 136.7, 156.3, 157.0, 158.7, 158.8 (C in arom.)

MALDI-TOF MS: m/z $[M+Na]^+$ calculated for $C_{36}H_{50}O_7S$: 589.31 ; found:589.38

IR (cm^{-1}): 3459, 2920, 2851, 1586, 1511, 1486, 1466, 1392, 1288, 1239, 1175, 1124, 1068, 1023, 888, 866, 839, 811, 773, 751, 723, 698, 692, 655, 636, 486

Alkali treatment

Monitoring of the reaction

γ-Sulfone **7G** (4 mg) was dissolved in dioxane (0.9 ml). The degradation was initiated by adding 0.3 M NaOH aqueous solution (0.1 ml) at r.t. to the solution. An aliquot of the reaction mixtures (100 ml) was

sampled after 0.5, 1, 2, and 3 h, and mixed with 100 ml of 0.03 M AcOH solution (dioxane/ H_2O=9/1). The mixture was subjected to HPLC on a Shimadzu LC-20AT with a PDA detector (SPD-M20A, monitoring at 280 nm) under the following conditions. Column: Cosmosil 5C18-MS (4.6=150 mm; Nacalai Tesque, Kyoto, Japan); eluent: H_2O/MeOH [initially H_2O/MeOH: 20/80 (v/v), linear gradient over 10 min to H_2O/MeOH: 80/20 (v/v), held isocratically at H_2O/MeOH: 80/20 (v/v) for 50 min: flow rate: 1.0 ml min^{-1}]. The degradation of **7S** and **7H** was monitored by the same procedure.

Reaction under optimum conditions

γ-Sulfone **7G** (5.1 mg, 0.0081 mmol) was dissolved in 1.275 ml of 0.03 M NaOH solution (dioxane/H_2O=9/1) and stirred for 2 h at 25°C Then, the reaction mixture was neutralized with 0.03 M AcOH solution (dioxane/ H_2O=9/1), extracted with ethyl acetate, washed with brine, dried over Na_2SO_4, and concentrated in vacuo to give a colorless syrup which was purified by P-TLC developed with ethyl acetate/n-hexane (1:2, v/v) to give **8G** (2.9 mg, 72.0% yield) as crystal. **7S** (8.7 mg, 0.0127 mmol) and **7H** (3.5 mg, 0.00618 mmol) were treated in the same manner to give **8S** (4.3 mg, 63.4% yield) and **8H** (2.4 mg, 82.5% yield), respectively.

Compound 8G

^{1}H NMR δ ($CDCl_3$): 0.88 (3H, t *J*=6.9, $CH_3C_{11}H_{22}SO_2$), 1.26 (16H, s, $CH_3CH_2C_8H_{16}CH_2CH_2SO_2$), 1.40 (2H, t *J*=6.9, $CH_3CH_2C_{10}H_{20}SO_2$), 1.76 (2H, m, $C_{10}H_{21}CH_2CH_2SO_2$), 2.98 (2H, t *J*=8.1, $C_{11}H_{23}CH_2SO_2$), 3.89 (3H, s, OCH_3), 5.16 (2H, s, $CH_2C_6H_5$), 5.37 (1H, dd *J*α-β=1.8 *J*α–γ-=3.3, Hα), 6.69 (1H, dd *J*γ–α=1.8 *J*γ–β=15.2, Hγ), 6.78 (1H, dd $J_{H\text{-}H}$ (ortho) =8.3, $J_{H\text{-}H}$ (meta) =1.8, H-6 in arom.), 6.86 (1H, d $J_{H\text{-}H}$ (meta) =1.8, H-2 in arom.), 6.86 (1H, d, $J_{H\text{-}H}$ (ortho) =8.1, H-5 in arom.), 6.98 (1H, dd, *J*β-α=3.3 *J*β-γ=15.2, Hβ),7.28-7.44 (5H, m, $C_6H_5CH_2$)

^{13}C NMR δ ($CDCl_3$): 14.1, 22.4, 22.7, 28.4, 29.1, 29.3, 29.3, 29.5, 29.6, 31.9, 54.7 ($C_{12}H_{25}SO_2$), 56.0 (OCH_3), 70.9 ($CH_2C_6H_5$), 72.6 (Cα), 110.0, 113.9, 119.0 (C-2, C-5, C-6 in arom.), 126.7 (Cγ), 127.2,

127.9, 128.6 (C in benzyl), 148.8 (Cβ), 132.7, 136.7, 148.5, 150.1 (C in arom.)

MALDI-TOF MS: m/z $[M+Na]^+$ calculated for $C_{29}H_{42}O_5S$: 525.70 ; found:525.26

Compound 8S

^1H NMR δ ($CDCl_3$): 0.88 (3H, t *J*=6.3, $CH_3C_{11}H_{22}SO_2$), 1.26, 1.40 (18H, broad, $CH_3CH_2C_8H_{16}CH_2CH_2SO_2$), 1.76 (2H, m, $C_{10}H_{21}CH_2CH_2SO_2$), 2.98 (2H, t *J*=7.8, $C_{11}H_{23}CH_2SO_2$), 3.81 (6H, s, OCH_3), 4.99 (2H, s, $CH_2C_6H_5$), 5.35 (1H, s, Hα), 6.68 (1H, dd, *J*=15.0, 1.5, Hγ), 6.97 (1H, dd, *J*=15.0, 3.6, Hβ), 6.51-7.49 (7H, m, H in arom.)

^{13}C NMR δ ($CDCl_3$): 14.1, 22.5, 22.7, 28.4, 29.1, 29.3, 29.5, 29.6, 31.9, 38.1, 54.7 ($C_{12}H_{25}SO_2$), 56.1 (OCH_3), 75.1 ($CH_2C_6H_5$), 72.9 (Cα), 103.4, 128.2, 128.5 (C in arom.)

MALDI-TOF MS: m/z $[M+Na]^+$ calculated for $C_{29}H_{42}O_5S$: 555.29 ; found:555.29

Compound 8H

^1H NMR δ ($CDCl_3$): 0.88 (3H, t, *J*=6.6, $CH_3C_{11}H_{22}SO_2$), 1.26 (16H, broad, $CH_3CH_2C_8H_{16}CH_2CH_2SO_2$), 1.40 (2H, m, $CH_3CH_2C_8H_{16}CH_2CH_2SO_2$), 1.77 (2H, m, $C_{10}H_{21}CH_2CH_2SO_2$), 2.98 (2H, m, $C_{11}H_{23}CH_2SO_2$), 5.07 (2H, s, $CH_2C_6H_5$), 5.39 (1H, dd, *J*=3.3, 1.8, Hα), 6.70 (1H, dd, *J*=20.0, 4.8, Hγ), 6.98 (1H, dd, *J*=20.0, 4.8, Hβ), 7.23-7.45 (7H, m, H in arom.)

^{13}C NMR δ ($CDCl_3$): 14.1, 22.4, 22.7, 28.3, 29.0, 29.2, 29.3, 29.5, 29.6, 31.9, 54.8 ($C_{12}H_{25}SO_2$), 70.0 ($CH_2C_6H_5$), 72.4 (Cα), 115.3, 127.4, 128.1, 128.1, 128.6, 132.0, 136.6, 159.1 (C in arom.)

MALDI-TOF MS: m/z $[M+Na]^+$ calculated for $C_{29}H_{42}O_5S$: 495.26 ; found:495.29

Chapter 3

Mesurements

A Bruker (Ettlingen, Germany) Avance 600 MHz spectrometer equipped with a cryogenic probe at 323 K was used. The solvent was deuterated dimethyl sulfoxide (DMSO-d_6) with 4,4-dimethyl-4-silapentane-1-sulfonic acid (DSS) as internal standard. The samples (DHPs **1**–**5**)

without acetylation were dissolved in 0.5 ml of DMSO-d_6. The spectral widths were 7788 and 21,135 Hz for the ^{1}H and ^{13}C dimensions, respectively. The number of collected complex points was 1536 for the 1H dimension, with a recycle delay of 1.5 or 2.5 s. The number of transients was 16 or 32, and 256 time increments were always recorded in the ^{13}C dimension. Gaussian multiplication (LB=-0.20) and squared sinebell (SSB=3) window functions were applied in ^{1}H and ^{13}C dimensions, respectively. Prior to FT, the data matrices were zero-filled up to 2048 and 1024 points in the ^{1}H and ^{13}C dimensions, respectively. FT-IR was performed with a Perkin Elmer Spectrum FT-IR spectrometer (Perkin Elmer, Boston, MA, USA). The technique of attenuated total reflectance (ATR) was applied. After acetylation, number-averaged molecular weight (*M*n) of each product was analyzed by gel permeation chromatography (GPC) in chloroform at 40°C with a Shimadzu (Kyoto, Japan) LC instrument: injector (LC-20AT), column oven (CTO-20A), UV-Vis detector (SPD-20A), detector (RID-10A), communication bus module (CBM- 20A), LC work solution (CLASS-LC solution), and Shodex columns (KF-804L and KF-803L). Calibration curves were obtained by polystyrene standards (Showa Denko, Tokyo, Japan). The flow rate is 1.0 ml min^{-1}.

Preparation of DHP

A DHP was prepared from coniferyl alcohol in the dark according to the Zutropf method (gradual monolignol addition); see Wayman and Obiaga (1974). Three solutions were prepared: (1) solution A: 2.5 mg of horseradish peroxidase (HRP) (100 U mg-1) (Wako, Osaka, Japan) in 250 ml of 0.1 m phosphate buffer (pH 6.5); (2) solution B: 1 g of coniferyl alcohol in 500 ml of distilled water; (3) solution C: 500 ml of 0.2% H_2O_2 aqueous solution. Solutions B and C were added dropwise together to solution A over a period of 60 h. During the addition of solutions B and C, 2.5 mg of HRP was added to the solution mixture after 24 and 48 h. Then, another 2.5 mg of HRP was added to the reaction mixture, which was kept at room temperature (r.t.) for 24 h. The precipitate of the resulting polymer was

collected by centrifugation at 36 618 ×*g* for 15 min and washed twice with distilled water. The precipitate was dissolved in 10 ml of dioxane/water (9:1, v/v) and filtered for purification. The solution was lyophilized to give powdered DHP (917.9 mg).

Reduction of olefins in the DHP

Palladium-carbon (5%, 150 mg) was added to a stirred solution of DHP (917.9 mg) dissolved in 20 ml of dioxane/water (9:1, v/v). The re- action mixture was stirred at r.t. under hydrogen atmosphere for 12 h. Then, the reaction mixture was filtered and washed with dioxane/ water (9:1, v/v). The combined filtrate and washings were dropped into 200 ml of distilled water to make the suspension, which was cen- trifuged at 36,618 ×*g* for 15 min to give the precipitate. The precipitate was suspended again and this suspension was lyophilized, resulting in the product referred to as **DHP1** (905.4 mg).

γ-Tosylation

TsCl (1.90 g, 10.0 mmol) was added to a stirred solution of **DHP1** (393.7 mg) dissolved in 5 ml of pyridine. The reaction mixture was kept at r.t. for 5 h and then was poured onto ethanol to remove excess TsCl. The suspension was centrifuged at 36,618 ×*g* for 15 min to give the precipitate. The precipitate was washed with ethanol until the odor of pyridine could not be detected, and then the precipitate was suspended in distilled water. The suspension was lyophilized and yielded **DHP2** (547.8 mg, 139.1%).

Thioetherification

K_2CO_3 (3.550 g, 25.7 mmol) and Dod-SH (1.228 ml, 5.14 mmol) were added to a stirred solution of **DHP2** (448.1 mg) dis- solved in 17 ml of dimethylformamide (DMF). The reaction mixture was kept at 70°C for 20 h and then cooled. The mixture was extracted with *n*-hexane (10 ml) for removal of

excess Dod-SH. The obtained DMF solution was concentrated in *vacuo*. The residue was suspended with distilled water (100 ml). This suspension was centrifuged at 36,618 ×*g* for 15 min. The obtained precipitate was washed with distilled water and the suspension was lyophilized, resulting in **DHP3** (361.2 mg, 80.6%).

Sulfonylation (Oxidation)

Oxone (purchased from Tokyo Chemical Industry Co., Ltd., Tokyo, Japan) containing over 45% of potassium peroxymonosulfate (1.3214 g) was added to a solution of **DHP3** (295.5 mg) dissolved in 5 ml of dioxane/H_2O (9:1, v/v). After stirring at r.t. for 2 h, the reaction mixture was diluted with distilled water. This suspension was centrifuged at 36,618 ×*g* for 15 min. The resulting precipitate was washed with distilled water (100 ml) five times and then suspended with distilled water and lyophilized to give the product **DHP4** (278.9 mg, 94.4%).

Alkali treatment

A 0.3 M NaOH aqueous solution (1 ml) was added to a solution of **DHP4** (47.2 mg) dissolved in dioxane (9 ml). The reaction mixture was stirred at 25°C for 2 h and then neutralized with 0.3 M HCl solution. The solution was concentrated in *vacuo*. The obtained product **DHP5** (47.2 mg, 100%) was subjected to FT-IR, NMR, and GPC measurements without further purification.

Chapter 4

Mesurements

A Bruker (Ettlingen, Germany) Avance 600 MHz spectrometer equipped with a cryogenic probe at 323 K was used. The samples (**pMWL1**–**4**) and **pMWL5** without acetylation were dissolved in 0.5 ml of DMSO-d_6 and $CDCl_3$, respectively. The spectral widths were 7788 and 21,135 Hz for the ^1H and

^{13}C dimensions, respectively. For the ^{1}H dimension, 1536 complex points were collected with a recycle delay of 1.5 or 2.5 s. In the ^{13}C dimension, the number of transients was 16 or 32, and 256 time increments were recorded. Gaussian multiplication (LB = -0.20) and squared sinebell (SSB = 3) window functions were applied in ^{1}H and ^{13}C dimensions, respectively. Prior to FT, the data matrices were zero-filled up to 2048 and 1024 points in the ^{1}H and ^{13}C dimensions, respectively.

FT-IR was performed with a Perkin Elmer Spectrum FT-IR spectrometer (Perkin Elmer, Boston, MA, USA). The technique of ATR was applied. After acetylation (Ac_2O/pyridine/r.t/over night), the *Mn* of each sample was analyzed by GPC in chloroform at 40°C with a Shimadzu (Kyoto, Japan) LC instrument: injector (LC-20AT), column oven (CTO-20A), UV-Vis detector (SPD-20A), detector (RID-10A), communication bus module (CBM- 20A), LC work solution (CLASS-LC solution), Shodex columns (KF-804L and KF-803L), and flow rate (1.0 ml min^{-1}). The system was calibrated with polystyrene standards (Showa Denko, Tokyo, Japan).

Preparation of the purified milled wood lignin (pMWL)

The wood (from 8-years-old *E. globulus*) provided by Oji paper Co., Ltd. (Tokyo, Japan) was premilled (Wiley-mill), extracted with EtOH/toluene (1/2) for 6 h, dried, and finely ball-milled for 48 h under nitrogen gas. Then the milled wood was extracted with dioxane/water (9/1) to obtain the crude MWL (Björkman 1956). The crude MWL was dissolved in 90% acetic acid and the solution was poured into distilled water. The suspension was centrifuged at 18,000 rpm (36,618 ×*g*) for 15 min to give the purified MWL (**pMWL1**).

γ-Tosylation

TsCl (2.15 g, 11.3 mmol) was added to a stirred solution of **pMWL1** (399.5 mg) dissolved in 5 ml of pyridine. The reaction mixture was kept at r.t. for 5 h and then was poured into EtOH to

remove excess TsCl. The suspension was centrifuged at 18,000 rpm (36,618 ×*g*) for 15 min. The precipitate was washed with EtOH until the pyridine odor disappeared and suspended in distilled water. The suspension was lyophilized to yield **pMWL2** (617.2 mg, 154.5%). The yield percentage is the weight of the product as percent of the weight of the starting material.

Thioetherification

K_2CO_3 (732.4 mg, 5.30 mmol) and Dod-SH (250 μl, 1.04 mmol) were added to a stirred solution of **pMWL2** (96.5 mg) dissolved in 5 ml of DMF. The reaction mixture was kept at 70°C for 20 h and then cooled. The mixture was extracted with *n*-hexane (100 ml) for removing of excess Dod-SH. The obtained DMF solution was concentrated in *vacuo*. The residue was suspended with distilled water (100 ml). This suspension was centrifuged at 18,000 rpm (36,618 ×*g*) for 15 min. The obtained precipitate was washed with distilled water until the filtrate became pH 7. The aqueous suspension of the precipitate was lyophilized resulting in **pMWL3** (80.1 mg, 83.0%).

Sulfonylation (oxidation)

Oxone (129.9 mg, 0.211 mmol) was added to a solution of **pMWL3** (29.9 mg) dissolved in 2 ml of dioxane/H_2O (9/1). After stirring at r.t. for 2 h, the reaction mixture was diluted with distilled water. This suspension was centrifuged at 18,000 rpm (36,618 ×*g*) for 15 min. The resulting precipitate was washed with distilled water (100 ml) five times and then suspended with distilled water and lyophilized to give the product **pMWL4** (25.1 mg, 83.9%).

Mild alkali treatment

A 0.3 N NaOH aqueous solution (1.0 ml) was added to a solution of **pMWL4** (19.5 mg) dissolved in dioxane (9.0 ml). The reaction mixture was stirred at 25°C for 2 h and then neutralized with

0.3 N HCl solution. The solution was concentrated in *vacuo* to obtain the product **pMWL5** (19.5 mg, 100%).

Chapter 5

Measurement

A Bruker (Ettlingen, Germany) Avance 600 MHz spectrometer equipped with a cryogenic probe at 323 K was used. The solvent was DMSO-d_6. The samples except **cMWL2** without acetylation were dissolved in 0.5 ml of DMSO-d_6. In case of the **cMWL2**, the sample after acetylation was dissolved in 0.5 ml of DMSO-d_6. The spectral widths were 7788 and 21,135 Hz for the ^{1}H and ^{13}C dimensions, respectively. The number of collected complex points was 1536 for the 1H dimension, with a recycle delay of 1.5 or 2.5 s. The number of transients was 16 or 32, and 256 time increments were always recorded in the ^{13}C dimension. Gaussian multiplication (LB=-0.20) and squared sinebell (SSB=3) window functions were applied in ^{1}H and ^{13}C dimensions, respectively. Prior to FT, the data matrices were zero-filled up to 2048 and 1024 points in the ^{1}H and ^{13}C dimensions, respectively. FT-IR was performed with a Perkin Elmer Spectrum FT-IR spectrometer (Perkin Elmer, Boston, MA, USA). The ATR technique was applied. Number-averaged molecular weight (*Mn*) of each product after acetylation was analyzed by GPC in chloroform at 40°C with a Shimadzu (Kyoto, Japan) LC instrument: injector (LC-20AT), column oven (CTO-20A), UV-Vis detector (SPD-20A), detector (RID-10A), communication bus module (CBM- 20A), LC work solution (CLASS-LC solution), and Shodex columns (KF-804L and KF-803L). Calibration curves were obtained by polystyrene standards (Showa Denko, Tokyo, Japan). The flow rate is 1.0 ml min^{-1}.

Preparation of the crude milled wood lignin (cMWL1)

The wood (from 8-years-old *Eucalyptus globulus*) provided by Oji paper Co., Ltd. (Tokyo,

Japan) was premilled (Wiley-mill), extracted with EtOH/toluene (1/2, v/v) for 6h, dried, and finely ball-milled for 48 h under nitrogen gas. Then the milled wood was extracted with dioxane/water (9/1, v/v) to obtain the crude MWL (Björkman 1956). The crude MWL was dissolved dioxane/water (9/1, v/v). The solution was poured onto distilled water. This suspension was centrifuged at 18,000 rpm (36,618 g) for 15min to give the **cMWL1**.

γ-Tosylation

TsCl (5.40 g, 28.3 mmol) was added to a stirred solution of **cMWL1** (998.1 mg) dissolved in 12.5 ml of pyridine. The reaction mixture was kept at r.t. for 5 h and then was poured onto ethanol to remove excess TsCl. The suspension was centrifuged at 18,000 rpm (36,618 ×*g*) for 15 min. The precipitate was washed with EtOH until the odor of pyridine could not detected, and suspended in distilled water. The suspension was lyophilized and yielded **cMWL2** (1.627 g, 163.0 %). The yield percentage is the weight of the product as percent of the weight of starting material.

Thioetherification

K_2CO_3 (11.0 g, 79.9 mmol) and Dod-SH (3.83 ml, 16.0 mol) were added to a stirred solution of **cMWL2** (1.40 g) dissolved in 25 ml of DMF. The reaction mixture was kept at 70 ^{o}C for 21 h and then cooled. The mixture was extracted with *n*-hexane (500 ml) for removal of excess Dod-SH. The obtained DMF solution was concentrated in *vacuo*. The residue was suspended with distilled water (500 ml). This suspension was neutralized at pH 7 by 1N HCl aqueous solution and centrifuged at 18,000 rpm (36,618 ×*g*) for 15 min. The obtained precipitate was washed with distilled water and the suspension was lyophilized, resulting in **cMWL3** (1.20 g, 85.7 %).

Sulfonylation (oxidation)

Oxone (3.39 g, 5.51 mmol) was added to a solution of **cMWL3** (1.08 g) dissolved in 30 ml of dioxane/H_2O (9/1, v/v). After stirring at r.t. for 2 h, the reaction mixture was diluted with distilled water (500 ml). This suspension was centrifuged at 18,000 rpm (36,618 ×*g*) for 15 min. The resulting precipitate was washed with distilled water (100 ml) five times and then suspended with distilled water and lyophilized to give the product **cMWL4** (1.06 g, 98.1 %).

Mild Alkali treatment

A 0.3N NaOH aqueous solution (10.0 ml) was added to a solution of **cMWL4** (100.9 mg) dissolved in dioxane (90.0 ml). The reaction mixture was stirred at 25°C for 2h and then neutralized with 0.3N HCl solution. The solution was concentrated in *vacuo* to obtain the product **cMWL5** (100.9 mg, 100 %).

Fractionation of the cMWL5

The **cMWL5** was successively extracted two times with 50ml of Et_2O, EtOAc, THF each. At first, **cMWL5** was extracted with Et_2O (100 ml) to get the Et_2O extractive (**cMWL5-1**) (40.3 mg, 40 %) and the Et_2O residue. Then, the Et_2O residue was extracted with EtOAc (100 ml) to obtain the EtOAc extractive (**cMWL5-2**) (18.6 mg, 19 %) and the EtOAc residue. Finally, the EtOAc residue was extracted with THF to take the THF extractive (**cMWL5-3**) (15.8 mg, 16 %) and the THF residue (**cMWL5-4**) (24.8 mg, 25 %).

References

Balakshin, M.Y., Capanema, E.A., Chen, C.-L., Gracz, H.S. (2003) Elucidation of the structures of residual and dissolved pine kraft lignins using an HMQC NMR technique. J. Agric. Food Chem. 51:6116–6127.

Balakshin, M.Yu., Capanema, E.A., Chang, H. (2007) MWL fraction with a high concentration of lignin carbohydrate linkages: isolation and 2D NMR spectroscopic analysis. Holzforschung 61:1-7.

Balakshin, M., Capanera, E., Grecz, H., Chang, H., Jameel, H. (2011) Quantification of lignin-carbohydrate linkages with high-resolution NMR spectroscopy. Planta 233: 1097-1110.

Björkman, A. (1956) Studies on finely divided wood. Part 1. extraction of lignin with neutral solvents. Svensk Papperstidn., 59:477-485.

Björkman, A. (1957) Finely divided wood. III. Extraction of lignin-carbohydrate complexes with neutral solvents. Svensk Papperstidn., 60:243-251.

Brodin, I., Sjöholm, E., Gellerstedt, G. (2009) Kraft lignin as feedstock for chemical products: The effects of membrane filtration. Holzforschung, 63(3):290-297.

Boerjan, W., Ralph, J., Baucher, M. (2003) Lignin biosynthesis, Annu. Rev. Biol., 54: 519-546.

Capanema, E.A., Balakshin, M.Y., Chen, C.-L., Gratzl, J.S., Gracz, H. (2001) Structural analysis of residual and technical lignins by 1H-13C correlation 2D NMR-spectroscopy. Holzforschung 55:302–308.

Capanema, E.A., Balakshin, M.Y., Kadla, J.F. (2004) A comprehensive approach for quantitative lignin characterization by NMR spectroscopy. J. Agric. Food Chem. 52:1850–1860.

Capanema, E.A., Balakshin, M.Y., Kadla, J.F. (2005) Quantitative characterization of a hardwood milled wood lignin by nuclear magnetic resonance spectroscopy. J. Agric. Food Chem. 53: 9639–9649.

Cherubini, F. and Stromman, A. H. (2011) Chemicals from lignocellulosic biomass: opportunities, perspectives, and potential of biorefinery systems. Biofuels Bioproducts & Biorefining 5: 548-561.

Choi, J.W., Choi, D.H. and Faix, O. (2007) Characterization of lignin-carbohydrate linkages in the residual lignins isolated from chemical pulps of spruce (*Picea abies*) and beech wood (*Fagus sylvatica*). J. Wood Sci., 53: 309-313.

Dos Santos M., Marcelo C., Pedrazzi, C., Colodette, J.L. (2011) Xylan deposition onto eucalypt pulp fibers during oxygen delignification. Holzforschung, 65(4):605-612.

Du, X., Gellerstedt, G. and Li, J. (2013) Universal fractionation of lignin-carbohydrate complexes (LCCs) from lignocellulosic biomass: an example using spruce wood. The plant journal, 74: 328-338.

Durst, T. (1979) In comprehensive organic chemistry, Edn. Barton, D., Ollis, W. D., Pergamon, Oxford, Vol. 3, p174.

Enoki, A., Yaku, F., Koshijima, T. (1983) Synthesis of LCC model compounds and their chemical and enzymatic stabilities. Holzforschung 37:135–141.

Fantoni, A.C. and Marañón, J. (1996) Conformational Properties of Methyl Vinyl Sulfone: Ab Initio Giometry Optimization and Vibrational Analysis. Structural Chemistry, 7:51-58.

Forzelius, S., Jerkeman, P., Lindberg, B. (1963) Sulphones of some lignin models. Acta Chemica Scandinavica, 17:1470-1471.

Freudenberg, K. and Dietrich, G. (1949) Vergleichende untersuchung des fichten-lignins und buchen-lignins. *Annalen der chemie-justus liebig*, 563: 146-156.

Furuno, H., Takano, T., Hirosawa, S., Kamitakahara, H. and Nakatsubo, F. (2006) Chemical structure elucidation of total lignin in woods. Part II: Analysis of a fraction of residual wood left after MWL isolation and solubilized in lithim chloride/*N*,*N*-dimethylacetamide. Holzforschung, 60: 653-658.

Guerra, A., Lucia, L.A., Argyropoulos, D.S. (2008) Isolation and characterization of lignins from *Eucalyptus grandis* Hill ex Maiden and *Eucalyptus globulus* Labill. by enzymatic mild acidolysis (EMAL). Holzforschung, 62(1):24-30.

Hansen, C.M. (1969) The universality of the solubility parameter. Industrial & engineering chemistry product research and development, 8: 2-11.

Heikkinen, S., Toikka, MM., Karhunen, T., Kilpelainen, IA. (2003) Quantitative 2D HSQC (Q-HSQC) via suppression of *J*-dependence of polarization transfer in NMR spectroscopy: Application to wood lignin. J. Am. Chem. Soc. 125: 4362-4367.

Henriksson, G., Lawoko, M., Martin, M.E.E. and Gellerstedt, G. (2007) Lignin-carbohydrate network in wood and pulps: A determinant for reactivity. Holzforschung, 61: 668-674.

Higuchi, T. (2006) Look back over the studies of lignin biochemistry. J. Wood Sci. 52:2–8.

Hirosawa, S., Katahira, R. and Nakatsubo, F. (2002) Chemical structural elucidation of total lignins in woods I: fractionation of the lignin in residual wood meal after extraction of milled wood lignin. J. Wood Sci., 48: 46-50.

Holtman, K.M., Chang, H.M., Jameel, H., Kadla, J.F. (2003) Elucidation of lignin structure through degradative methods: comparison of modified DFRC and thioacidolysis. J. Agric. Food Chem. 51:3535–3540.

Ibarra, D., Chavez, M. I., Rencoret, J., Del Rio, J. C., Gutierrez, A., Romero, J., Camarero, S., Martinez, M. J., Jumenez-Barbero, J., Martinez, A. T. (2007) Lignin modification during *Eucalyptus globulus* kraft pulping followed by totally chlorine-free bleaching: a two- dimensional nuclear magnetic resonance, Fourier transform infrared, and pyrolysis-gas chromatography/mass spectrometry study. J. Agric. Food Chem. 55:3477–3490.

Jerkeman, P. and Lindberg, B. (1964) Sulphones of lignin models, synthesis and reactions in alkali. Acta Chemica Scandinavica, 18:1477-1482.

Katahira, R., Ujihara, M., Nakatsubo, F. (2003) A novel selective cleavage method for β-O-4 substructure in lignins named TIZ method. I. Degradation of guaiacyl and syringyl models. J. Wood Chem. Technol. 23:71–87.

Katahira, R., Kamitakahara, H., Takano, T., Nakatsubo, F. (2006) Stability of α-ether substructures in lignins under TIZ reaction conditions. Cellulose Chem. Technol. 40:19–34.

Koshijima, T., Watanabe, T. (2003) Association between lignin and carbohydrates in wood and other plant tissues. Springer, Berlin.

Landucci, L.L., Ralph, S.A., Hammel K.E. (1998) ^{13}C-NMR characterization of guaiacyl, guaiacyl/syringyl, and syringyl dehydrogenation polymers. Holzforschung, 52:160-170.

Lapierre, C., Monties, B., Roland, C. (1986) Preparative thioacidolysis of spruce lignin: isolation and identification of main monomeric products. Holzforschung 40:47–50.

Lawoko, M., Henriksson, G. and Gellestedt, G. (2003) New method for quantitative preparation of lignin-carbohydrate complex from unbleached softwood kraft pulp: lignin-polysaccharide networks I. Holzforschung, 57: 69-74.

Lawoko, M., Henriksson, G., Gellerstedt, G. (2005) Structural differences between the lignin-carbohydrate complexes present in wood and in chemical pulps. Biomacrom. Chem. 6:3467-3473.

Lawoko, M., Henriksson, G. and Gellestedt, G. (2006) Characterisation of lignin-carbohydrate complexes (LCCs) of spruce wood (*Picea abies* L.).isolated with two methods. Holzforschung, 60: 158-161.

Lenihan B.D., Shechter H., (1998) Synthesis and conversions of substituted *o*-(trimethylsilyl)methylxbenzyl-*p*-tolyl sulfones to o-quinodimethanes and products thereof. J. Org. Chem. 63: 2072–2085.

Leschinsky, M., Zuckerstätter, G., Weber, H.K., Patt, R., Sixta, H. (2008a) Effect of autohydrolysis of *Eucalyptus globulus* wood on lignin structure. Part 1: Comparison of different lignin fractions formed during water prehydrolysis. Holzforschung, 62(6):645-652.

Leschinsky, M., Zuckerstätter, G., Weber, H.K., Patt, R., Sixta, H. (2008b) Effect of autohydrolysis of *Eucalyptus globulus* wood on lignin structure. Part 2: Influence of autohydrolysis intensity. Holzforschung, 62:653–658.

Leskinen, T., King, A.W.T., Kilpeläinen and Argyropoulos, D.S. (2011) Fractionation of lignocellulosic materials with ionic liquids. 1. effect of mechanical treatment. Ind. Eng. Chem. Res., 50: 12349-12357.

Leskinen, T., King, A.W.T., Kilpeläinen and Argyropoulos, D.S. (2013) Fractionation of lignocellulosic materials using ionic liquids: Part 2. Effect of particle size on the mechanisms of fractionation. Ind. Eng. Chem. Res., 52: 3958-3966.

Li, J., Martin-Sampedro, R., Pedrazzi, C., Gellerstedt, G. (2011) Fractionation and characterization of lignin-carbohydrate complexes (LCCs) from eucalyptus fibers. Holzforschung, 65(1):43-50.

Lindberg, B., Lundstro¨m, H. (1966) 6-Deoxy-6-*p*-tolylsulphonyl-D-glucopyranosides. Acta Chem. Scand. 20: 2423–2426.

Ljunggren, S., Ljungquist, P. O., Wenger, U. (1983) The significance of α-sulfone and α-sulfonate groups for the cleavage of β-aryl ether structures in lignin. Acta Chemica Scandinavica, B37, 313-320.

Lu, F., Ralph, J. (1997a) Derivatization followed by reductive cleavage (DFRC method), a new method for lignin analysis:protocol for analysis of DFRC monomers. J. Agric. Food Chem. 45: 2590–2592.

Lu, F., Ralph, J. (1997b) DFRC method for lignin analysis. 1. New method for beta aryl ether cleavage: lignin model studies. J. Agric. Food Chem. 45:4655–4660.

Lundquist, K. (1992) Methods in Lignin Chemistry. Eds. Stephen, Y.L., Carlton, W.D. Springer, Berlin. pp. 289-300.

Matsumoto, Y., Ishizu, A., Nakano, J. (1980) Selective cleavage of arylglycerol-β-aryl ether type structure in lignin I. Model experiment. Mokuzai Gakkaishi 26:806–810.

Matsumoto, Y., Ishizu, A., Iiyama K., Nakano, J. (1982) Selective cleavage of arylglycerol-β-aryl ether type structure in lignin II. Determination of the arylglycerol-β-aryl ether type structure in milled wood lignin of spruce. Mokuzai Gakkaishi 28:249–254.

Mendes, C.V.T., Baptista, C.M.S.G., Rocha, J.M.S., Carvalho, M.G.V.S. (2009) Prehydrolysis of *Eucalyptus globulus* Labill. hemicelluloses prior to pulping and fermentation of the hydrolysates with the yeast *Pichia stipitis* 10th EWLP, Stockholm, Sweden, August 25–28, 2008. Holzforschung, 63(6):737-743.

Miyagawa, Y., Kamitakahara, H., Takano, T. (2013) Fractionation and characterization of lignin-carbohydrate complexes (LCCs) of Eucalyptus globulus in residues left after MWL isolation. Part II: Analyses of xylan-lignin fraction (X-L). Holzforschung 67:629-642.

Nakatsubo, F., Sato, K., Higuchi, T. (1976) Enzymatic dehydrogenation of *p*-coumaryl alcohol. IV. reactivity of quinonemethide. Mokuzai Gakkaishi 22:29–33.

Nakatsubo, F., Sato, K., Higuchi, T. (1975) Synthesis of guaiacylglycerol-β-guaiacyl ether. Holzforschung 29:165–168.

Nicholson, D.J., Duarte, G.V., Alves, E.F., Kiemle, D.J., Francis, R.C. (2012) Preliminary Results on an Approach for the Quantification of Lignin-Carbohydrate Complexes (LCC) in Hardwood Pulps. Journal of wood chemistry and technology, 32: 238-252.

Nieminen, K., Sixta, H. (2012) Comparative evaluation of different kinetic models for batch cooking: A review. Holzforschung, 66(7):791-799.

Node, M., Kumar, K., Nishide, K., Ohsugi, S., Miyamoto, T. (2001) Odorless substitutes for foul-smelling thiols: syntheses and applications. Tetrahedron Lett. 42: 9207–9210.

Patt, R., Kordsachia, O., Fehr, J. (2006) European hardwoods versus *Eucalyptus globulus* as a raw material for pulping. Water Science and Technology. 40:39-48.

Ralph, J., Lu, F. (1998) The DFRC method for Lignin Analysis. 6. A sample modification for identifying natural acetates on lignins. J. Agric. Food Chem. 46:4616–4619.

Ralph, J., Marita, J.M., Ralph, S.A., Hatfield, R.D., Lu, F., Ede, R.M., Peng, J., Quideau, S., Helm, R.F., Grabber, J.H., Kim, H., Jimenez-Monteon, G., Zhang, Y., Jung, H. J. G., Landucci, L.L., MacKay, J.J., Sederoff, R.R., Chapple, C., Boudet, A.M. (1999) Solution-state NMR of lignin. In: Advances in Lignocellulosics Characterization. Ed. Argyropoulos, D.S. Tappi Press, Atlanta, GA. pp. 55–108.

Ralph, J., Akiyama, T., Kim, H., Lu, F., Schatz, P. F., Marita, J. M., Ralph, S. A., Reddy, M. S. S., Chen, F., Dixon, R. A. (2006) Effects of coumarate 3-hydroxylase down-regulation on lignin structure. J. Biol. Chem. 281:8843-8853.

Ralph, S.A., Ralph, J., Landucci, L. (2004) NMR Database of Lignin and Cell Wall Model Compounds. US Forest Prod. Lab., Madison, WI (http://ars.usda.gov/Services/docs.htm? docids10491) (accessed July 2006).

Rencoret, J., Marques, G., Gutiérrez, A., Ibarra, D., Li, J., Gellerstedt, G., Ignacio Santos, J., Jiménez-Berbero, J., Martínez, Á. T., del Río, J. C. (2008) Structural characterization of milled wood lignins from diffent eucalypt species. Holzforschung 62:514-526.

Rodríguez-López, J., Romaní, A., González-Muñoz, M.J., Garrote, G., Parajó, J.C. (2012) Extracting value-added products before pulping: Hemicellulosic ethanol from *Eucalyptus globulus* wood. Holzforschung, 66(5):591-599.

Roland, C., Monties, B., Lapierre, C. (1992) Methods in Lignin Chemistry. Eds. Stephen, Y.L., Carlton, W.D. Springer, Berlin. pp. 334–349.

Salanti, A., Zoia, L., Tolppa, E.L., Orlandi, M. (2012) Chromatographic detection of lignin-carbohydrate complexes in annual plants by derivatization in ionic liquid. Biomacromoleclules, 13: 445-454.

Silverstein, R.M. (1967) Spectrometric Identification of Organic Compounds. 2nd Rev. Edn. John Wiley & Sons, New York.

Terashima, N., Atalla, R.N., Ralph, S.A., Landucci, L.L., Lapierre, C., Monties, B. (1995) New preparation of lignin polymer models under conditions that approximate cell wall lignification. I. Synthesis of novel lignin polymer models and their structural characterization by ^{13}C NMR. Holzforschung, 49:521-527.

Terashima, N., Atalla, R.N., Ralph, S.A., Landucci, L.L., Lapierre, C., Monties, B. (1996) New preparations of lignin polymer models under conditions that approximate cell wall lignification. II. Structural characterization of the models by thioacidolysis. Holzforschung 50:9-14.

Vila, C., Francisco, J.L., Santos, V., Parajó, J.C. (2013) Effects of hydrothermal processing on the cellulosic fraction of *Eucalyptus globulus* wood. Holzforschung, 67(1):33-40.

Watanabe, T. (1995) Important properties of lignin-carbohydrates complexes (LCCs) in environmentally safe paper making. Trends Glycosci. Glycotechnol. 33:57-68.

Wayman, M., Obiaga, T.I. (1974) The modular structure of lignin. Can. J. Chem. 52:2102–2110.

William, J., Boehm, J.C. (1995) The syntheses of 3b-steroidal diacylglyceryl sulfides, sulfoxides, and sulfones. Steroids 60: 321–323.

Yuan, T.Q., Sun, S.N., Xu, F., Sun, R.C. (2011) Characterization of Lignin Structures and Lignin-Carbohydrate Complex (LCC) Linkages by Quantitative 13C and 2D HSQC NMR Spectroscopy. J. Agric. Food Chem., 59: 10604-10614.

Zhang, L., Gellerstedt, G. (2007) Quantitative 2D HSQC NMR determination of polymer structures by selecting suitable internal standard reference. Magn. Res. Chem. 45:37-45.

Publications

The present study has been reported in the following papers.

1) Daisuke Ando, Toshiyuki Takano, Fumiaki Nakatsubo "Multi-step degradation method for β-O-4 linkages in lignins: α-TSA method. Part 1: Reaction of non-phenolic dimeric β-O-4 model compound" Holzforschung, 2013, *accepted* [Chapter 1]

2) Daisuke Ando, Toshiyuki Takano, Fumiaki Nakatsubo "Multi-steps degradation method for β-O-4 linkage in lignins: γ-TTSA method. Part 1. Reaction of non-phenolic dimeric β-O-4 model compounds" Holzforschung, 2012, 66, 3, 331-339. [Chapter 2]

3) Daisuke Ando, Fumiaki Nakatsubo, Toshiyuki Takano, Hiroshi Nishimura, Masato Katahira, Hiroyuki Yano "Multistep degradation method for β-O-4 linkage in lignins: γ-TTSA method. Part 2: reaction of lignin model polymer (DHP)" Holzforschung, 2013, 67, 3, 249-256. [Chapter 3]

4) Daisuke Ando, Fumiaki Nakatsubo, Toshiyuki Takano, Hiroshi Nishimura, Masato Katahira, Hiroyuki Yano "Multi-step degradation method for β-O-4 linkages in lignins: γ-TTSA method. Part 3. Degradation of Milled Wood Lignin (MWL) from *Eucalyptus globulus*" Holzforschung, 2013, 67, 8, 835-842 [Chapter 4]

5) Daisuke Ando, Fumiaki Nakatsubo, Toshiyuki Takano, Hiroshi Nishimura, Masato Katahira, Hiroyuki Yano "Multi-step degradation method for β-O-4 linkages in lignins: γ-TTSA method. Part 4. Selective cleavage of β-O-4 linkages in the LCC sample (crude Milled Wood Lignin) from *Eucalyptus globulus*" Holzforschung, 2014, *to be submitted* [Chapter 5]

Acknowledgements

The author wishes to express his sincerest thanks to Professor Dr. Toshiyuki Takano, Laboratory of Chemistry of Biomaterials Science, Division of Forest and Biomaterials Science, Graduate school of Agriculture, Kyoto University, and also Emeritus Professor Dr. Fumiaki Nakatsubo, Laboratory of Active Bio-based Materials, Research Institute for Sustainable Humanosphere (RISH), Kyoto University, for their kindest guidance and encouragements during the entire process.

The author is deeply grateful to Professor Dr. Yoshiyuki Nishio, Laboratry of Chemistry of Composite Materials, Division of Forest and Biomaterials Science, Graduate school of Agriculture, Kyoto University, and Professor Dr. Toshiaki Umezawa, Laboratory of Metabolic Sciences of Forest Plants and Microorganisms, Research Institute for Sustainable Humanosphere (RISH), Kyoto University, and for their invaluable suggestions and critical readings of the manuscript.

Thanks are also due to Professor Dr. Hiroyuki Yano, Laboratory of Active Bio-based Materials, Research Institute for Sustainable Humanosphere (RISH), Kyoto University.

The author wishes to thank Professor Dr. Masato Katahira, Structural Energy Bioscience Research Section Institute of Advanced Energy, Bioenergy Research Section, Department of Fundamental Energy Science, Graduate School of Energy Science, Kyoto Unversity, and Assistant Professor Dr. Hiroshi Nishimura, Laboratory of Biomass Conversion, Research Institute for Sustainable Humanosphere (RISH), Kyoto University, for the HSQC-NMR analysis and Dr. Kazutsune Tsurumi, Oji Holdings Corporation, for providing the wood sample of *Eucalyptus globulus*.

Thanks are also due to Associate Professor Dr. Hiroshi Kamitakahara, Laboratory of

Chemistry of Biomaterials Science, Division of Forest and Biomaterials Science, Graduate school of Agriculture, Kyoto University, and Associate Professor Dr. Fumio Tanaka, Associate Professor Dr. Toshiro Morooka, and Assistant Professor Dr. Kentaro Abe, Laboratory of Active Bio-based Materials, Research Institute for Sustainable Humanosphere (RISH), Kyoto University, for their helpful suggestions.

The author wishes to thank for the members in Laboratory of Chemistry of Biomaterials Science, Division of Forest and Biomaterials Science, Graduate school of Agriculture, Kyoto University, and Laboratory of Active Bio-based Materials, Research Institute for Sustainable Humanosphere (RISH), Kyoto University, for their co-operation in this work.

Finally, the author is much indebted to his family and his friends for their sincere supports and continuous encouragements throughout his research.

January 2014 Daisuke Ando